Comparison of different methodologies to estimate the freshwater-saltwater distribution in coastal aquifers

Betsy Daniela Romero Verástegui

Thesis to obtain the Master of Science Degree in

Environmental Engineering

Supervisors:
Dr. Gualbert Oude Essink
Dr. Maria Teresa Condesso de Melo

Examination Committee
Chairperson:
Supervisor:
Members of the Committee:

September 2019

Comparison of different methodologies to estimate the freshwater-saltwater distribution in coastal aquifers

Master of Science Thesis
by
Betsy Daniela Romero Verástegui

Supervisors
Gualbert Oude Essink
Daniel Zamrsky
Maria Teresa Condesso de Melo

Examination committee
[examination committee member 1]
[examination committee member 2]
[examination committee member 3]
etc.

This thesis is submitted in partial fulfilment of the requirements for the academic degree of

Master of Science in Water Science and Engineering
IHE Delft Institute for Water Education, Delft, the Netherlands

Master of Science in Environmental Engineering
Instituto Superior Técnico, Universidade de Lisboa, Portugal

Master of Science in Hydro Science and Engineering
Technische Universität Dresden, Germany

MSc research host institution
Instituto Superior Técnico, Universidade de Lisboa, Portugal

September 2019

Acknowledgements

Firstly, I would like to thank dr. ir. Gualbert Oude Essink for giving me the opportunity of doing this research and for all his valuable guidance which helped to successfully finish this thesis.

I am also very thankful to Daniel Zamrsky for his contributions and time to discuss the different parts of the research, as well as providing the necessary information for developing the thesis.

I finally want to address a special thanks to Teresa Melo for her much valuable support and advice during all these months.

Abstract

Coastal aquifers are at risk of salinization due to human pressures and the effect of climate change. It is important to evaluate these effects using methodologies that adequately represent the freshwater-saltwater distribution in these areas. The objective of this research was to compare different methodologies for the estimation of the saltwater intrusion in coastal aquifers. The case study areas evaluated are in Australia, because they had data available for this purpose. The first step was assessing the parameters to be used, which were obtained from local and global sources. Subsequently, this information was the input data in five methodologies that ranged from the simplest to the most complex. Finally, climate change simulations were done to evaluate future stress scenarios. The comparison of data showed large differences between the values of the parameters obtained from local and global sources. The results obtained from the methodologies were influenced by the hydraulic conductivity, the geological layering and the hydraulic gradient. Climate change scenarios presented high levels of saltwater intrusion and decreased volumes of fresh groundwater. The global datasets should be used carefully but are a good starting point in areas where there is no information available. All methodologies were able to represent the saltwater-freshwater distribution, but its accuracy is highly influenced by the input data used.

Keywords: Freshwater-saltwater distribution, coastal aquifer, variable-density groundwater flow, global datasets, saltwater intrusion, analytical solution, iMOD-SEAWAT, SEAWAT.

Table of Contents

List of Figures

List of Tables

Chapter 1 Introduction

Coastal areas are very important for the development of communities. They are the most densely populated areas in the world (Post, 2005). Historically, communities have naturally migrated to the coastal areas due to the transport, food and ecological benefits. It is estimated that 44% of the world's population live within 150 km of the coast, while in 2001 more than half of the world's population lived within 200 km of a coastline (UN-Oceans, n.d.). This increase of human settlements, agricultural and economic activities causes shortages of fresh groundwater in these coastal areas (Oude Essink, 2001).

The use of groundwater, in comparison to surface water, has benefits such as good quality, the minimal seasonal effects, low storage costs and it is available in high quantities. However, it also has disadvantages such as the extraction costs, high mineral content, potential land subsidence and the threat of saltwater intrusion (Oude Essink, 2001).

1.1 Problem definition

Coastal aquifers are important sources of freshwater which are under risk of being salinized because of human intervention or climate change effects. Because of their high sensitivity, it would be ideal to have appropriate methodologies and the necessary amount of data to accurately represent the current freshwater-saltwater distribution and future variations due to human intervention and climate change. These tools would be advantageous for governmental agencies, water managers and users to ensure an appropriate and sustainable use of these fresh groundwater resources, seeking to safeguard the fresh groundwater volumes available.

Currently, there are two types of methodological approaches to evaluate the freshwater-saltwater distribution in aquifers: (1) through analytical formulas and (2) using variable-density groundwater and coupled salt transport modelling. An example of (1) is the methodology proposed by Werner et al. (2012), where specific formulas have been defined for a general conceptual model of a coastal aquifer defined by the author. In the case of (2), it is a more complex approach which needs the use of computer codes such as SEAWAT (Langevin et al., 2008) for the calculations. In this case, different conceptualizations of the groundwater system can be defined. These can be simple and use, for example, average values of recharge and hydraulic conductivity for the whole area or be more complex and treat these as spatially variable parameters.

To be able to apply these methodologies, it is necessary to count with hydrogeological and climatic data of the area. Nevertheless, on a global scale, there is not enough data available to accurately model coastal aquifers and salinization effects. Therefore, it is important to focus on the development of new methodologies that, even with a limited amount of data or by using global datasets, can help to represent these processes and evaluate the sensitivity of coastal aquifers to different anthropogenic and climate change scenarios.

This research aims to compare the use of different methodologies (analytical formulas and different conceptualizations using variable-density groundwater and coupled salt transport modelling) as well as the use of different input data (local or global-scale information) to evaluate how these represent the freshwater-saltwater distribution in the subsurface under present and future scenarios. By assessing their similarities and differences, these results will be a reference for the use of these methodologies.

To evaluate this, it is necessary to have a case study area that already has saltwater intrusion (SWI) studies and counts with the necessary amount of local data to use as a benchmark to test the different methodology approaches. Because of this, Australia was chosen as the area of evaluation. The project "A national-scale vulnerability assessment of seawater intrusion" (Ivkovic, Marshall, et al., 2013) has defined case study areas in Australia's territory which are at risk of SWI and has already compiled relevant data and applied analytical calculations to evaluate this effect. These were used as a baseline for this evaluation.

1.2 Research questions and objectives

The aim of this research is to answer the following research questions:

- What are the differences between the local-scale and global-scale data collected for the case study areas to be used in the proposed methodologies to evaluate the freshwater-saltwater distribution in coastal aquifers?
- How influential are the input data and the conceptualizations in the different methodologies for the evaluation of the freshwater-saltwater distribution in coastal aquifers and how do these affect the calculated results?
- What are the possible effects of climate change on the saltwater intrusion process in coastal aquifers?

The following objectives were identified to answer the previous research questions:

Main objective

- Compare different methodologies to estimate the freshwater-saltwater distribution in coastal aquifers.

Secondary objectives

- Gather coastal aquifers data from local-scale and global-scale sources and do a comparison between them.
- Evaluate the saltwater – freshwater distribution in coastal aquifers using different methodologies.
- Assess the effects of possible climate change scenarios in coastal aquifers and its influence on the saltwater intrusion processes.

Chapter 2 Background information

2.1 Saltwater intrusion (SWI)

Seawater intrusion (also called saltwater intrusion) is “the encroachment of saline water into fresh groundwater regions in coastal aquifer settings” (Werner & Simmons, 2009). Seawater intrusion (SWI) is a process where, in coastal aquifers, changes in the hydrology of the coastal zone can cause landward movement of seawater (Morgan, Werner, Morris, et al., 2013).

This process is related to the effect of human intervention, for example, the reclamation of coastal areas, impoldering, groundwater extraction, irrigation, drainage, reduction of recharge areas, among others (Oude Essink, 2001), but also due to climate change impacts (e.g. sea-level rise or decrease in aquifer recharge). This has led to significant losses in the availability of freshwater resources in coastal aquifers (Morgan, Werner, Morris, et al., 2013) and changes in the hydrogeological regime (e.g. decreasing the outflow of fresh groundwater). The response of groundwater to these effects is to reach a new equilibrium in relation to the distribution of fresh and saline groundwater (Oude Essink, 2001).

The process of reaching an equilibrium state can take from tens of years to even hundreds or thousands of years, mainly depending on the geological characteristics. In consequence, most counter measures will also take a long time before they are effective (Oude Essink, 2001). As a result, the future fresh water availability (at any time, in enough volumes, with the right quality, at the right location) will be threatened and uncertain.

2.1.1 Density of water

Density is a function of pressure, fluid temperature and concentration of dissolved solids. However, pressure can be neglected in most hydrogeological systems, while the influence of dissolved solids concentration on density is of major importance in comparison to the influence of temperature (Oude Essink, 2001) (Figure 1).

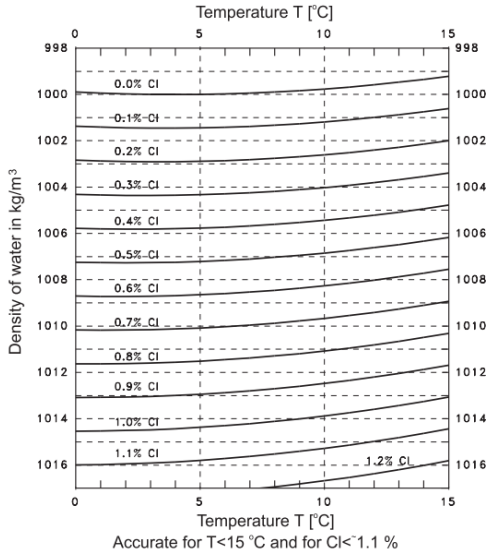

Figure 1: Density of water as a function of the chlorinity and temperature (Oude Essink, 2001).

This indicated that the groundwater density is generally only related to the dissolved solids concentration in groundwater. The temperature is assumed as constant.

The salinity or total dissolved solids (TDS) is used to assess the quality of groundwater. The concentration of dissolved solids is composed of anions and cations (Oude Essink, 2001). For coastal groundwater, chloride (Cl-) is the predominant cation so it is considered that its distribution represents the distribution of all dissolved solids.

Stuyfzand (1993) presented a classification of fresh, brackish and saline groundwater based on chloride concentrations, however other classifications are also possible as the definition for fresh groundwater depends on its application.

Table 1: Classification into eight main types of fresh, brackish or saline groundwater depending on the basis of chloride concentration, after Stuyfzand (1993) (Oude Essink, 2001).

Main type of groundwater	**Chloride concentration (mg Cl^-/l)**
Oligohaline	0 - 5
Oligohaline-fresh	5 - 30
Fresh	30 - 150
Fresh-brackish	150 - 300
Brackish	300 - 1 000
Brackish-saline	1 000 - 10 000
Saline	10 000 - 20 000
Hyperhaline or brine	≥ 20 000

2.1.2 Fresh-saline interface

The density differences influence the groundwater system, by affecting the piezometric heads. This occurs in coastal aquifers, however, many times only fresh groundwater in considered in the

evaluations. The interface approximation based on the Badon Ghijben- Herzberg principle is a straightforward concept which considers density flow in a simple way.

The Badon Ghijben- Herzberg principle describes the location of a fresh and saline groundwater interface. This is represented by the relationship in Equation 1 (Oude Essink, 2001):

Pressure saline groundwater = Pressure fresh groundwater

$$h = \frac{\rho_s - \rho_f}{\rho_f} H \leftrightarrow h = \alpha H$$

Equation 1

Where:

- h = piezometric head of with respect to mean sea level (L),
- H = depth of the fresh–salt interface below mean sea level (L),
- ρ_f = reference density, usually the density of fresh water without dissolved solids (M/L^3),
- ρ_s = density of saline groundwater (M/L^3) and
- $\alpha = \frac{\rho_s - \rho_f}{\rho_f}$ the relative density difference (dimensionless).

For ρ_s=1025 kg/m^3 and ρ_f=1000 kg/m^3, the relative density difference α = 0.025.

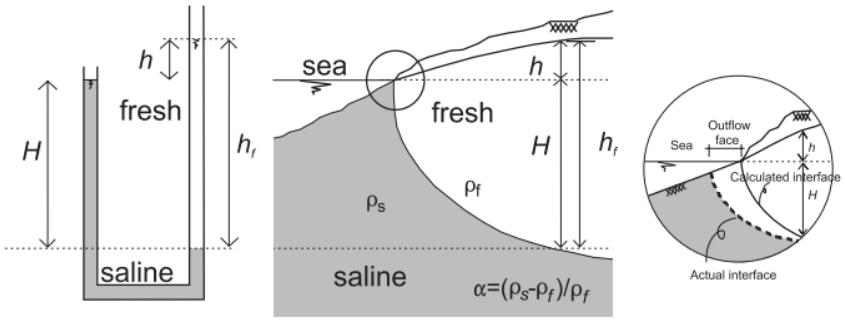

Figure 2: The Badon Ghijben-Herzberg principle: a fresh-salt interface in an unconfined coastal aquifer (Oude Essink, 2001).

This equation considers that in the freshwater zone there is only horizontal flow and the saline water is stagnant. The principle also considers that the transition zone between fresh and saline groundwater is only a small percentage of the thickness of the saturated freshwater body. This occurs in unspoiled sand-dune areas or (coral)islands. Also, it can only be applied if the vertical flow component in the freshwater body is negligible. However, systems are not in hydrostatic conditions most of the time, so the formula can lead to small errors mostly in the vicinity of the outflow zone. This is a good approximation of the reality, nonetheless.

The conditions required to apply this principle are the following:

- Homogeneous aquifer
- The hydrodynamic dispersion is negligible
- Only vertical flow in the aquitard
- Only horizontal flow in the aquifer
- Saline groundwater is at rest

2.2 Saltwater intrusion investigations

There are still important gaps in knowledge related to the saltwater intrusion investigations, such as the difficulties in the prediction of how the seawater intrusion extent will vary depending on changes in management at basin scale. Even though there are recent advances in modelling codes for this purpose, there is still uncertainty in the prediction capabilities due to the large data requirements needed (Werner, 2009).

Numerical models need reliable and enough data to prove its predictive capability, accuracy and reliability; however, in many cases this is scarce. For example, geohydrologic information is mostly obtained from a point or line source and it has to be extrapolated/interpolated. Furthermore, the calibration of variable-density groundwater models requires long time series of monitored salinities since the groundwater flow and the transport of constituents is a slow process. This, it is often recommended to intensify the collection and analysis of reliable groundwater data, which includes subsoil parameters, solute concentrations and piezometric levels (Oude Essink & Boekelman, 1996).

Because of these disadvantages, Morgan & Werner (2015) specified that methods that rely on limited information are needed for a national overview of SWI (for the particular case of Australia), since SWI is a complex process that makes this assessment relatively difficult and expensive.

2.3 Methods to estimate and evaluate saltwater intrusion

A characteristic of saltwater intrusion models is the variation of density due to the difference in salinity between seawater and freshwater, which causes an important impact even though this variation is only 2.5% (Werner, Bakker, et al., 2012). The authors also mention that there are two types of flow models for the simulation of seawater intrusion:

- Interface models: Based on the interface assumption. Freshwater and saltwater considered as two immiscible fluids which are separated by an interface.
- Variable-density models: Solved using numerical solutions. Transition zone between freshwater and saltwater has a finite thickness and density of water is not constant.

Werner (2017) indicates that in the case of simple coastal aquifer situations where a fresh-saline interface, under steady-state and homogeneous conditions occurs, analytical methods can be applied. However, these are not suitable for transient problems where freshwater and seawater are in movement. In addition, he indicated that the understanding of SWI is mainly focused on steady-state models, while general research about transient SWI has been underdeveloped.

In cases where the transition zone between fresh and saline groundwater is influenced by the circulation of brackish groundwater due to inflow of saline groundwater, tidal regime and human activities, it is required to use distributed numerical models that consider variable densities (Oude Essink & Boekelman, 1996).

2.3.1 Analytical solution

This methodology is presented in the article "Vulnerability Indicators of Sea Water Intrusion" (Werner, Ward, et al., 2012) and it is based on the analytical solution developed by Strack (1976, 1989) for the calculation of the steady-state extent of the freshwater-saltwater interface.

The parameters considered in this conceptualization and can be seen in Figure 3 are described as follows:

- W_{net} = Distributed net recharge, which includes the effect of infiltration, evapotranspiration and distributed pumping (L/T),
- q_b = Lateral flow exchange with aquifers landward of the inland boundary (L^2/T),
- q_0 = Discharge to the sea (L^2/T),
- z = Depth of the interface (L),
- z_0 = Horizontal base of the aquifer below sea level (L),
- h = Thickness of fresh water (L),
- x_T = Location of the salt water wedge toe (L),
- h_f = hydraulic head (L) by the Badon Ghijben-Herzberg relation $z = h_f/\delta$ (Badon Ghijben 1888, Herzberg 1901),
- δ = dimensionless density term $\delta = (\rho_s - \rho_f)/\rho_f$,
- ρ_s = sea water density (M/L^3),
- ρ_f = fresh water density (M/L^3).

Likewise, the conceptualization considers two zones: (1) Zone 1, where there is only fresh water and complies with the condition $x \geq x_T$; and (2) Zone 2, which contains both fresh and salt water and $0 \leq x < x_T$.

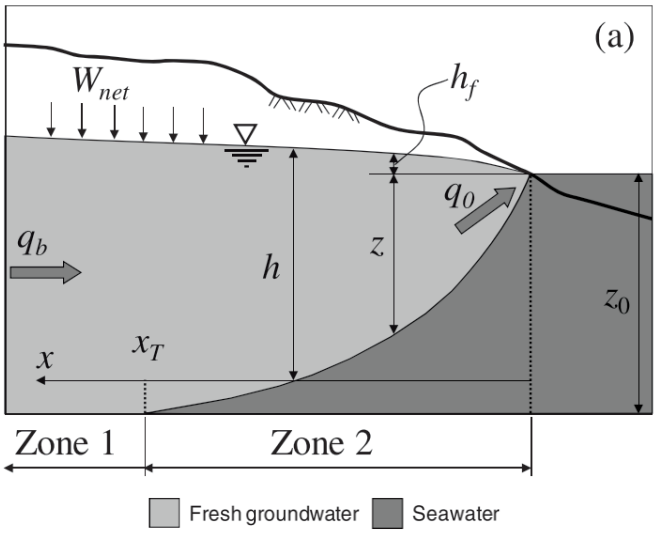

Figure 3: Conceptualization of a steady-state sharp-interface: (a) unconfined aquifer setting (Werner, Ward, et al., 2012)

This methodology is based on the use of mathematical equations for the calculation of the different vulnerability parameters. The equations that define the steady-state sharp-interface in an unconfined aquifer will be presented as follows.

The hydraulic head for an unconfined aquifer, using the method of Strack (1976) and under the conditions in Figure 3:

For Zone 2: $x \leq x_T$

$$hf = \sqrt{\left(\frac{\rho_s - \rho_f}{\rho_s}\right)\frac{2q_0x - W_{net}x^2}{K}}$$

Equation 2

For Zone 1: $x \geq x_T$

$$hf = \sqrt{\frac{2q_0x - W_{net}x^2}{K} + \left(\frac{\rho_s}{\rho_f}\right)z_0^2} - z_0$$

Equation 3

Being K the hydraulic conductivity (L/T).

These equations can be re-arranged to estimate q_0 for a given h_b.

For Zone 1:

$$q_0 = \frac{K((h_b + z_0)^2 - (1+\delta)z_0^2) + W_{net}x_b^2}{2x_b}$$

Equation 4

For Zone 2:

$$q_0 = \left(\frac{1+\delta}{\delta}\right)\frac{K}{2x_b}h_b^2 + \frac{W_{net}x_b}{2}$$

Equation 5

Being h_b the head level at the inland boundary condition (L) and x_b the distance of the inland boundary from the coastal boundary (L).

Knowing that $hf = \delta z_0$ at the wedge toe, the equation for the calculation of the toe position is (Cheng and Ouazar, 1999) (Equation 6):

$$x_T = \frac{q_0}{W_{net}} - \sqrt{\left(\frac{q_0}{W_{net}}\right)^2 - \frac{K\delta(1+\delta)z_0^2}{W_{net}}} \; (W_{net} > 0)$$

Equation 6

The volume of sea water (V_{sw}) in an aquifer is important in water resources management and to assess SWI. Equation 7 presents the calculation of this parameter in an unconfined aquifer:

$$V_{SW} = \varphi z_0 \left(x_T - \frac{x_n}{2} \left(\sqrt{\frac{1}{M}}\, arcsin\left(\sqrt{M}\right) - \sqrt{1-M} \right) \right)$$

Equation 7

Where φ is porosity and M is the mixed convection ratio, calculated using Equation 8:

$$M = \frac{K\delta(1+\delta)z_0^2}{W_{net}x_n^2}$$

Equation 8

This methodology considers simplification assumptions and does not make it possible to consider time scales since it is a steady-state analysis, allowing only for simple estimates of the extent of the interface and its variations. However, it is possible to use it to rank coastal aquifers regarding their vulnerability to SWI; on top, it is useful in cases where the existing data is scarce while also the investigative resources are limited.

This mathematical approach has some limitations, due to the simplification of the conceptual system and assumptions in the analytical model. These are presented as follows (Morgan, Werner, Ivkovic, et al., 2013):

- There is a sharp interface between fresh and sea water.
- Aquifers are evaluated as cross sections, and its characteristics are vertically integrated.
- Transient conditions are not considered. It presents long-term situation and not a current status in case of aquifers that have not reached steady-state (equilibrium conditions) yet.
- No recharge variation: low precipitation periods combined with increase of extraction could increase SWI.
- No influence of wells; they are not direct part of the methods, no upconing effect of specific well.
- Recharge is evenly distributed along the aquifer section.
- Fixed coastal boundary: it could vary, for example, in flat areas were sea-level rise could cause intrusion of saline water from the ocean.
- Only horizontal flow of fresh groundwater is considered.
- No head losses in the saltwater zone are considered.
- No heterogeneity. In reality, the interface location varies within an aquifer, due to the spatial variability of the aquifer conditions. Here it is assumed that these are homogeneous, isotropic and geometrically uniform.
- No offshore freshwater discharge, assumes that freshwater discharges at the coast (aquifer ends at the coastline)
- A constant coastal boundary is assumed, so no effect of tidal impacts,
- Management and knowledge of the system, along with elements such as population growth and supplementary supplies of freshwater are not part of the method.

2.3.2 Variable-density groundwater and coupled salt transport modelling

a) Groundwater flow equation

MODFLOW is a finite-difference groundwater model developed by the United States Geological Survey (USGS). To represent the three-dimensional movement of groundwater of constant density through porous earth material, it is described by the following partial-differential equation (Equation 9) (Harbaugh, 2005):

$$\frac{\partial}{\partial x}\left(K_{xx}\frac{\partial h}{\partial x}\right)+\frac{\partial}{\partial y}\left(K_{yy}\frac{\partial h}{\partial y}\right)+\frac{\partial}{\partial z}\left(K_{zz}\frac{\partial h}{\partial z}\right)+W=\ S_s\frac{\partial h}{\partial t}$$

Equation 9

Where:

- K_{xx}, K_{yy}, and K_{zz} = hydraulic conductivity along the x, y, and z coordinate axes, which are assumed to be parallel to the major axes of hydraulic conductivity (L/T);
- h = potentiometric head (L);
- W = volumetric flux per unit volume representing sources and/or sinks of water (T^{-1});
- S_S = specific storage of the porous material (L^{-1});
- t = time (T).

b) Variable density groundwater flow equation.

MODFLOW by itself is not capable of simulating variable density groundwater flow. Because of this, SEAWAT was developed to simulate three-dimensional, variable-density groundwater flow. It is a coupled version of MODFLOW and MT3DMS. This computer program can solve the variable-density groundwater flow equation (Equation 10) (Langevin et al., 2008).

$$\nabla\cdot\left[\rho\frac{\mu_0}{\mu}\mathbf{K_0}\left(\nabla h_0+\frac{\rho-\rho_0}{\rho_0}\nabla z\right)\right]=\rho S_{s,0}\frac{\partial h_0}{\partial t}+\theta\frac{\partial\rho}{\partial C}\frac{\partial C}{\partial t}-\rho_s q'_s$$

Equation 10

Where:

- ρ_0 = fluid density [ML^{-3}] at the reference concentration and reference temperature;
- μ = dynamic viscosity [$ML^{-1}\,T^{-1}$];
- K_0 = hydraulic conductivity tensor of material saturated with the reference fluid [LT^{-1}];
- h_0 = hydraulic head [L] measured in terms of the reference fluid of a specified concentration and temperature (as the reference fluid is commonly freshwater).
- $S_{s,0}$ = specific storage [L^{-1}], defined as the volume of water released from storage per unit volume per unit decline of h0;
- t = time [T];
- θ = porosity [-];
- C = salt concentration [ML^{-3}];
- q'_s = source or sink [T^{-1}] of fluid with density ρ_s.

In addition, SEAWAT can also solve the solute transport equation (Equation 11) (Langevin et al., 2008):

$$\left(1+\frac{\rho_b K_d^k}{\theta}\right)\frac{\partial\left(\theta C^k\right)}{\partial t}=\nabla\cdot\left(\theta\mathbf{D}\cdot\nabla C^k\right)-\nabla\cdot\left(\mathbf{q}C^k\right)-q'_s C_s^k$$

Equation 11

Where:

- ρ_b = bulk density (mass of the solids divided by the total volume) [ML^{-3}],
- K_d^k= distribution coefficient of species k [L^3M^{-1}],
- C^k = concentration of species k [ML^{-3}],
- D = hydrodynamic dispersion coefficient tensor [L^2T^{-1}],
- q = specific discharge [LT^{-1}],
- C_s^k = source or sink concentration [ML^{-3}] of species k.

Equation 12 is a general equation of state for fluid density, which correlates concentration, temperature and pressure (Langevin et al., 2008):

$$\rho=\rho_0\exp\left[\beta_C\left(C-C_0\right)+\beta_T\left(T-T_0\right)+\beta_P\left(P-P_0\right)\right]$$

Equation 12

Where:

- C = concentration [ML^{-3}],
- T = temperature [K],
- P = pressure [$ML^{-1}T^{-2}$].
- β_C,β_T,β_P = Volumetric expansion coefficients for solute concentration, temperature and pressure, respectively. These are calculated as:

$$\beta_C=\frac{1}{\rho}\left(\frac{\partial\rho}{\partial C}\right)_{T,P},\quad \beta_T=\frac{1}{\rho}\left(\frac{\partial\rho}{\partial T}\right)_{C,P},\text{ and }\quad \beta_P=\frac{1}{\rho}\left(\frac{\partial\rho}{\partial P}\right)_{C,T}$$

Equation 13 is the form of the equation of state used in SEAWAT that accounts for the transport of multiple solute species (NS), where the concentration of each of them can affect fluid density (Langevin et al., 2008):

$$\rho=\rho_0+\sum_{k=1}^{NS}\frac{\partial\rho}{\partial C^k}\left(C^k-C_0^k\right)+\frac{\partial\rho}{\partial T}\left(T-T_0\right)+\frac{\partial\rho}{\partial\ell}\left(\ell-\ell_0\right)$$

Equation 13

Where $\frac{\partial\rho}{\partial l}$ can be calculated based on β_P.

c) iMOD-SEAWAT

iMOD-SEAWAT is a modified version of SEAWAT v4.00.05 (Langevin et al., 2008), with changes that make it compatible with iMOD's (Vermeulen et al., 2018) input and output file formats, such as IDF grid files and IPF point files. In addition, it uses a fully keyword driven run-file which is more user-friendly when working with many layers (Verkaik & Janssen, 2015).

Chapter 3 Research method

This chapter presents the research methodology steps that were followed to answer to the research questions. Figure 4 shows a general description of the methodology to have an overview of the steps. In the following sections, these steps will be explained.

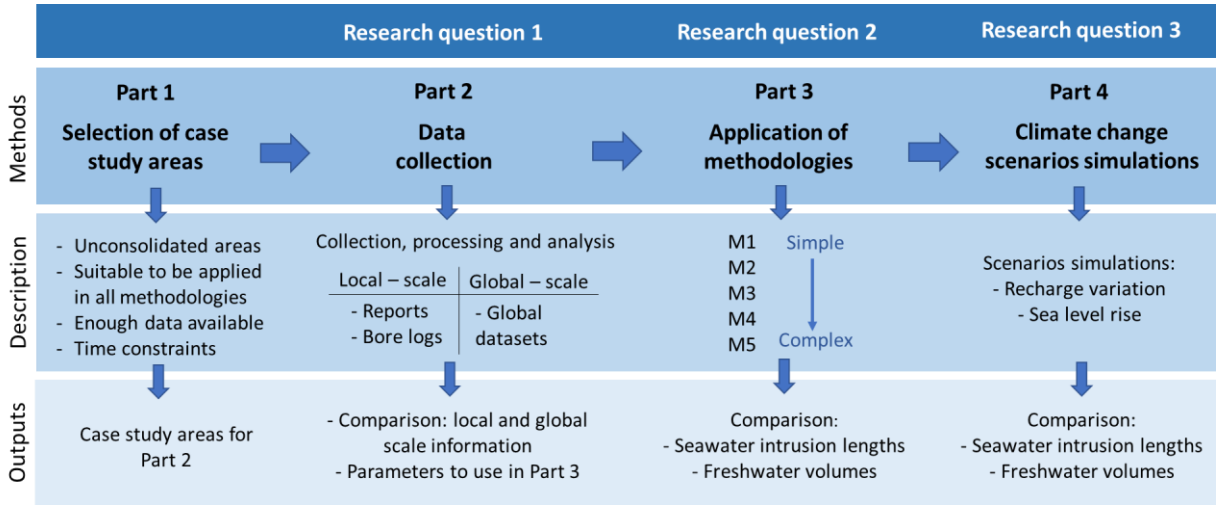

Figure 4: Methodology workflow.

3.1 Selection of case study areas

The main task of this research is being able to compare different approaches to evaluate the freshwater-saltwater distribution in coastal aquifers. To do this, it was necessary to choose an area with enough local information to do the input data comparisons and the calculations and simulations. Australia, known for their current studies related to saltwater intrusion (Morgan, Werner, Ivkovic, et al., 2013), presented the information needed for this purpose. Furthermore, they had already performed an analytical evaluation of the SWI in case study areas in Australian territory.

The project "A national-scale vulnerability assessment of seawater intrusion" (Morgan, Werner, Ivkovic, et al., 2013) was used as the baseline for this analysis. It presents 28 zones at risk of saltwater intrusion, or case study areas (Figure 5). To define the case study areas considered in their analysis, reports and journal papers indicating Australia areas with incidence or threat of seawater intrusion and consultation with stakeholders were considered. These areas are characterized for being exploitable aquifers (for example with salinity less than 3000 Cl^- mg/l and depths of less than 400 m) located within 15 km from the coast. It was also important that these areas would cover different

jurisdictions, geologies and land uses. Also, these zones needed to have enough hydrogeological data available for the mathematical analysis. The data used came from literature (for example, from specific locations previously studied for groundwater development and modelling or prior SWI monitoring) and groundwater databases (Ivkovic, Marshall, et al., 2013; Ivkovic et al., 2012).

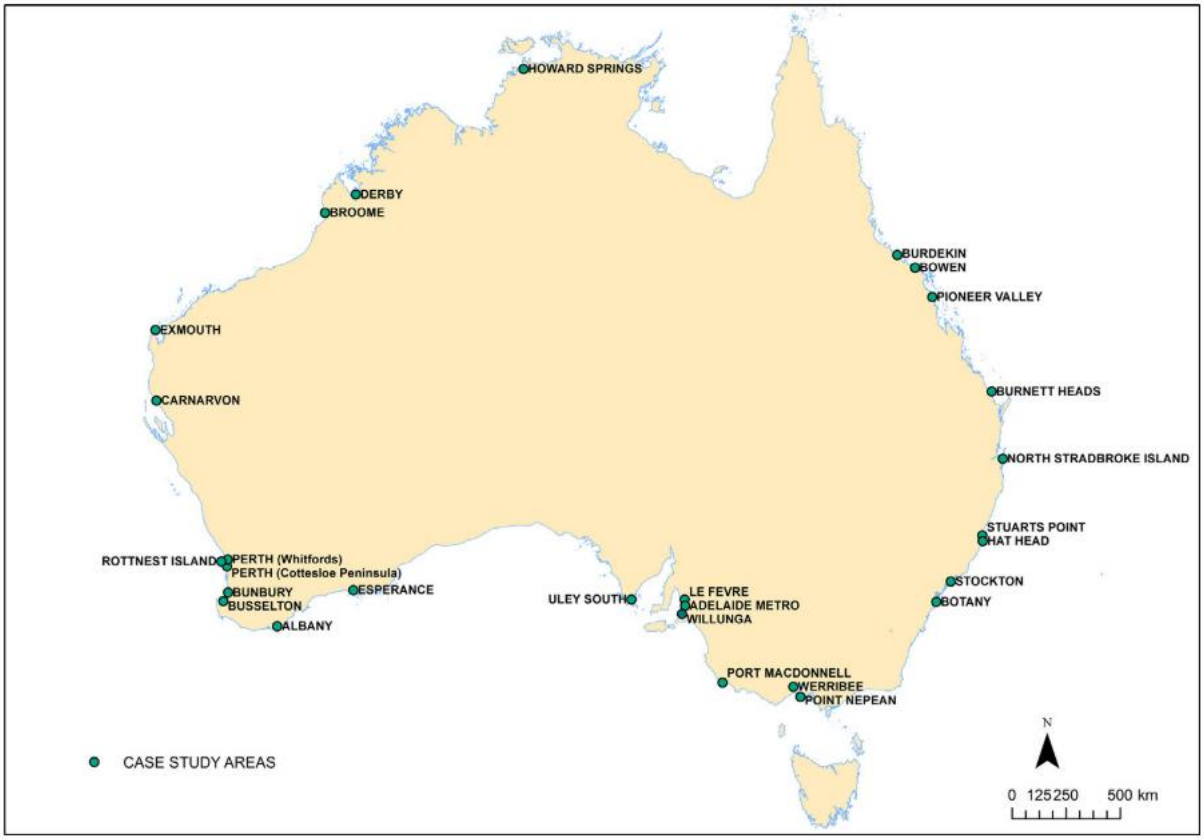

Figure 5: Case study area locations (Morgan & Werner, 2015)

However, some points had to be taken into consideration before applying all the data belonging to these areas into the methodologies. For example, not all 28 case study areas were considered because the interest of this research is only groundwater systems composed of unconsolidated sediments. Another factor considered is if all these areas would be suitable to be applied in all the methodologies, based on the input data requirements and the aquifer characteristics that each of them needed. In addition, the methodologies evaluated contemplated a data collection process for each of them, as well as the amount of calculations and simulations to be performed. These steps consumed a lot of time, so it was also necessary to consider this factor when defining the total number of case study areas.

Firstly, an analysis was performed for all the proposed case study areas to evaluate the geological composition of the groundwater systems, to keep the ones composed only of unconsolidated sediments. This analysis was based on the following information:

1) The report “A national-scale vulnerability assessment of seawater intrusion - Coastal aquifer typology” (Ivkovic, Marshall, et al., 2013)
2) Bore logs information obtained from the Australian Groundwater Explorer website (Australian Government - Bureau of Meteorology, n.d.)

At first, the information from (1) would have been enough for defining these characteristics, however, the information of (2) was also relevant as a supplementary check. Furthermore, the borehole analysis was also used to identify the sediment layers along the profile as well as estimating the depth to bedrock.

After the analysis, it was found that the case study areas that met the criteria were 8, out of 28. For these, it was necessary to check if these had the necessary local-scale information for the simulation. This was found in the several reports that encompass the project “A national-scale vulnerability assessment of seawater intrusion” (Morgan, Werner, Ivkovic, et al., 2013) for the Australian territory. Furthermore, it was defined that time-wise it would be possible to perform the data collection, calculations and simulations for all these case study areas.

Finally, the 8 case study areas chosen for this research are the following:

1) Botany
2) Bowen
3) Burdekin
4) Burnett Heads (Moore Park)
5) Hat Head
6) Pioneer Valley
7) Stockton
8) Stuarts Point

Detailed information about the characteristics of the areas can be found in Appendix A. Its location is presented in Figure 6.

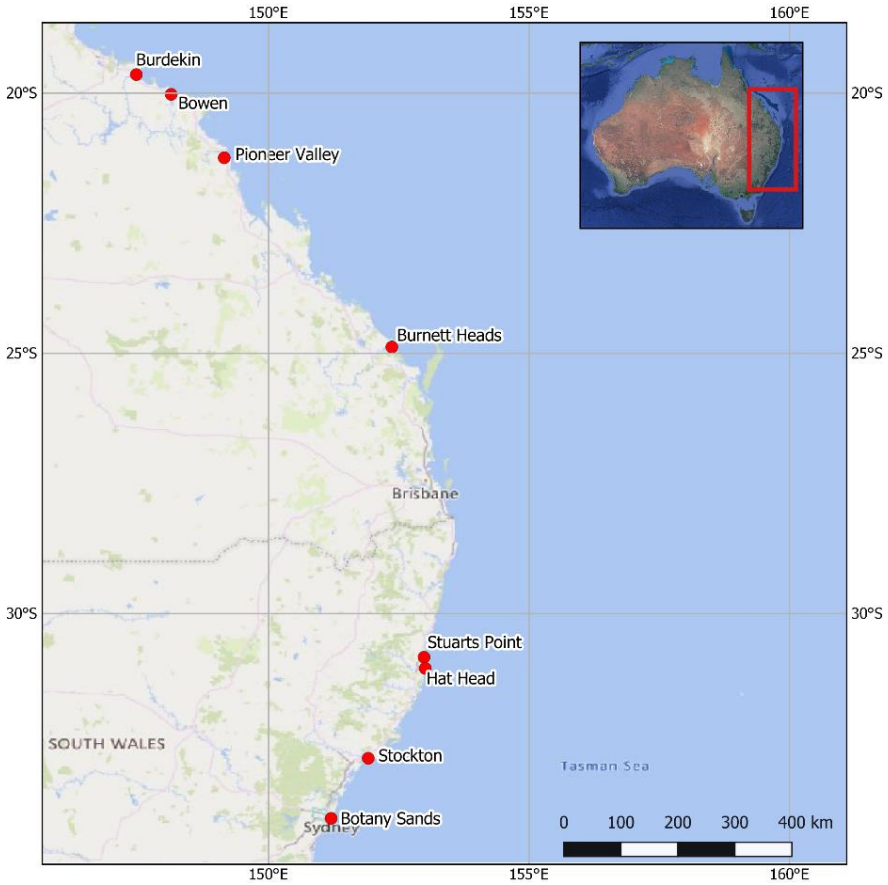

Figure 6: Location of case study areas (WGS 84 coordinate system)

The list of bore logs analysed as well as a synthesis of the type of sediments found in each of them can be found in Appendix B.

3.2 Data collection: local-scale and global-scale information sources

This step of the methodology is related to the first research question, which aims to assess the differences in the local-scale and global-scale information sources to be used as input in the simulations for the determination of the freshwater-saltwater interface in coastal aquifers. This provided a first look at how these could possibly be influencing the results of the saline water intrusion calculations and simulations when using them as input data. In order to do this, the steps followed were collection, processing and analysis of the data.

The sources considered in this research are (1) reported hydrogeological data by the Australian government (Morgan, Werner, Ivkovic, et al., 2013) and (2) global datasets obtained from freely available sources. Details and characteristics of each of these sources are presented in the following sections.

3.2.1 Local-scale data

a) Data from reports

As mentioned in Chapter 2, case study areas which are under saltwater intrusion threat have been defined for Australia. Detailed information for each of them was compiled in the several reports which are part of the project "A national-scale vulnerability assessment of seawater intrusion" (Morgan, Werner, Ivkovic, et al., 2013). The data presented in these reports comes from publicly available reports, journal articles, documents and presentations provided by the Australian states and territories. The main sources from this project used in this research are:

1. First-order assessment of seawater intrusion for Australian case study (Morgan, Werner, Ivkovic, et al., 2013)
2. Coastal aquifer typology (Ivkovic, Marshall, et al., 2013)
3. Literature review, data review, and method development (Ivkovic, Dixon-Jain, et al., 2013)

From these sources, the main information related to the aquifer characteristics and climatic parameters which are relevant for the calculation of the freshwater-saltwater distribution was extracted. The parameters collected from this source which are required for the calculations are:

- K (m/d) = Hydraulic conductivity
- W_{net} (m/d) = Net recharge (accounting for infiltration, evapotranspiration and distributed pumping)
- z_0 (m) = Base of the aquifer below sea level
- x_b (m) = Distance of the inland boundary from the coastal boundary
- h_b (m) = Head level at the inland boundary condition x_b
- n (-) = Porosity

b) Bore logs interpretation

An important task of this research was to analyse the bore logs information obtained from the Australian Groundwater Explorer website (Australian Government - Bureau of Meteorology, n.d.). It was not only used as an additional verification to select the case study areas, but it also provided information about the aquifer layers present in the groundwater system and it helped with the understanding of the simplifications done to the aquifer characterisation in the local-scale data reports.

The Australian Groundwater Explorer website provides information in csv format that contains the bore logs identification numbers and the corresponding sediments found at different depths. These depths did not follow a constant spacing, making the comparison between boreholes more complex. Due to this reason, a Python script was developed to obtain data description every meter. For each case study area, the deepest boreholes were selected and, using the results from the Python script, the information was compared at each of the depths among the different boreholes. For each depth, the most common sediment type was considered, obtaining an average bore geology for each area.

As well, from the bore logs interpretation, it was possible to extract the information related to the depth to the basement rock, which was correlated to the depth to the aquifer base from mean sea level.

3.2.2 Global-scale data

The use of global datasets in groundwater evaluations is important due to the current lack of measured and accurate data in many parts of the world. Also, considering that these are freely available, these are an interesting option in areas where there are no resources available for field campaigns or installation of measurement devices. Still, it is important to assess the accuracy of this data and evaluate if it can accurately represent climatic and aquifer characteristics on a smaller local scale.

This section presents the global datasets used in this evaluation, which will be used for comparison with the local-scale information and for the saline water intrusion assessment. Most of the global datasets used for the global-scale analysis were the same considered by Zamrsky (2019) in his PhD research to perform a rapid coastal groundwater modelling based on global data. This approach is one of the methodologies in evaluation, to keep a consistency in the analysis.

a) Hydraulic conductivity

The hydraulic conductivity information came from the GLHYMPS 2.0 global dataset (Huscroft et al., 2018b). Hydraulic conductivity information can be obtained based on the information from "Compiling and Mapping Global Permeability of the Unconsolidated and Consolidated Earth: GLobal HYdrogeology MaPS 2.0 (GLHYMPS 2.0)" (Huscroft et al., 2018b). This research presents a global, two-layer map of shallower and deeper permeability values based on geological mapping. This new dataset has improved the previous GLHYMPS datasets (Gleeson et al., 2014), by coupling it with the Global Unconsolidated Map (GUM) (Börker et al., 2018) and depth to bedrock information from SoilGrids (Shangguan et al., 2017) (Figure 7).

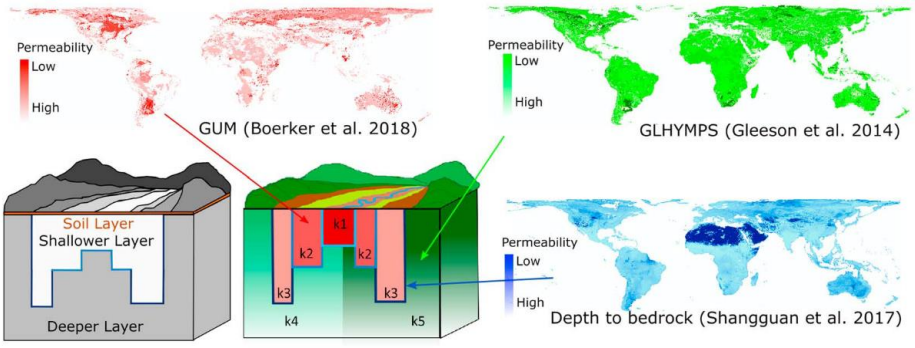

Figure 7: The structure of GLobal HYdrogeology MaPS 2.0. (Huscroft et al., 2018b)

Note: Surficial materials representative of Global Unconsolidated Map (GUM, red), near-surface materials taken from GLobal HYdrogeology MaPS outside of GUM coverage areas (green), and GUM surface layer thickness taken from SoilGrids depth to bedrock map in (blue).

In GLHYMPS, this dataset compiled permeability for major rock types and paired it with the Global Lithological Map (GLiM) (Hartmann & Moosdorf, 2012). GLiM has the limitation of not having a detailed refinement of unconsolidated sediment types and some areas there are no surface sediments on top of deeper lithological units. In parallel, GUM database (Börker et al., 2018) addresses this concern by increasing the unconsolidated sediment land area coverage, however, there is still remaining uncovered land area due to lack of accessible data or the exclusion of mapped consolidated surface sediments. The information provided by GUM is sediment type, sediment subtype and grain size (if available), which is used by Huscroft et al. (2018b) to develop a permeability classification system. This was done through a literature compilation, using textbooks, field data from hydraulic tests and calibrated groundwater models as sources. After the analysis, it was determined that the permeability compilation would focus on grain sizes, since most sediment types represent a mixture of these (Huscroft et al., 2018b).

GUM only covers 55% of the global land surface, so in the areas where GUM was not mapped, GLHYMPS data was directly assigned in these cases. For the GUM polygons with grain size information, this was used to pair it with permeability values. However, in 68% of the GUM polygons there is no grain size information available, so the permeability had to be paired to sediment subtype and or sediment type (Huscroft et al., 2018b). Figure 8 shows a map representing the final permeability values.

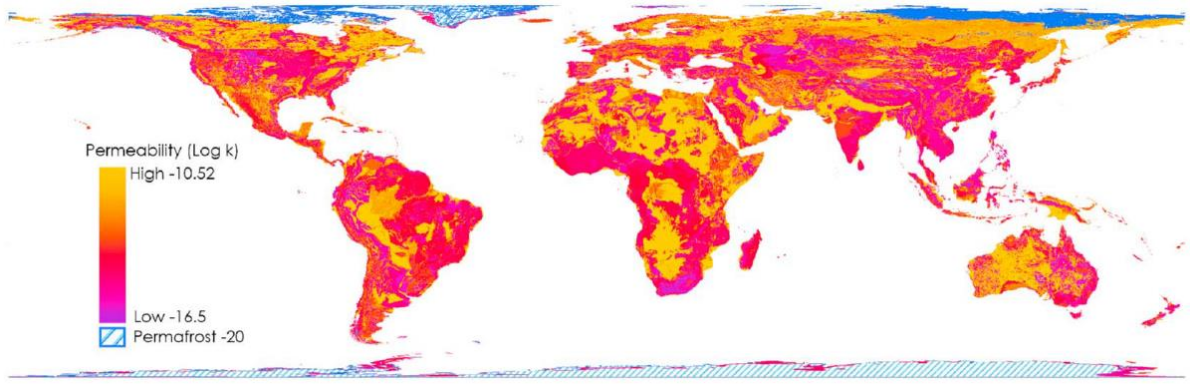

Figure 8: New representation of high-resolution surficial unconsolidated sediments and associated global permeability, GLobal HYdrogeology MaPS 2.0. Permafrost areas included and with assumed log(k)= -20. (Huscroft et al., 2018b)

The GLHYPMS 2.0 data set provides permeability (κ) represented as log(k)*100 or log permeability*100 so that it is an integer. The following formula (Huscroft, Gleeson, Hartmann, & Börker, 2018a) is used to convert the permeability values into hydraulic conductivity values, which were the ones needed for the simulations. Therefore,

$$\kappa = 10^{\kappa/100}$$

Equation 14

And, to obtain hydraulic conductivity:

$$K = \frac{\kappa \rho g}{\mu}$$

Equation 15

Where:

- *K* (m/s) is hydraulic conductivity which is dependent on fluid viscosity and density
- ρ (kg/m^3) is the density of the fluid, normally water = 999.97 kg/m^3
- g (m/s^2) is the acceleration due to gravity = 9.81 m/s^2
- μ (kg/m.s or Pa.s) is the viscosity of the fluid, normally water = 1e^{-3}

This information came in a shapefile format, so it was spatially distributed and most of the case study areas presented more than one hydraulic conductivity value inside their limits. To define which value to use, it was considered to keep the values that were located closer to the coast, as they would be the most relevant for the SWI analysis. At the same time, it was seen that the higher hydraulic conductivity values were also the ones found near the coastline. Nonetheless, this simplification of selecting only one hydraulic conductivity value may not be accurate enough since details of the geology that may affect the groundwater flow movement could be omitted.

In the case of the local-scale data, the Australian reports presented only a single hydraulic conductivity value for each case study area, as a way of simplification of the system. Because of this, the selection from the global-scale datasets also had to follow a simplification, however, the use of this simplification depended on the methodology in evaluation.

b) Recharge

The recharge calculation is based on precipitation and evapotranspiration values from MODIS (NTSG, n.d.). These datasets were also used by Zamrsky (2019) for the same purpose, so the final raster was provided by the author to be used in this evaluation, and also keep a level of consistency in the analysis.

The base datasets have a resolution of 1 km and cover the whole world. These are Long-term MODIS estimated ET (mm/y) and Long-term estimated Precipitation (mm/y). To calculate the recharge values based on this information, Equation 16 was used:

$$RCH = (P - (ET * 0.1)) / 365.25$$

Equation 16

Where,

- RCH = Recharge (mm/d)
- P = Precipitation (mm/y)
- ET = Evapotranspiration (mm/y)
- 0.1 = Multiplication factor mentioned in (NTSG, n.d.)

A final raster of recharge was obtained from this calculation. As it is only calculated as the difference between the precipitation and evapotranspiration, this global recharge does not account for the effects of pumping or irrigation or other specific processes affecting the recharge in the area in evaluation.

From the result raster, an average recharge value for each case study area is needed. By using the GDAL batch mode in Python, first the raster was resampled to have a better representation of the dataset, and then cropped to the boundary limits of each area defined by a corresponding shapefile. After this, the GetStatistics tool was applied to obtain an average recharge value for each of the areas.

c) Depth to aquifer base from mean sea level

This information is related to the unconsolidated aquifer thickness estimation as presented in the article "Estimating the thickness of unconsolidated coastal aquifers along the global coastline" (Zamrsky et al., 2018). This peer-reviewed article presents profiles along the global coastline, where an average aquifer thickness in meters above sea level (m a.s.l.) is presented for each of them (see for an example, Figure 9). In some of the areas, more than one profile was present, so only the most representative ones were selected, and an average thickness was calculated.

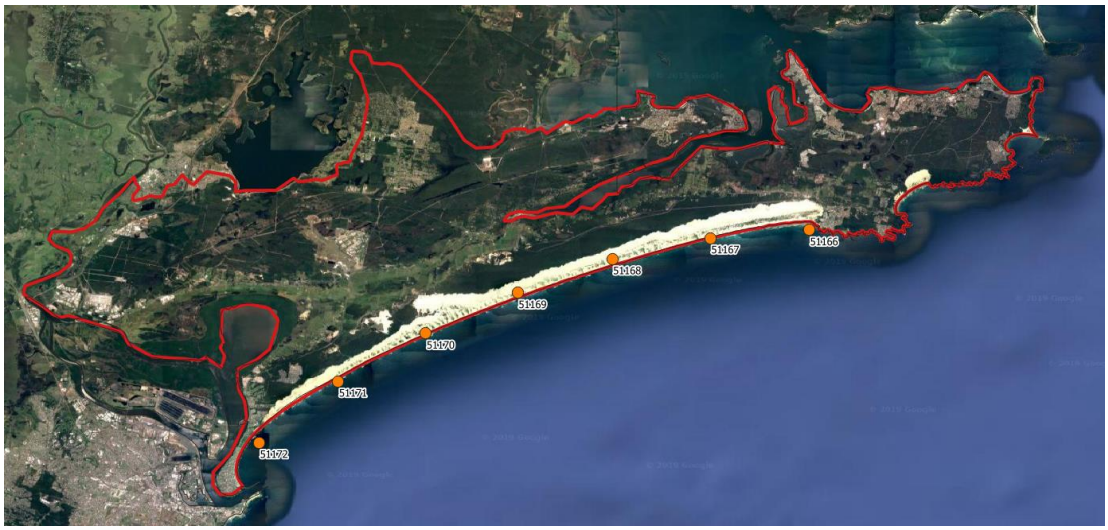

Figure 9: Example of Stockton, Australia – Location of points where aquifer thickness is estimated.
Note: Labels represent the id_cs, which is the cross-section identification number according to Zamrsky et al. (2018)

The research "Estimating the thickness of unconsolidated coastal aquifers along the global coastline" (Zamrsky et al., 2018) provides values of unconsolidated aquifer thickness on a global scale. It is focused in aquifer systems formed by unconsolidated sediments, based on the GLiM (Hartmann & Moosdorf, 2012) dataset, along the global coastline. By combining topographical and lithological information, a methodology was developed to find the topographical slope of outcropping bedrock formations and the coastal plain extent.

This method uses already available open-source global datasets that provide the following information:

Table 2: Summary of the global datasets used for aquifer thickness estimation (Zamrsky et al., 2018)

Dataset name	Description	Resolution	Reference
GEBCO 2014	Global topography and bathymetry	30 arcsec	Weatherall et al. (2015)
Average soil and sedimentary deposit thickness	A gridded global dataset of soil, intact regolith, and sedimentary deposit thicknesses for regional and global land surface modelling; max. estimated depth is 50 m.	30 arcsec	Pelletier et al. (2016)
PCR-GLOBWB	Thickness of the groundwater layer from the global model (5 arcmin)	5 arcmin	de Graaf et al. (2015)
GLiM	Global Lithological Map – Rock types of the Earth surface (16 basic classes), more than 1 200 000 polygons	vector	Hartmann and Moosdorf (2012)
Natural Earth coastline	Global coastline	vector	Natural Earth (2017)

To represent the coastal zones, cross sections placed every 5 km and perpendicular to the coastline are considered. They span 200 km inland and offshore to obtain the topographical and bathymetrical information. These cross sections have a set of points every 0.5 km from where the global information is extracted.

Based on the global datasets in Table 2, the coastal plain extent was determined and, afterwards, four estimation techniques plus a first and second-order curve fitting for each were used to estimate the bedrock slope. Based on the resulting points, the mean, minimum and maximum aquifer thickness is estimated (Figure 10).

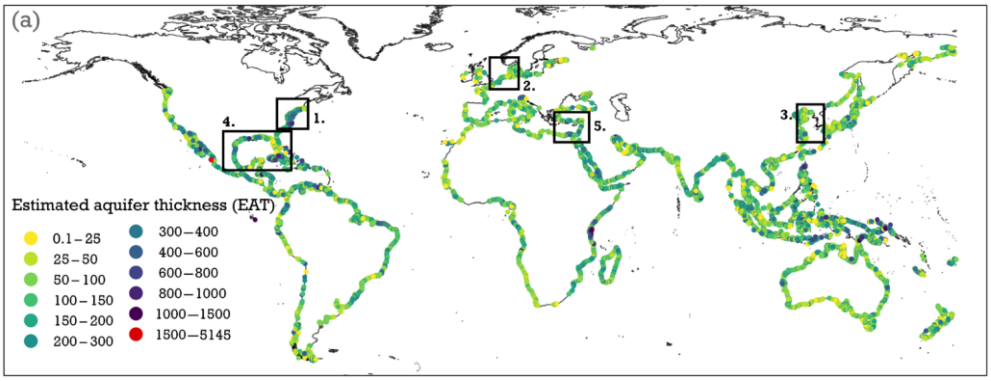

Figure 10: Global map of EAT (estimated aquifer thickness) at the coastline (Zamrsky et al., 2018).
Note: Minimum and maximum values not displayed in the figure.

d) Distance to the inland boundary condition and head level

The inland boundary head (h_b) is described as the groundwater level that remains constant regardless of a change in sea level, and it's located at a distance x_b (Werner, Ward, et al., 2012). In the case of

these two parameters, there was no global dataset available which could directly provide their corresponding values. Because of this limitation, they were inferred from the GEBCO dataset for topography (and bathymetry) (Weatherall et al., 2015) and the global water table depth estimated by Fan, et al. (2013).

GEBCO is the General Bathymetric Chart of the Oceans (Weatherall et al., 2015). This dataset merges a digital bathymetric model of the world ocean floor with land topography from digital elevation models freely available to the public. The GEBCO_2014 grid, it is the update version of GEBCO_08. Its grid spacing is 30 arc sec and includes information from sources such as The Australian Bathymetry and Topography Grid. Figure 11 shows a worldwide image of the values from GEBCO_2014.

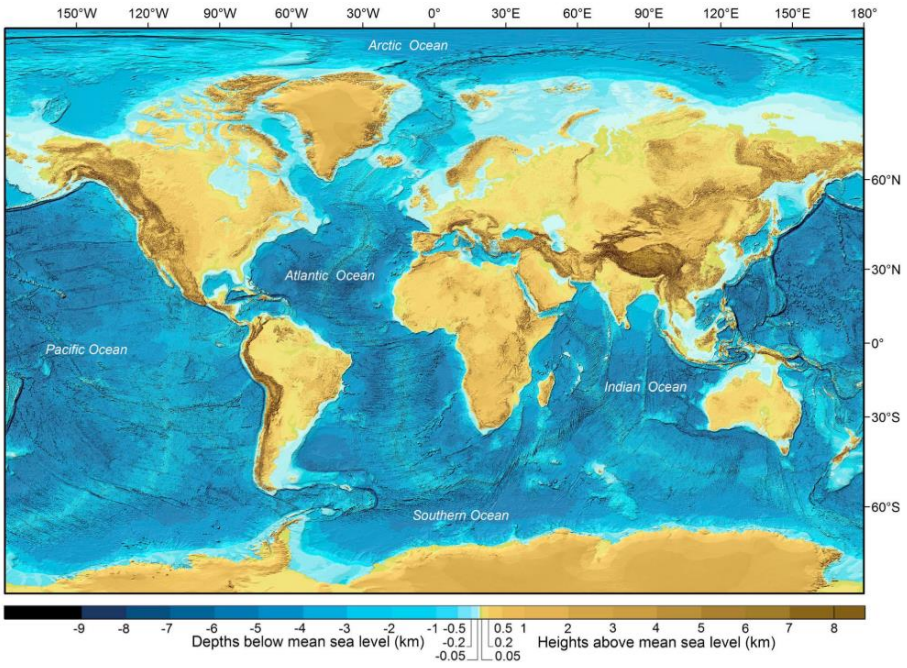

Figure 11: GEBCO_2014 grid (Weatherall et al., 2015).
Note: The colors denote ocean floor (blues) and land (browns)

The research ”Global patterns of groundwater table depth” (Fan et al., 2013) presents a dataset of global observations of water table depth based on data compiled from governmental sources and literature. In the areas where data gaps were found, these were filled in by using a groundwater model considering the influences of modern climate, terrain and sea level. This provided a global-scale simulation of the water table depth (m) (which are constrained by observations) at 30 arc-sec grid (~1 km).

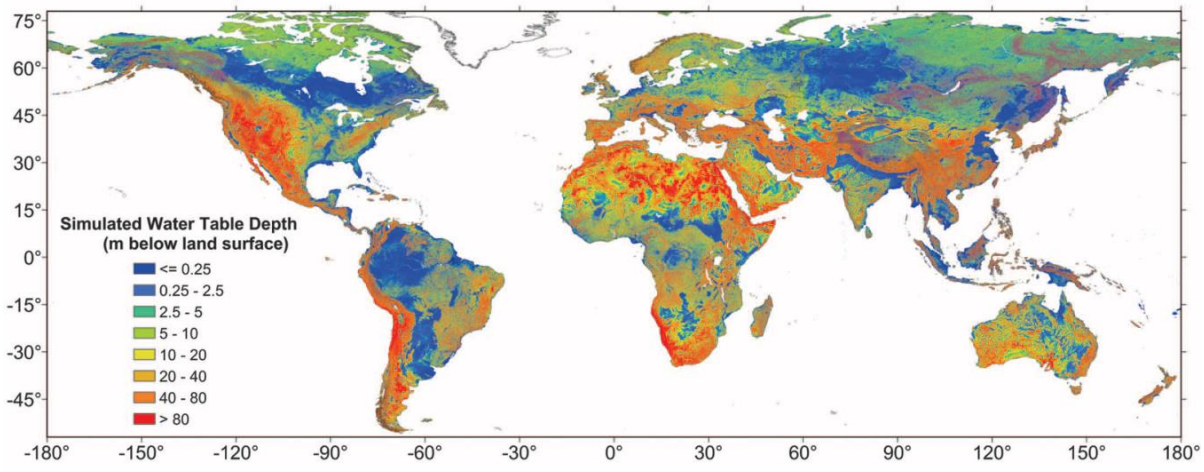

Figure 12: Simulated water table depth (m) at 30-arc-sec grid (~1 km) (Fan et al., 2013).

To estimate the parameters, firstly, the shapefiles that delimitate to the case study areas were overlapped with the locations of cross sections defined by Zamrsky (2018) in his analysis of aquifer thickness estimation. These sections are located equidistantly every 5 km along the coastline and each of them have a set of points every 500 m along the cross section. For each case study area, representative cross sections were kept and considered for the analysis.

It was assumed that the x_b parameter would be located at a point with a high elevation, similar to a water divide. At each of the cross-section points, the topography value was obtained from GEBCO (the grid version used in this research is GEBCO_2014) and the x_b location was measured (Figure 13). Consequently, the inland boundary head (h_b) would have to be determined at the same location. This was calculated as the difference between the topography at this point and the distance to the water table from the global datasets (Fan et al., 2013). Out of all the x_b and h_b values obtained for several cross section in a same case study area, they were averaged to obtain one value.

Figure 13: Example of Stockton, Australia – Cross-section points (Background: GEBCO dataset)

e) Porosity

For this parameter, there was no global dataset available that defined this parameter. In consequence, based on the porosity values indicated in the "A national-scale vulnerability assessment of seawater intrusion" reports, an average value equal to 0.25 was assumed for all the case study areas.

3.3 Application of methodologies for the estimation of the saltwater intrusion

This part of the research aimed to assess if it is possible to represent the freshwater-saltwater distribution using the previously gathered local-scale and global-scale data. Five different methodologies were tested to evaluate how these simulate the saltwater intrusion for the case study areas in consideration.

The methodologies considered are presented in the following sections from the simpler to the more complex procedures. However, this is not necessarily linked to the accuracy of the results that each of them can provide. For simplification, when referring to them in the text, the methodologies will be numbered from 1 to 5, and labelled as M1, M2, etc.

Firstly, each of the individual methodologies were assessed for local and global-scale data (where applicable). The parameters considered are the wedge toe location and the freshwater volume available. After gaining this first insight, a full comparison of the results obtained from all the methodologies was later done.

3.3.1 Methodology 1 (M1): Analytical solution

It is based on the methods presented by Werner et al. (2012), as previously described in Chapter 2.

This approach is the first methodology in evaluation because it is an analytical approach where direct formulas are applied, considering it to be a simple tool to use without the requirement of modelling knowledge tools. A Python script was developed to ease the insertion of the input data and the calculations.

For each of the 8 case study areas, the local-scale data and the global datasets information were used as input in this methodology obtaining a total of 16 calculations.

The parameters needed were the net recharge (W_{net}), hydraulic conductivity (K), horizontal base of the aquifer below sea level (z_0), distance of the inland boundary from the coastal boundary (x_b), the freshwater head at the inland boundary (h_b) and porosity (n) (Figure 14).

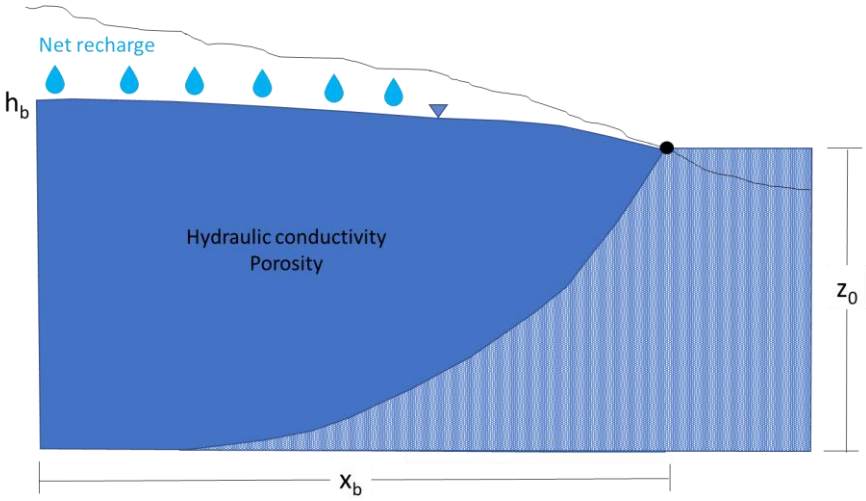

Figure 14: Conceptualization of Methodology 1 (M1)

3.3.2 Methodology 2 (M2): Henry case conceptualisation modelling

Model testing encompasses the verification of problems for which analytical solutions exist. The Henry problem has an analytical solution for density groundwater flow in combination with hydrodynamic dispersion. This case is used as a benchmark for codes that simulate density-driven groundwater flow. This problem was formulated in 1964 and represents a hypothetical rectangular coastal aquifer in Biscayne aquifer (Florida, U.S.A.) where saline water intrusion occurs in a homogeneous, isotropic, confined, rectangular aquifer, including dispersion (Oude Essink, 2001).

Figure 15 shows the boundary conditions for Henry's problem. A constant flux (Q) of fresh water enters the aquifer on the left side, along the whole depth, while on the right side, there is a constant saltwater head condition. The upper and lower boundaries are impermeable, so there is no flux along them (Oude Essink, 2001). In this case, the constant flux was specified by using a constant head along the left-side boundary. There is no anisotropy and the specific storativity is equal to zero.

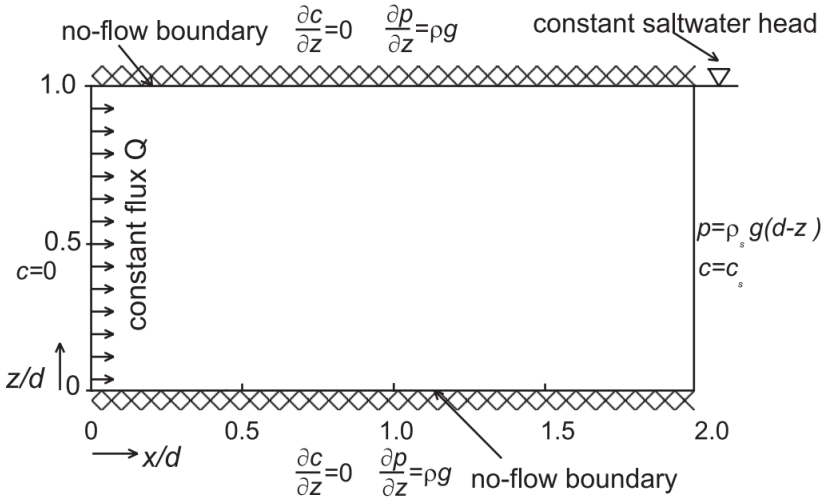

Figure 15: Henry's problem (1964): saline water intrudes in a hypothetical rectangular aquifer and merges by a constant dispersion coefficient (Oude Essink, 2001)

The original conceptualization considers certain relations associated to the aspect ratio, the net fresh water discharge related to the hydraulic conductivity and the aquifer height, or the hydrodynamic dispersion coefficient related to the net fresh water discharge. Nevertheless, these aspects were not taken into consideration in our modelling because the real parameters of the case study areas do not follow any specific pattern and it was necessary to represent them as closer to reality as possible.

For this Methodology 2, the input files were created using the iMOD-Python toolbox (Visser & Bootsma, 2019), while the iMOD-SEAWAT executable (Verkaik & Janssen, 2015) was used for the numerical simulation.

Figure 16 shows a schematic graph of the corresponding conceptualization.

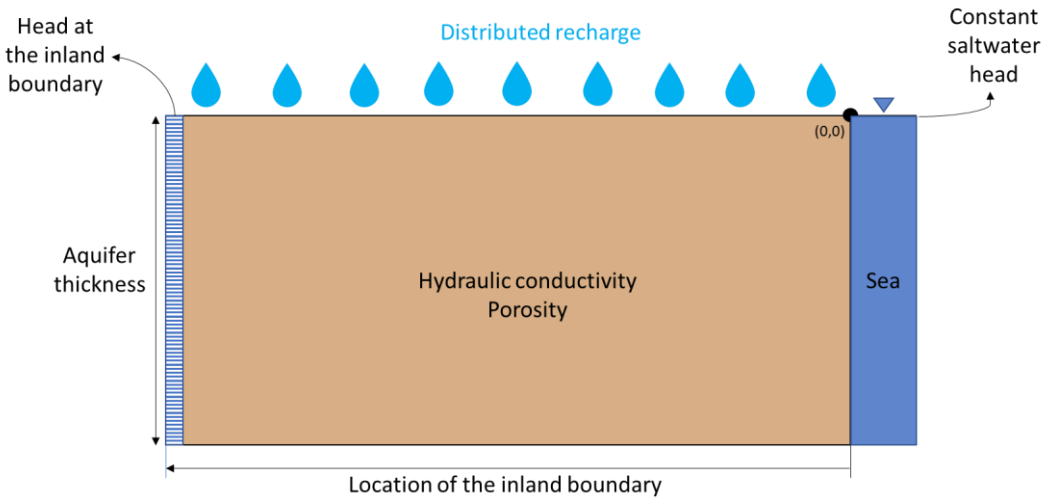

Figure 16: Conceptualization of Methodology 2 (M2)

For representing the recharge, the MODFLOW RCH package was used. The column where the inland head was defined, as well as for the coastal condition (head equal to zero), were set using IBOUND = -1. Regarding concentration, the concentration in the coastal boundary is equal to 35 Cl^- g/l, while in the rest of the model is initially equal to 0 Cl^- g/l.

The input data required in this methodology, such as the hydraulic conductivity (K), porosity (n), recharge rate (W_{net}), horizontal base of the aquifer below sea level (z_0) and the location of the inland boundary (x_b) and head at the inland boundary (h_b) were considered from the gathered data from local and global sources. In consequence, considering the 8 case study areas, a total of 16 model simulations were done for Methodology 2. Some of the most representative parameter values considered are shown in Table 3.

Table 3: Parameters used in Methodology 2

Parameter (units)	Symbol	Value
Inland head (m)	h_b	Variable*
Inland distance (m)	x_b	Variable*
Coastal head (m)	-	0
Horizontal base of the aquifer below sea level (m)	z_0	Variable*
Recharge (mm/y)	W_{net}	Variable*
Horizontal hydraulic conductivity (m/d)	K_x	Variable*
Vertical hydraulic conductivity (m/d)	K_z	Equal to Kx
Longitudinal dispersivity (m)	αL	1
Transverse dispersivity (m)	αT	0.1
Molecular diffusion (m^2/d)	D	9E-5
Effective porosity (-)	n	Variable*
Seawater density (kg/m^3)	ρ_s	1025
Seawater salinity (kg/m^3)	-	35

*Parameters vary for each individual model depending on the area and if a local or global source is being used.

3.3.3 Methodology 3 (M3): Synthetic conceptualisation modelling

The objective of using this model is to have a model case closer to reality, considering more specific boundary conditions. The SEAWAT (Langevin et al., 2008) code was used for the simulation of the synthetic Python model. The initial model was provided by Zamrsky and modified according to the needs of this research.

Methodology 3 considers the complete length of the continental shelf and continental slope, as well as its bathymetry. However, this could not be done as the large topographic distance between the inland boundary condition and the bottom of the continental slope bottom caused a large number of model layers, mainly focused in the offshore area and not providing a detailed representation in the main area of interest. In addition, the model would take too long to run. To accelerate the model simulation running time, the offshore distances were reduced up to a distance of around 4 times the length of the inland zone. Before doing this, a test model was used to check if the geometry of the coastal part of the aquifer does not have influence in the distribution of the saline water intrusion, as it would happen if paleo climatic reconstruction scenarios were being modelled. Different lengths of the coastal area of the aquifer were tested and the resulting saline intrusion was the same in all cases.

In this simulation, the bottom of the aquifer bedrock is not known, so it is assumed that the thickness is the same for the whole profile. Figure 17 shows the model conceptualization.

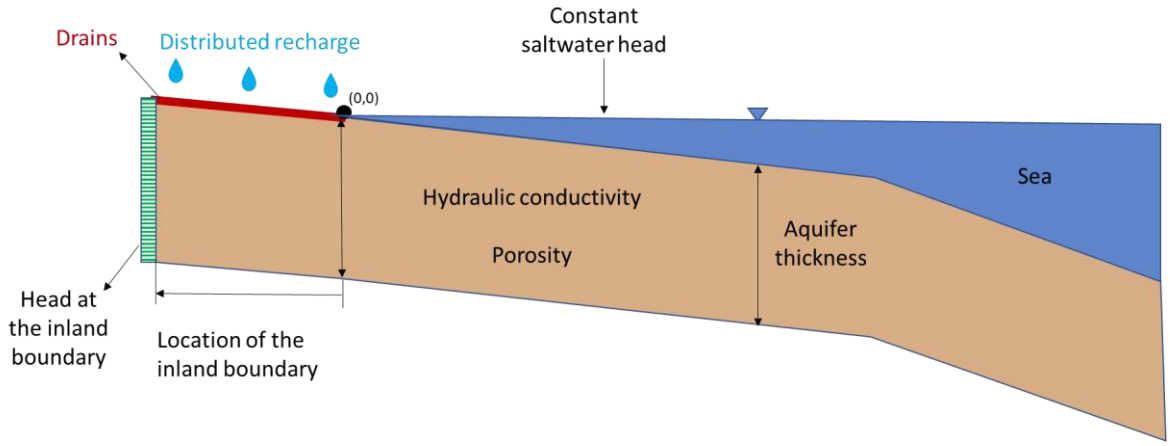

Figure 17: Conceptualization of Methodology 3 (M3)

The head at the inland boundary is represented using the General Head Boundary (GHB) MODFLOW package. The boundary head parameter is indicated as the inland head value known from the local and global compiled information. The conductance parameter is calculated by the script based on the cell dimensions and the hydraulic conductivity of the top layer cell, leading to a calculated head in each GHB model cells that corresponds with the inlead head.

The drains (MODFLOW DRN package) are assigned in the top cells located inland, where also the recharge condition (RCH package) is applied. These drains work as a system discharge and limit the recharge that can go into the system in case the heads would otherwise get too high in the system. The elevation assigned to the drain cells is the inland topography, and the conductance is also being calculated conceptually as in the case of the GHB, though represents a physical drainage system in each specific model cell.

The input data considered in this Methodology 3 was the local-scale Australian reported data and the global datasets information. This information was applied to the 8 case study areas, obtaining a total of 16 model simulations. Table 4 shows the parameters considered in M3.

Table 4: Parameters used in Methodology 3

Parameter (units)	Symbol	Value
Inland head (m)	h_b	Variable*
Inland distance (m)	x_b	Variable*
Coastal head (m)	-	0
Horizontal base of the aquifer below sea level (m)	z_0	Variable*
Recharge (mm/y)	W_{net}	Variable*
Horizontal hydraulic conductivity (m/d)	K_x	Variable*
Vertical hydraulic conductivity (m/d)	0.1 K_x	Variable*
Longitudinal dispersivity (m)	αL	1
Transverse dispersivity (m)	αT	0.1
Molecular diffusion (m^2/d)	D	9E-5
Effective porosity (-)	n	Variable*
Seawater density (kg/m^3)	ρ_s	1025
Seawater salinity (kg/m^3)	-	35

*Parameters vary for each individual model depending on the area and if a local or global source is being used.

3.3.4 Methodology 4 (M4): Complex conceptualisation modelling using global datasets

In this methodology, the conceptualizations of the model are becoming more complex in comparison to the previous ones. This step is based on the methodology from Zamrsky's PhD research "Rapid coastal groundwater modelling and scenarios for strategic policy development" (2019) which aims to assess the current and future distribution of fresh and saline groundwater on global scale by using computer modelling. This methodology is relevant to this analysis because its input data is based only in global datasets and statistical analysis for the determination of, for example, recharge, topography, bathymetry, thickness along the cross sections and the geological characteristics of the area. The processed input data and Python scripts currently being used in his evaluations were provided by the author and applied to a representative cross section for each case study area.

The first part of his research consisted in the determination of global coastal aquifer thicknesses (Zamrsky et al., 2018). This information was used to build regional representative 2D groundwater flow models along most of the coastal regions of the world. Furthermore, possible future climate change scenarios will be evaluated in upcoming articles.

The recharge rate considered in the modelling within this PhD research is from the MODIS datasets of evapotranspiration and precipitation. For each COSCAT area (Laruelle et al., 2013), values were measured and fitted to a lognormal distribution. From these, the mean and standard deviation were calculated. These two statistical parameters were used to obtain randomizations of recharge values by creating new datasets with these characteristics.

One important parameter for building these profiles is the geological complexity of the inland and shelf zones. The geology considered in this methodology is based on the research by Karssenberg (2018), in

which an estimation of the geology of the unconsolidated sedimentary cover of the global continental shelves is presented. These results are based on previous conceptual models that describe the continental shelf, case studies and global datasets (Figure 18). This geological information was used to run randomly generated realizations that varied parameters such as number and thickness of aquifer and aquitard layers are estimated based on previously defined ratios of fine and coarse sediments.

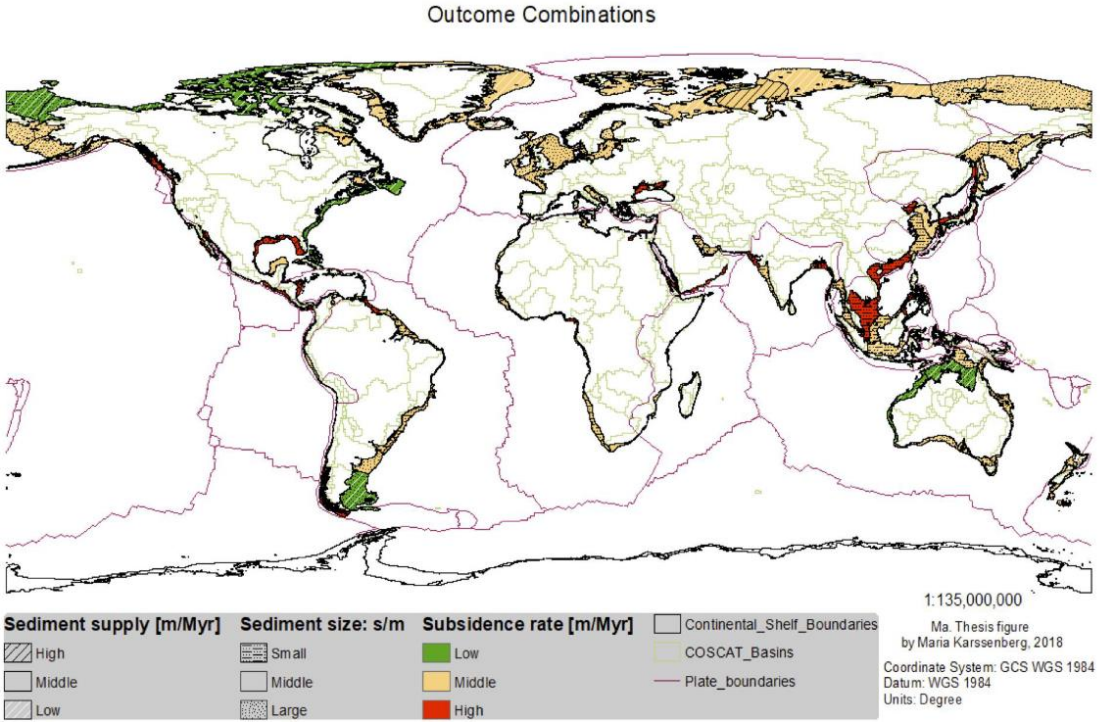

Figure 18: Map of the three main external controls on the continental shelf for each COSCAT shelf segment (Karssenberg, 2018)

Five realizations, that considered a varying recharge and geology, per cross section were considered in this evaluation to assess different scenarios of recharge and geology due to the uncertainty of these parameters. This was applied to 6 case study areas, as the other 2 were not available for use yet. Note that, this code is under development as part of an ongoing PhD research so some numerical subroutines are still under development and will not be considered as part of this research. In addition, the final version of the code to be presented in Zamrsky's final document could vary from the scripts used in this research depending on future improvements by the author. Figure 19 shows the conceptualization of M4.

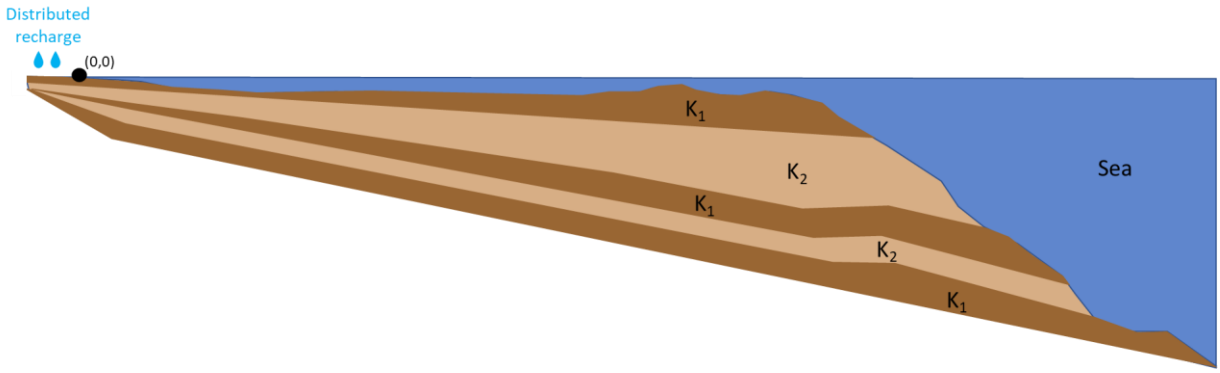

Figure 19: Conceptualization of Methodology 4 (M4)

3.3.5 Methodology 5 (M5): Complex conceptualisation modelling using collected bore log data

The hydraulic conductivity of the aquifers is considered as a determining factor for the groundwater flow movement and, as a consequence, for the saline water intrusion processes. This section of the methodology used as its basis the Python script applied to create the models in M4, maintaining all the boundary conditions and input data but modifying the geological information based on the bore log data analysis previously explained in Section 3.2.1 b) Bore logs interpretation. It was decided that this step was important in the methodology since it would help to reduce uncertainty in the geological layers estimated from the global datasets. The same six profiles from M4 were used in this section and 5 realizations for recharge were considered. Figure 20 shows the conceptualization of M5.

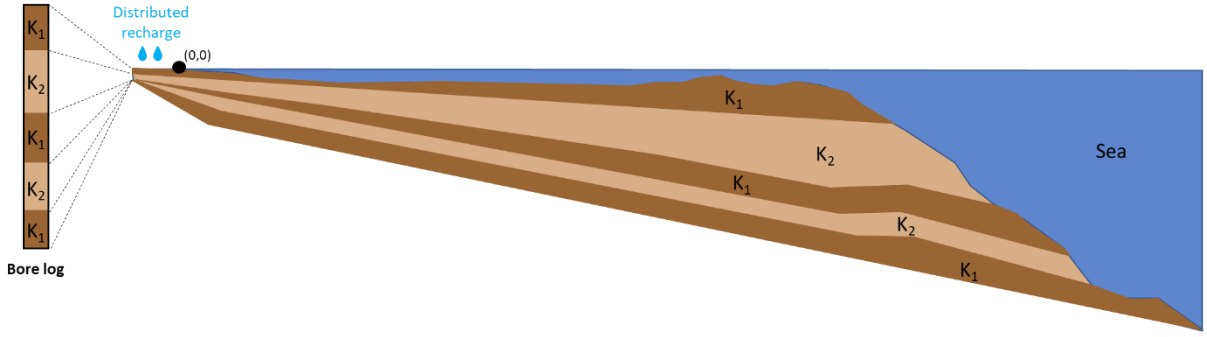

Figure 20: Conceptualization of Methodology 5 (M5)

3.3.6 Comparison between methodologies

The objective of this section is to compare between each other the previously seen results obtained from the five methodologies in evaluation. The parameters considered were the wedge toe location and the freshwater volume available in the inland part of the aquifer. Due to the different geometries of the aquifers depending on the input data used, the freshwater volume had to be normalised to be comparable with each other.

3.4 Climate change scenarios simulations

Climate change simulations were considered as part of the methodology to evaluate possible scenarios of sea-level rise and variation in the net recharge. The base models to be used for this analysis were the ones from Methodology 5 (M5), which consider the conditions from Methodology 4 (M4) plus the use of bore log information for the geology definition.

These scenarios considered the effect of recharge variations and the increase of sea level. For the recharge, two approaches were considered: (1) use the global recharge values (which are variable per top model cell) from M5 (which is the same as for M4 – see Appendix G) for the first randomization, and (2) use the constant recharge values from the local-scale data (Table 7). The baseline conditions are also considered, which do not have sea level rise and have a recharge multiplier of 1.

Due to the uncertainty in the future, multiple scenarios were considered for the climate change simulations. In the case of sea level rise, increases of 0.2 m, 1.0 m and 2.0 m were evaluated, while for recharge variation, multipliers equal to 0.25, 0.75 and 1.25. In total, 16 possible scenarios were evaluated (Table 5). The simulations for each scenario were run until reaching the amount of years necessary for steady state conditions of salinity distribution and, after this, 1000 extra years were simulated.

Table 5: Climate change scenarios to be considered

K_{RCH} / ΔH_{sea}	0.25	0.75	1	1.25
0				
0.2				
1				
2				

Note: K_{RCH} = Recharge multiplier, ΔH_{sea} = Change in sea level (m)

Due to the amount of simulations needed and the time constraints, these calculations were only performed for 2 case study areas (Stockton and Stuarts Point), which were used as a reference of the possible climate change effects.

Chapter 4 Results

This chapter presents the results obtained in each of the steps described in the methodology.

4.1 Data collection: local-scale and global-scale information sources

These results are linked to the first research question, which is focused on assessing the differences in local-scale and global-scale data collected for the case study areas. In the following sections, a comparison between the values obtained from both sources was done for each of the parameters.

4.1.1 Bore logs interpretation

Methodology 5 (M5) and the climate change scenarios simulations aim to better represent the conditions of the system by considering the sediment distribution obtained from the bore logs analysis and correlate it with hydraulic conductivity values. To do this, the bore logs located in each case study area were evaluated every 1 meter of depth, obtaining an average bore log description for every individual case.

Table 6 presents the percentages (from the surface to the basement rock) estimated for the average geology profiles that compose each of the groundwater system in evaluation. The sediments are classified in two groups: sediments with high permeability-HP (gravel and sand) and sediments with low permeability-LP (silt and clay). This is to follow the conceptualization considered in M5. For Botany, Hat Head, Stockton and Stuarts Point, the analysis indicated that its composition was of 100% highly permeable sediments. However, this percentage was reduced to 90%, and the 10% left assigned as low permeability sediments as, in reality, it is not expected to find a completely homogeneous media. Besides these groundwater systems, the other four (Bowen, Burdekin, Burnett Heads and Pioneer Valley), presented variable sediment types along the profile. A more detailed description of the layers found in each borehole and the simplifications done can be found in Appendix C.

Table 6: Composition of low and high permeable layers based on bore logs analysis

Case study area	Composition of low and high permeable layers
Botany	90% HP, 10% LP
Bowen	14% LP, 36% HP, 23% LP, 5% HP, 23% LP
Burdekin	13% LP, 8% HP, 19% LP, 54% HP, 6% LP
Burnett Heads	14% LP, 8% HP, 34% LP, 16% HP, 28% LP
Hat Head	90% HP, 10% LP
Pioneer Valley	18% HP, 73% LP, 9% HP
Stockton	90% HP, 10% LP
Stuarts Point	90% HP, 10% LP

*Where HP = High permeability, and LP = Low permeability. The percentages start from the surface towards the bottom.

4.1.2 Hydraulic conductivity

Figure 21 shows the hydraulic conductivity values in meters per day obtained from the local and global scale sources in the case study areas. In all cases, it showed that the values obtained from local sources are much larger than the global ones. This difference can reach up to five orders of magnitude, meaning that the global dataset used in the evaluation would be underestimating these parameters. Moreover, these values were compared to the ones found in literature (Freeze & Cherry, 1979), finding that all the local values are inside the category of clean sand, however, the bore log analysis indicated in half of the case study areas there is a mix of sediment types in the profile (of high and low permeability), and not only clean sand. However, this is also due to the simplification used by the local source. For the global information, the literature showed that the values are in the range of clean sand, silty sand and unweathered marine clay, but not all of these characteristics were seen in the bore logs analysis. For example, Botany and Stuarts Points bore logs showed mostly sand, while the global datasets assigned them a value corresponding to unweathered marine clay. For Hat Head and Stockton, these also showed logs composed of mostly highly permeable sediments but the global datasets value represents silty sand which is a mix of highly and low permeable sediments.

Furthermore, based on the bore logs analysis from the previous section, it was seen that at least in half of the evaluated areas, these groundwater systems are composed of sediment layers of different materials. This heterogeneity could have an important influence in the distribution of the groundwater flow, meaning that the hydraulic conductivity simplification may not be a completely correct option to represent the aquifer conditions.

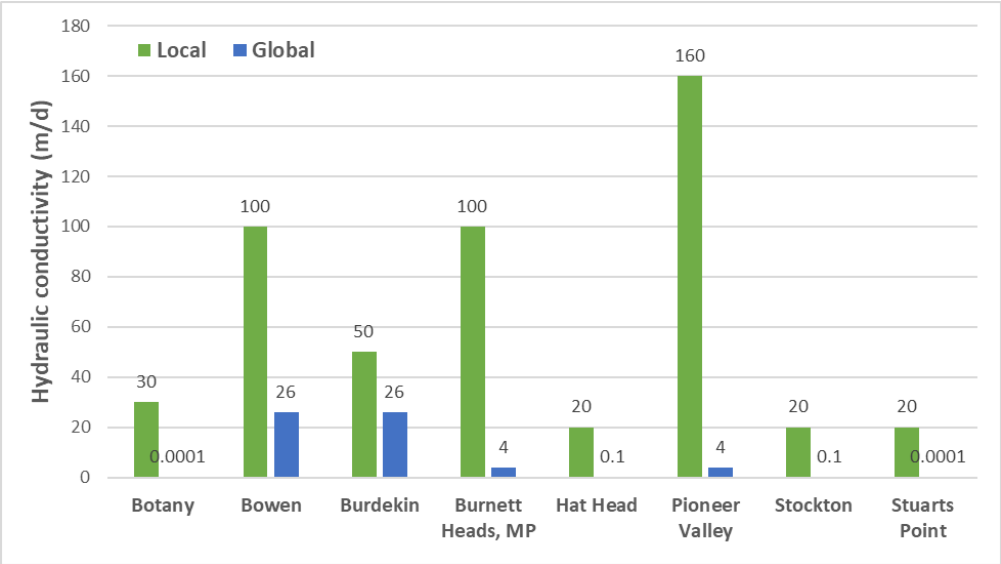

Figure 21: Hydraulic conductivity (m/d) per case study area.

4.1.3 Depth to aquifer base from mean sea level

When comparing the values of aquifer thicknesses estimated for both sources (Figure 22) it was seen that, in all cases, the values coming from the global datasets are larger than the ones obtained from local sources. The global information can be from 2 times larger up to 11 times larger than the local data. Appendix D provides detailed information about which cross sections from the global dataset were considered for estimating the average aquifer thickness per case study area, as well as the standard deviation values for each of the cross-section's estimations.

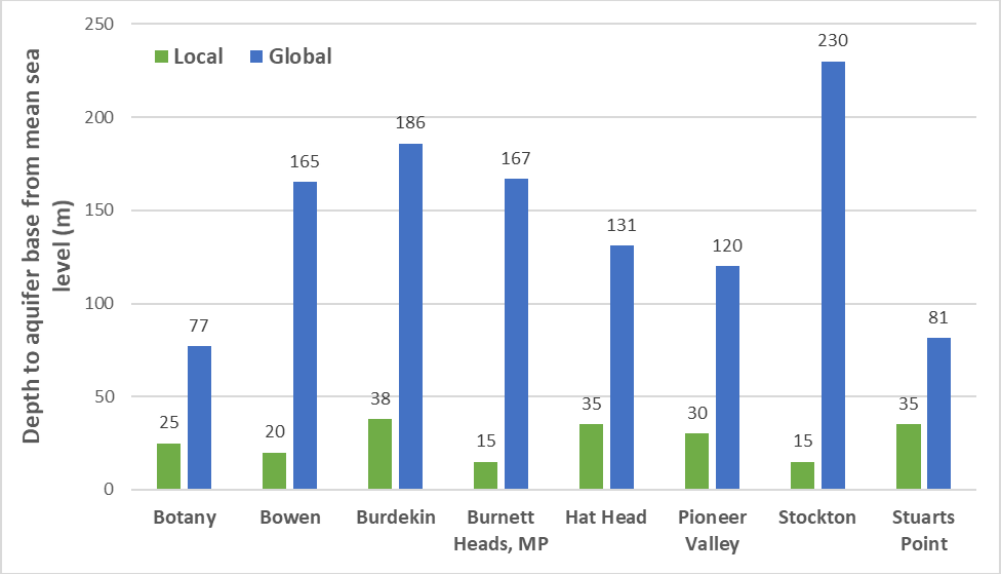

Figure 22: Depth to aquifer base from mean sea level (m) per case study area.

For this parameter it was possible to do a validation based on the bore logs interpretation by analysing the depth to bedrock in the boreholes which were drilled deep enough. Figure 23 presents the comparison between the depths to aquifer base obtained from the three sources in evaluation: the local and global scale data presented in Figure 22 plus the information obtained from the bore logs

analysis. For all case study areas, the deepest bore logs available were selected to determine the depth to bedrock.

Considering the bore logs information as the most reliable one, an overestimation of the aquifer depths was observed from global datasets. The global dataset uses a method where many possible aquifer depths at the coastline are calculated for each cross-section. The discrepancy could be related to the fact that, from all these estimations, only an average value at the coast is being considered, which may not be precise enough or could be affected by extreme depth values obtained from the different methods of evaluation to define the basement shape. This possibility can be supported by the standard deviation of the thicknesses calculated for each cross-section (see Appendix D) which are very large, meaning that there is a large amount of variation in the data. Furthermore, it can also be possible that this dataset may not be accurate enough to represent particular characteristics of the groundwater systems at this scale of evaluation. In addition, the global dataset could be taking into account more low-permeable systems that may have not been properly represented in the boreholes due to not being deep enough.

In contrast, it is seen that the local information is inside the limits defined by the bore logs analysis. However, in Burnett Heads the local information is below the limits. This is because the local information is only considering the uppermost formation (Elliot Formation), while there are still other formations below, which were not contemplated during the bore logs analysis. Information about the bore logs analysis, such as the logs considered, the estimated depths to basement rock and type of basement rock are found in Appendix E.

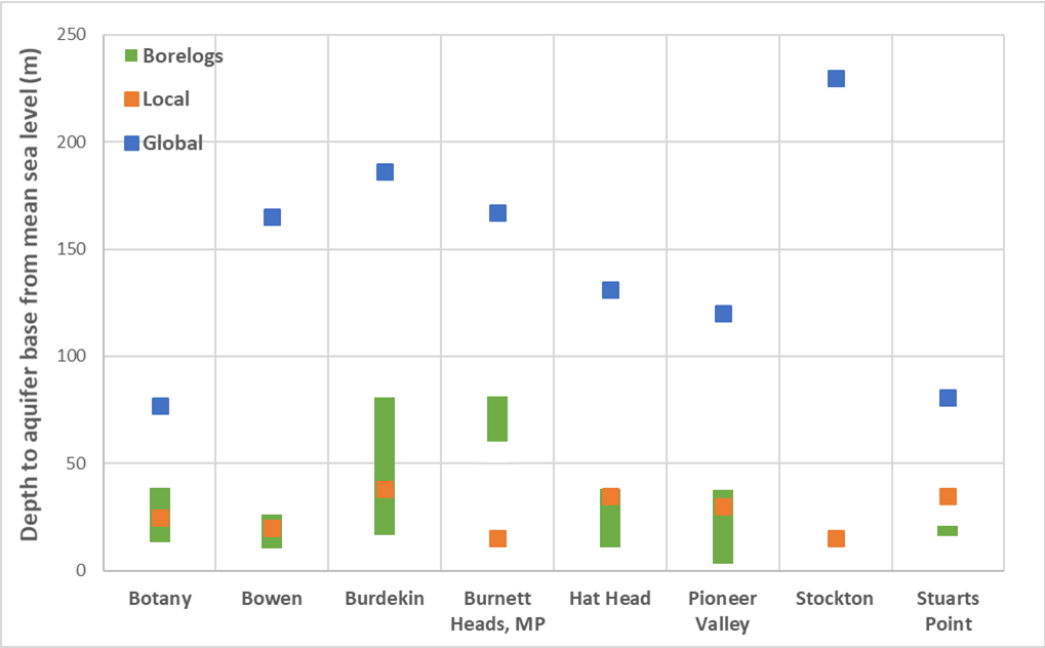

Figure 23: Depth to aquifer base from mean sea level (m).

Note: The blue squares represent the values from global sources, the orange ones are from the local sources and the green ones are from the bore logs analysis (the latter shown as a range from the largest and the smallest values found). In the case of Stockton, the bore logs available in the area were too shallow and did not reach the bedrock, so there was no information regarding this parameter to include in the graph.

4.1.4 Recharge

Figure 24 presents the comparison between the recharge values from the local and global sources. In general, the values obtained from the global datasets are lower in comparison to the local-scale values except in Botany and Bowen.

It is also important to consider that the global recharge does not account for the effects of pumping or irrigation, as it is only the difference between the precipitation and evapotranspiration. The local-scale recharge is accounting additionally for infiltration and distributed pumping (Werner, Ward, et al., 2012).

In Burdekin and Stuarts Point, the recharge from global sources has a negative value, which indicates that the evapotranspiration is higher than the precipitation in these areas, so there is a deficit in the available water. For the simulations, in these cases, a negligible value equal to 10 mm/y was considered as recharge to be able to apply the methodologies.

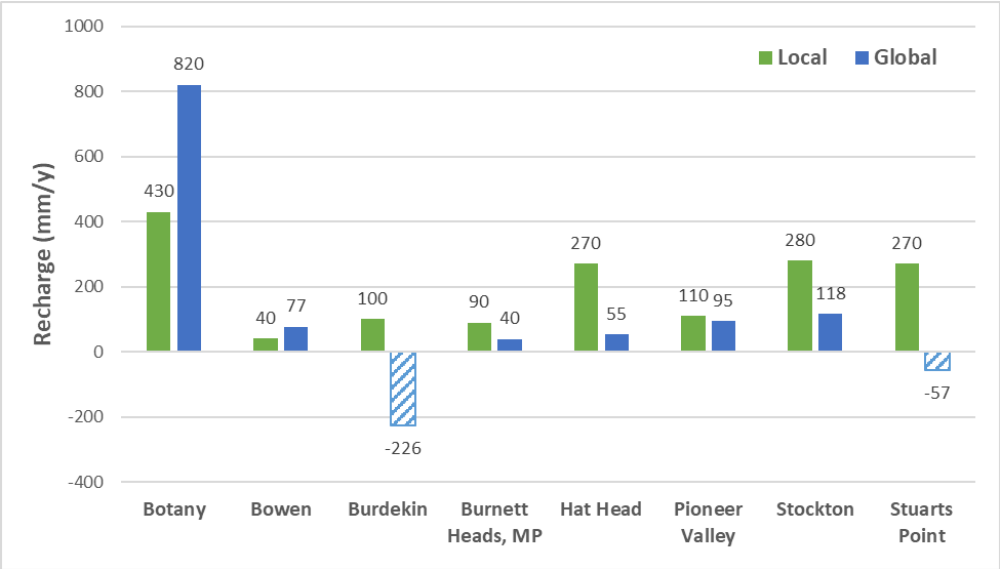

Figure 24: Recharge (mm/y) per case study area.

4.1.5 Distance to the inland boundary condition and head level

The distance to the inland boundary condition (Figure 25) for the local and global data sources does not follow a specific pattern. Nonetheless, 6 out of 8 case study areas showed a good match. An important condition is that this parameter did not have a defined method of calculation, so its determination could be influenced by the approach used. For the global datasets, it considered choosing the distance where, based on the topography, a water divide could exist. Another possible influencing factor on the determination of this parameter is that the topography dataset used may need a finer resolution for this type of analysis.

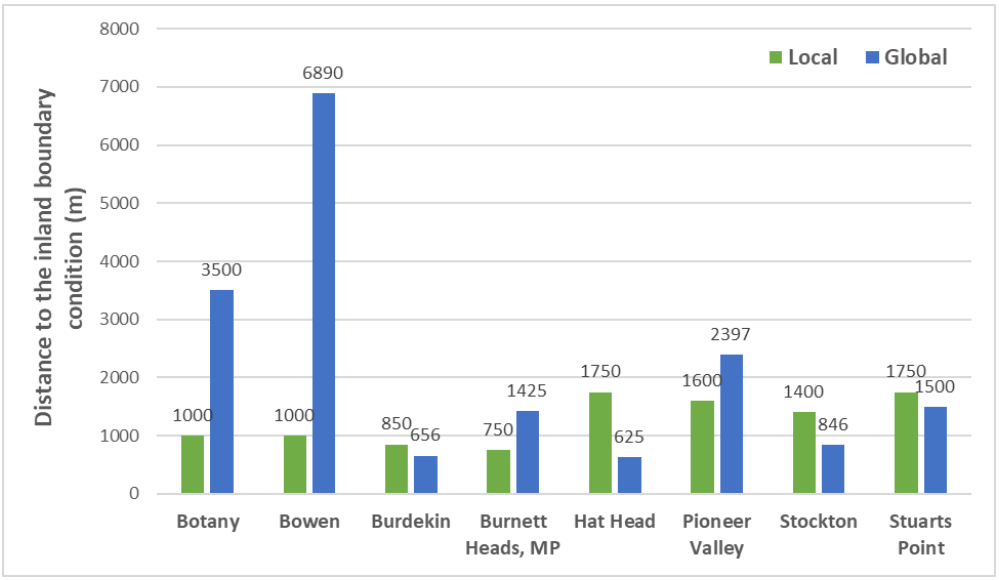

Figure 25: Distance to the inland boundary condition (m) per case study area.

As seen in Figure 26, for all zones except Stuarts Point, the global values of the head at the inland boundary condition were larger than the local values. This comparison also needs to be assessed carefully, as the heads were evaluated at different distances in both local and global sources for the

same case study area. For the global data, another factor that could influence the determination of this parameter is the resolution of the datasets used (topography and water table distance).

In most cases, the differences between the local and global information are not that big, but since this measurement is influenced by the location defined, it is automatically different too.

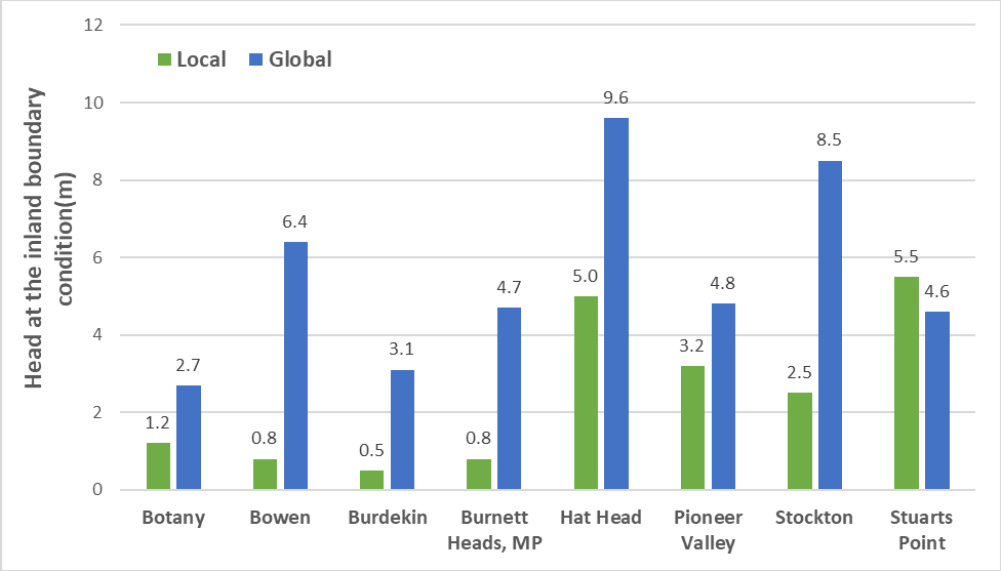

Figure 26: Head at the inland boundary condition (m a.s.l.) per case study area.

The detailed results from the determination of these two parameters using global data can be found in Appendix F.

4.1.6 Porosity

The porosity, based on the local data, has values of 0.1 and 0.3 for the different case study areas. For the global data, a constant value equal to 0.25 is assumed, since this figure is generally used as a default value, also for groundwater and solute transport modelling. Figure 27 shows that in five of the case study areas, the assumed global value is larger than the local ones, while in three of the cases it is smaller.

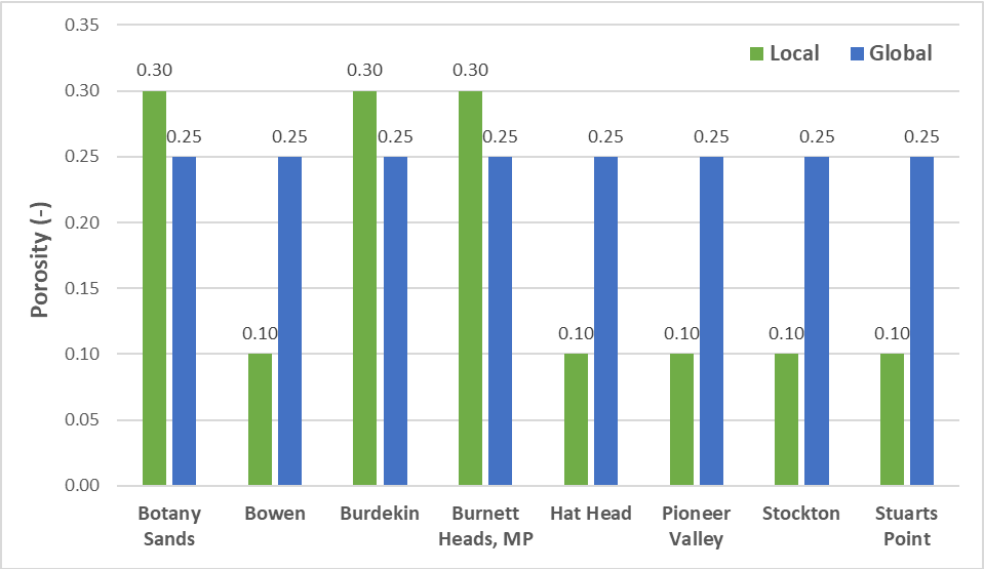

Figure 27: Porosity (-) per case study area.

4.1.7 Synthesis of the results

Table 7 synthetizes the comparison of all the input data collected at local and global scale for the analysis. In general, a discrepancy between the local and global-scale data was observed, being the most important the hydraulic conductivity and the depth to aquifer base.

Table 7: Comparison of local-scale and global-scale collected parameters.

Case study area	Hydraulic conductivity (m/d)		Recharge (mm/y)		Depth to aquifer base from mean sea level (m)		Head at the inland boundary condition (m)		Location of the inland boundary condition (m)		Porosity (-)	
	Local	Global	Local	Global	Local	Global	Local	Global	Local	Global	Local	Global
Botany	30	0.0001	430	820	25	77	1.2	2.7	1000	3500	0.3	0.25
Bowen	100	26	40	77	20	165	0.8	6.4	1000	6890	0.1	0.25
Burdekin	50	26	100	-226	38	186	0.5	3.1	850	656	0.3	0.25
Burnett Heads, MP	100	4	90	40	15	167	0.8	4.7	750	1425	0.3	0.25
Hat Head	20	0.1	270	55	35	131	5	9.6	1750	625	0.1	0.25
Pioneer Valley	160	4	110	95	30	120	3.2	4.8	1600	2397	0.1	0.25
Stockton	20	0.1	280	118	15	230	2.5	8.5	1400	846	0.1	0.25
Stuarts Point	20	0.0001	270	-57	35	81	5.5	4.6	1750	1500	0.1	0.25

4.2 Application of methodologies for the estimation of the saltwater intrusion

Based on the information gathered in the data collection step, the different data sources and parameters were applied to the proposed methodologies. The first sections show the comparison between the results obtained in each methodology, while the last section presents a final assessment between methodologies.

4.2.1 Methodology 1 (M1): Analytical solution

This methodology considered the use of analytical formulas for the determination of the saltwater intrusion length as well as the freshwater volume present in the aquifer. In this evaluation, the results obtained from using the local-scale data were compared to the ones obtained from the global datasets. The results from both can be observed in Figure 28.

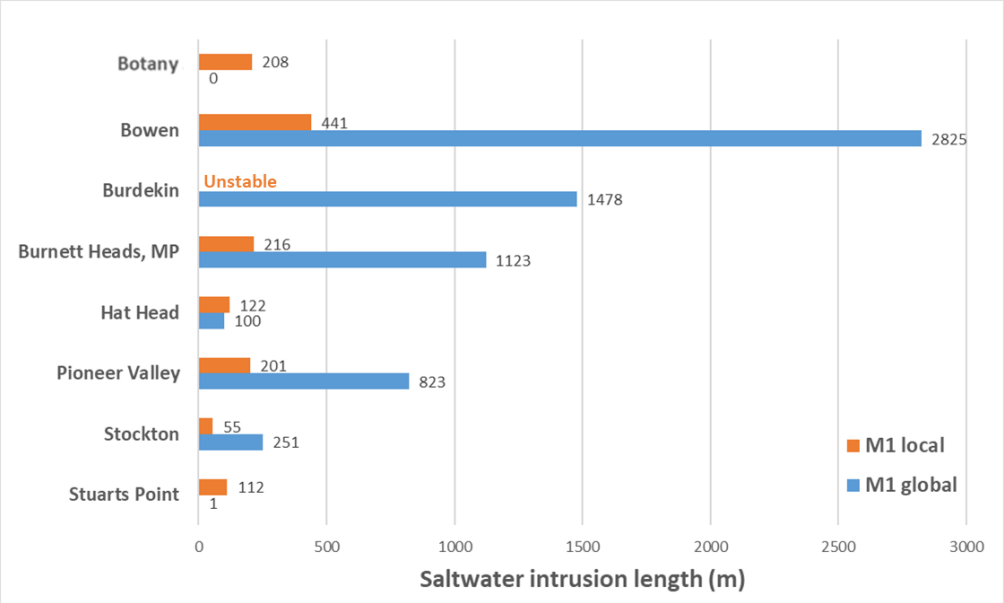

Figure 28: Methodology M1 – Saltwater intrusion length (m).
Note: In Burdekin – global, the saline intrusion length goes beyond the distance to the boundary condition.

When using the global information, in most of the cases the length of the saltwater intrusion is larger than when using the local information. However, in Stuarts Point and Botany, the intrusion is almost inexistent. This is linked to the hydraulic conductivity values obtained from the global sources, which are lower by many orders of magnitude in comparison to the values reported by the local sources. This difference is very relevant for the two areas mentioned. In addition, the sediment type corresponding to the global hydraulic conductivity, which is weathered marine clay in these two case study areas, is not representative of the real characteristics of the area.

According to Methodology 1, there is the possibility of having “unstable” conditions regarding the saltwater intrusion, which means that the freshwater that is discharging to the coast is not large enough to make the wedge toe reach a steady-state location (Morgan & Werner, 2015). In the case of Burdekin-local, this process is occurring, while for Burdekin global, the saltwater intrusion length is larger than the distance to the inland boundary condition.

Figure 29 shows a comparison between the saltwater intrusion calculated from the local and global data for the 8 case study areas.

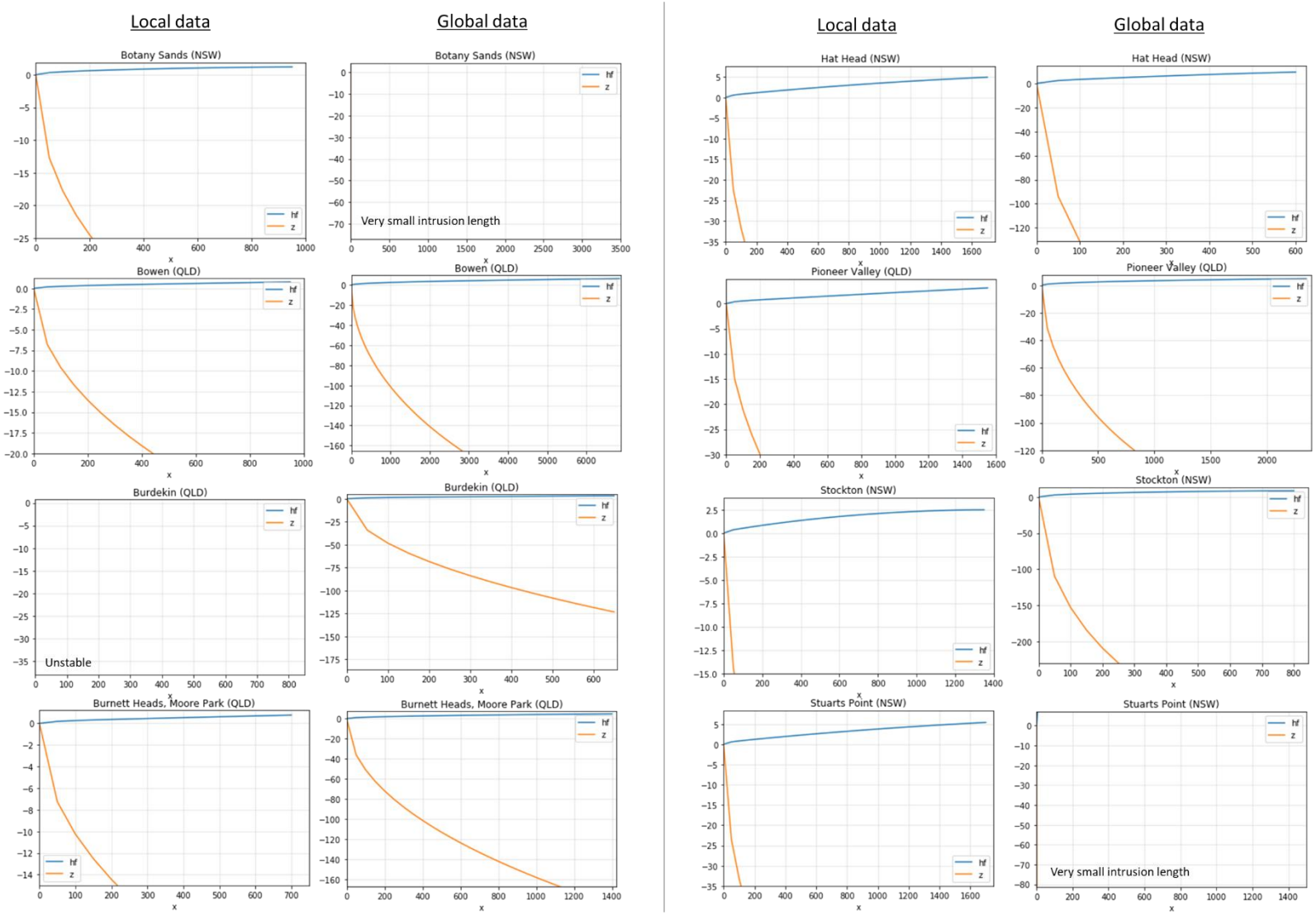

*Where h_f is the freshwater head above mean sea level (m) and z represents the depth to the interface (m)

Figure 29: Methodology 1 (M1) - Freshwater head and freshwater-saltwater interface location.

Figure 30 shows the freshwater volumes calculated for the case study areas applying M1. The difference between the results from using the two different input data sources is significant, obtaining from the global datasets much higher values of freshwater available in the aquifer for all the evaluation cases.

The freshwater volume is a parameter that will highly depend on the aquifer geometry, which is defined in the 2D profiles by the depth to the aquifer base and the distance to the inland boundary. In the case of the depth to the aquifer base, all the values obtained from the global sources were from 2 to 15 times larger than the corresponding local sources. In addition, the location of the inland boundary condition also influenced this calculation as, in some of the cases, the global values were also from 2 to 7 times larger than the corresponding local ones. All these conditions caused greater volumes in the case of the calculations based on the global datasets.

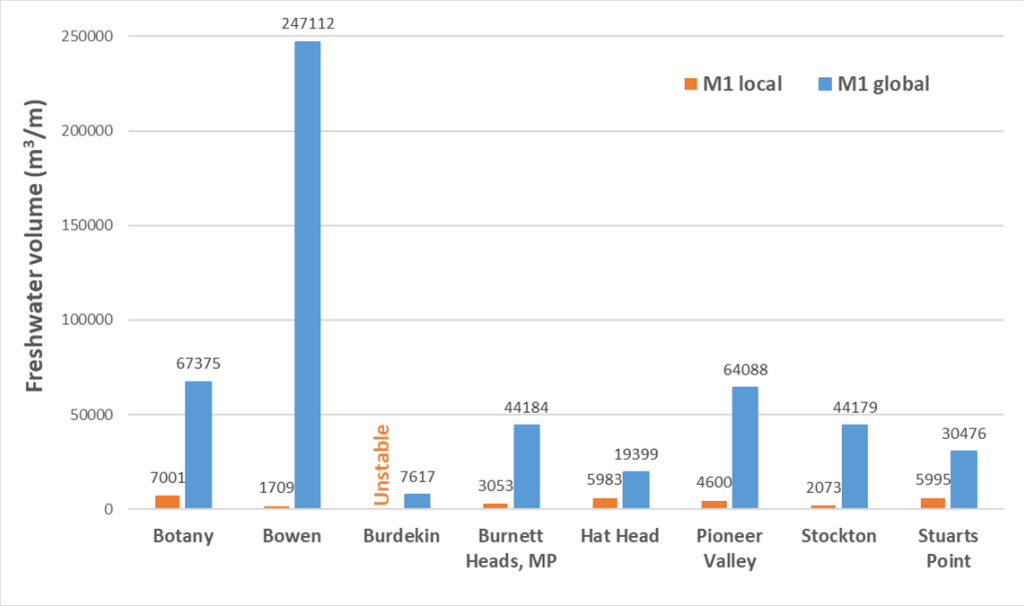

Figure 30: M1 – Freshwater volume (m^3/m).

4.2.2 Methodology 2 (M2): Henry case conceptualization modelling

Methodology 2 (M2) aimed to use the same input data used in M1 and run variable-density groundwater models based on the Henry case problem and using iMOD-SEAWAT.

Figure 31 shows the results obtained from these simulations. In most cases, the simulations using global datasets showed a larger saltwater intrusion than when using local datasets. The exceptions are Stuarts Point and Botany, that show no saltwater intrusion (because of the low hydraulic conductivity value obtained from the global sources). Burdekin showed in both simulations (global and local) that the intrusion reached the inland boundary condition.

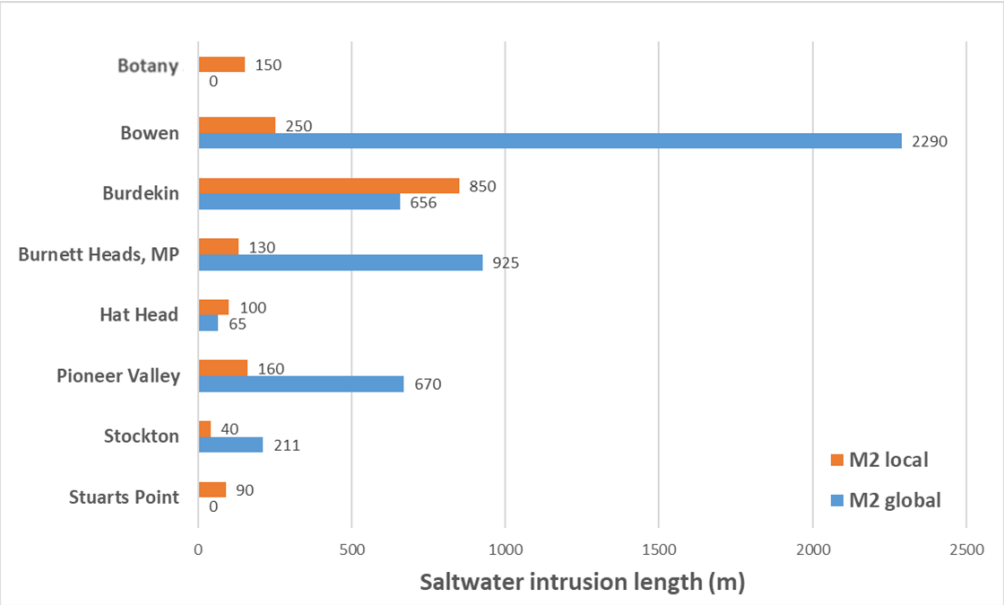

Figure 31: M2 – Saltwater intrusion length (m).

Note: In Burdekin local and global, the intrusion reaches the whole length of the model, reaching the inland boundary condition.

Figure 32 and Figure 33 show the concentration profiles for the 8 case study areas for local and global input data.

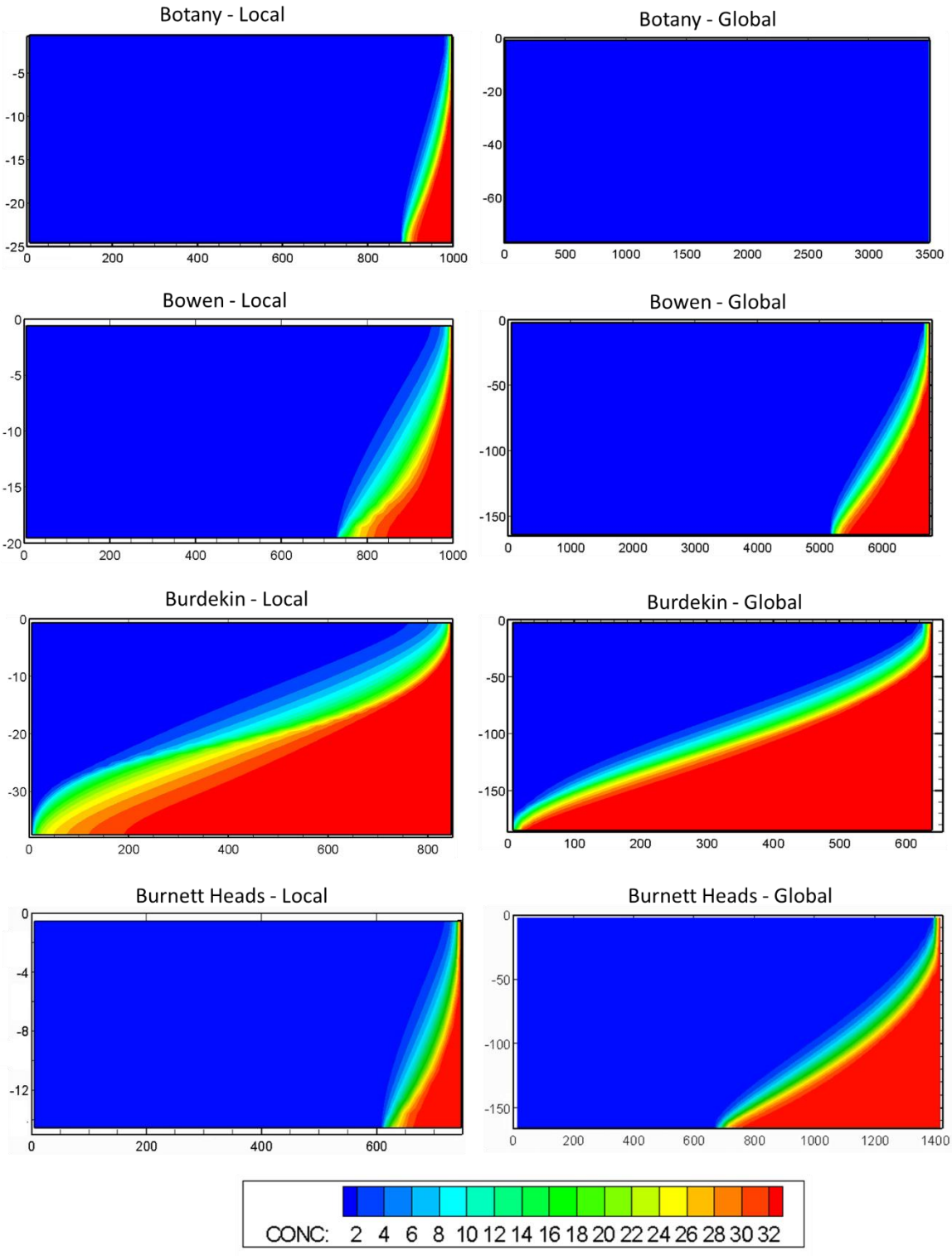

Figure 32: Concentration profiles (g Cl^-/l) for M2 - Part 1.

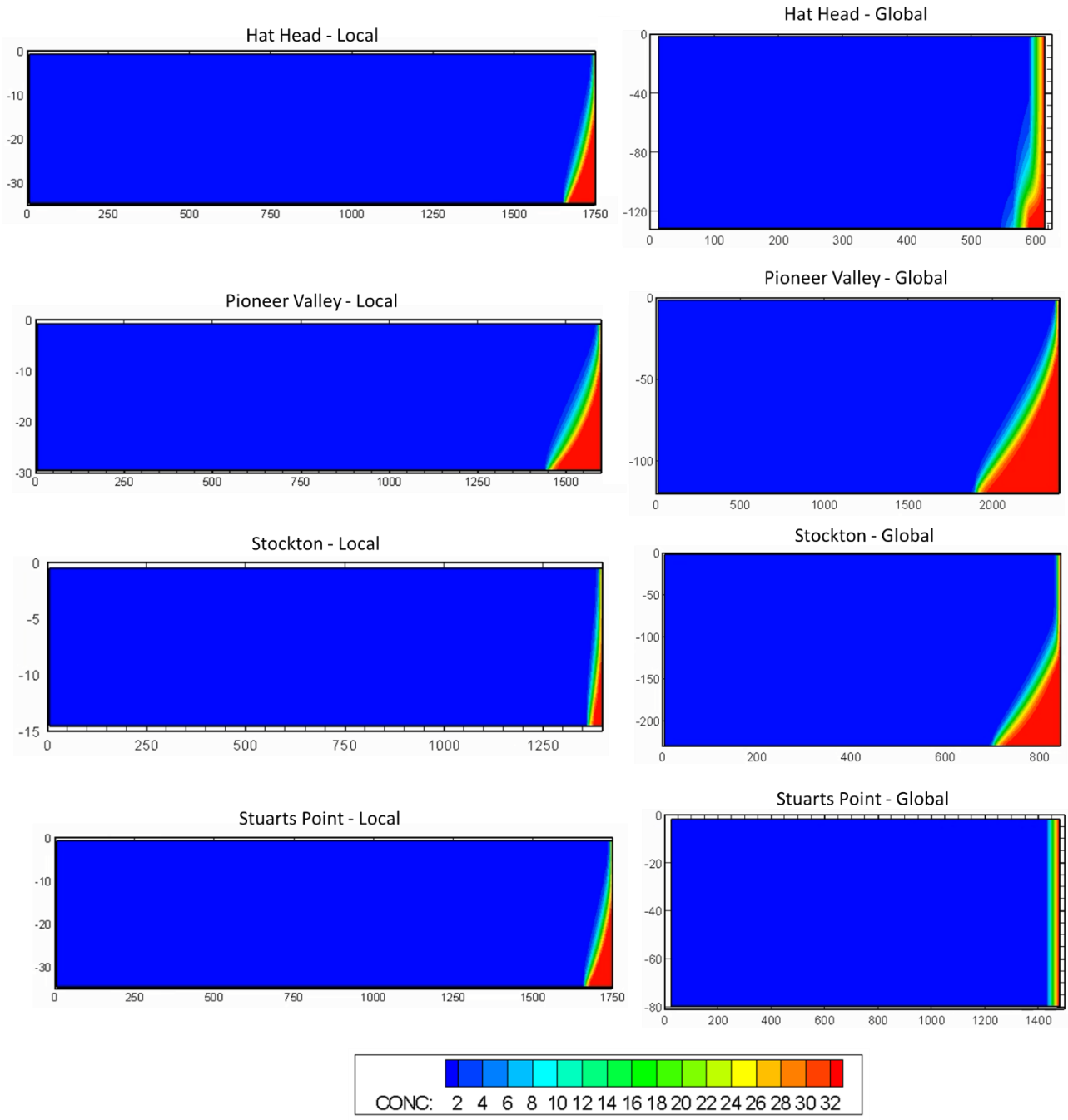

Figure 33: Concentration profiles (g Cl^-/l) for M2 - Part 1.

In Hat Head - global and Stockton – global the saltwater intrusion is not fully extended along the vertical boundary of the profile. This could be representing conditions where there is freshwater in the continental shelf area, however, this cannot be defined at this stage because the model conceptualisation considered does not show the behaviour of the flow in this offshore area.

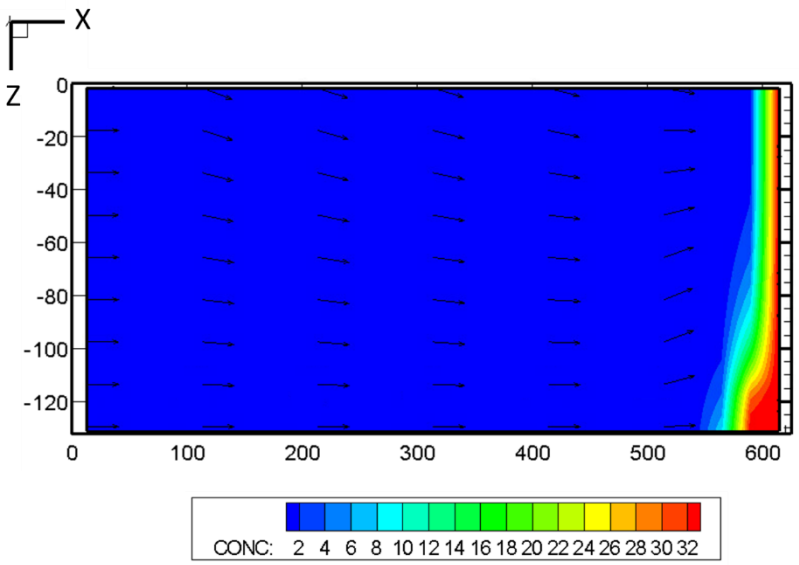

Figure 34: M2- Concentration profile Hat head (g Cl^-/l): global datasets.

Figure 35 shows the freshwater volumes calculated using this methodology. The volumes obtained from using the global datasets were a lot larger than in the case of the local ones. The same behaviour was observed in M1, and the reason are the dimensions of the distance to the inland boundary condition and the depth to the bottom of the aquifer, which are larger in the global data tan in the local one.

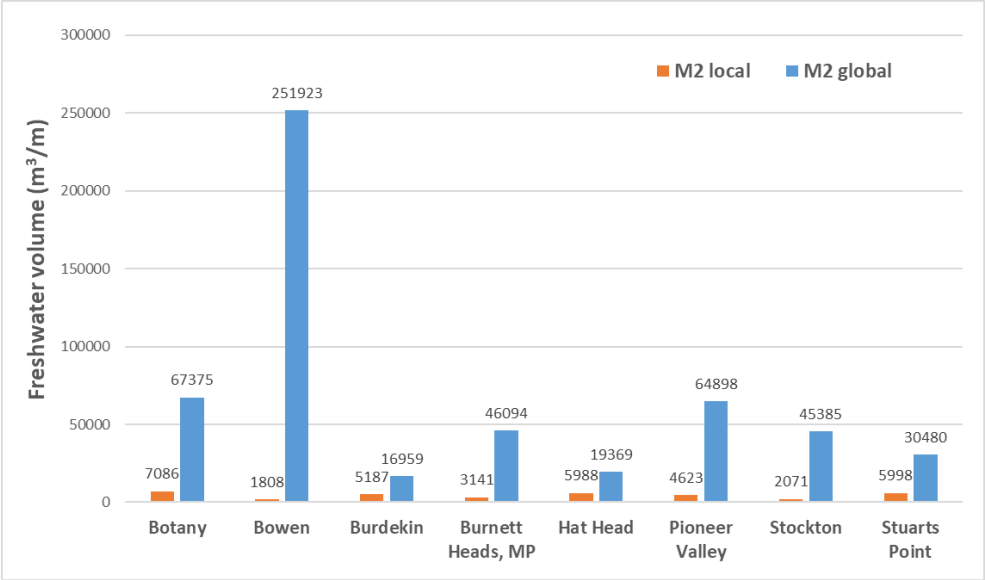

Figure 35: Methodology M2 – Freshwater volume (m³/m).

4.2.3 Methodology 3 (M3): Synthetic conceptualization modelling

Methodology 3 (M3) considered the use of SEAWAT for the simulation of a synthetic model, using local and global datasets. Figure 36 shows the comparison of saltwater intrusion lengths for the methodology M3. Figure 36 and Figure 37 represent the concentration profiles for the 8 case study areas using global and local data.

The saltwater intrusion was larger when using the global datasets than when using the local information. The saltwater intrusion in Burdekin reached the total length of the model, as in M2. For Stuarts Point and Botany there was no saltwater intrusion in the case of the global datasets, due to the small values of hydraulic conductivity found in these areas. These two cases showed that the freshwater-saltwater division stayed close to the coastline.

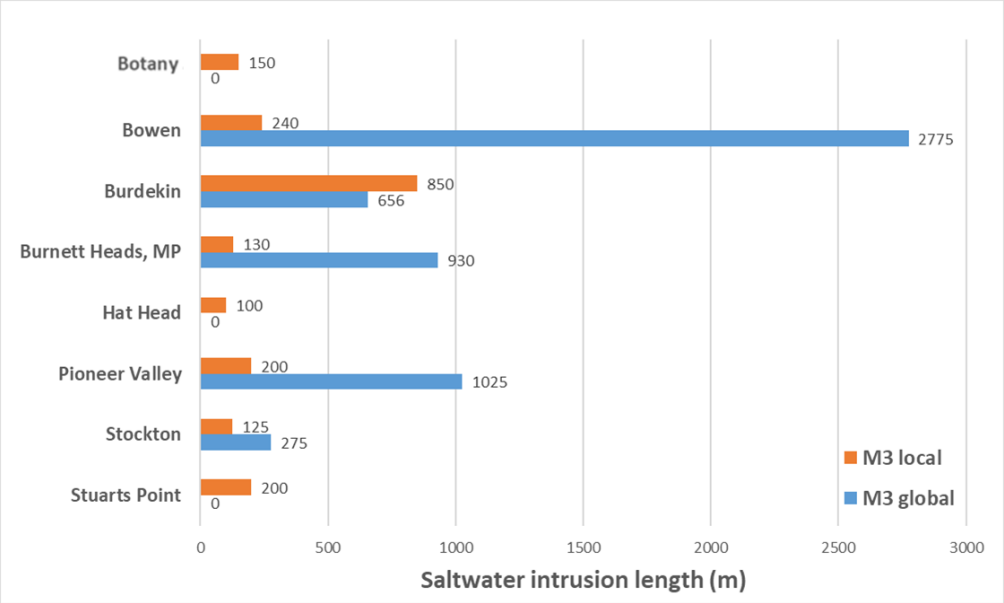

Figure 36: M3 – Saltwater intrusion length (m).

Note: In Burdekin local and global, the intrusion reaches the whole length of the model, reaching the inland boundary condition.

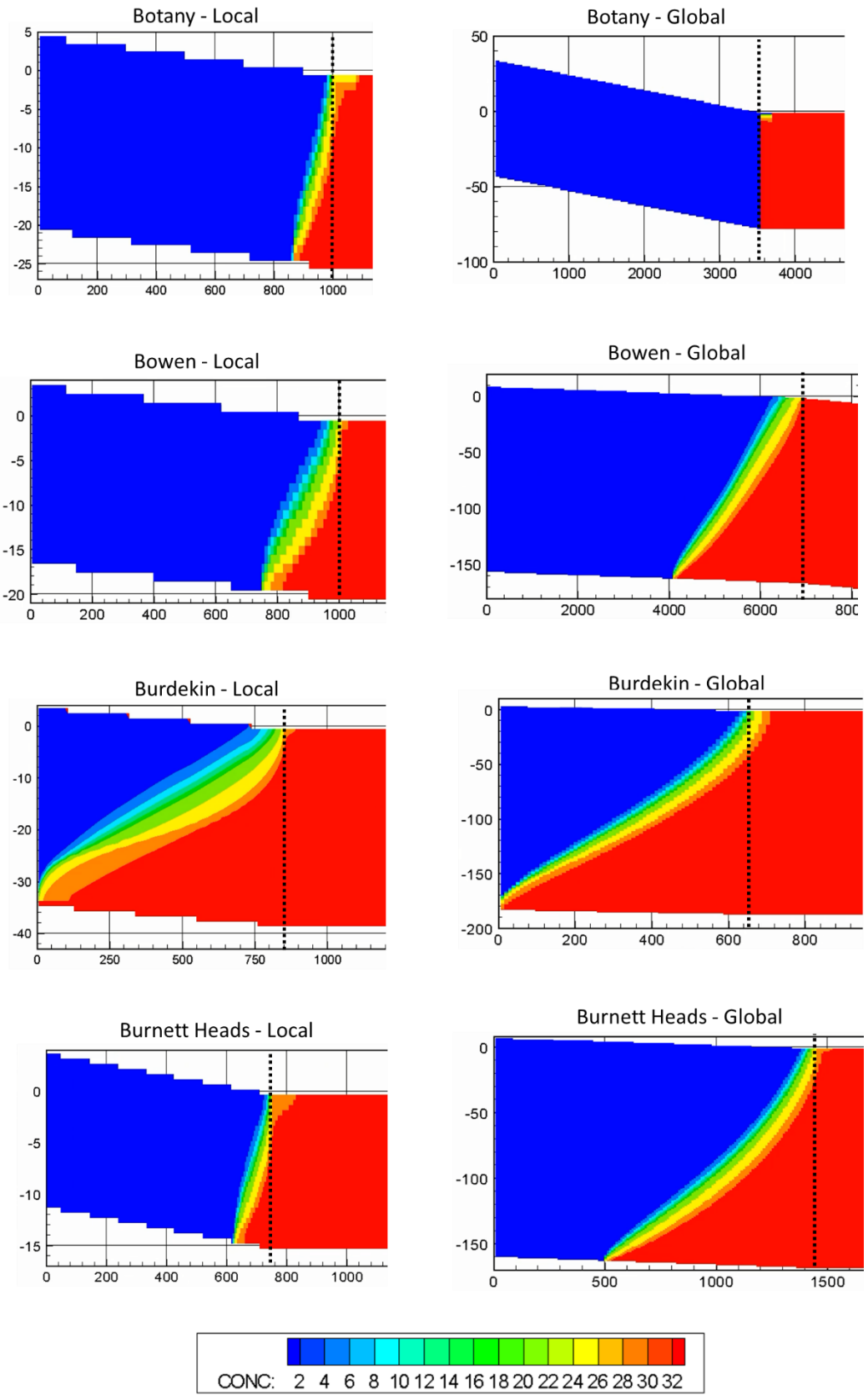

Figure 37: Concentration profiles (g Cl^-/l) for M3 - Part 1.

Note: The total length of the model was cropped in the images for a better visualization. The black dashed line represents the location of the coastline.

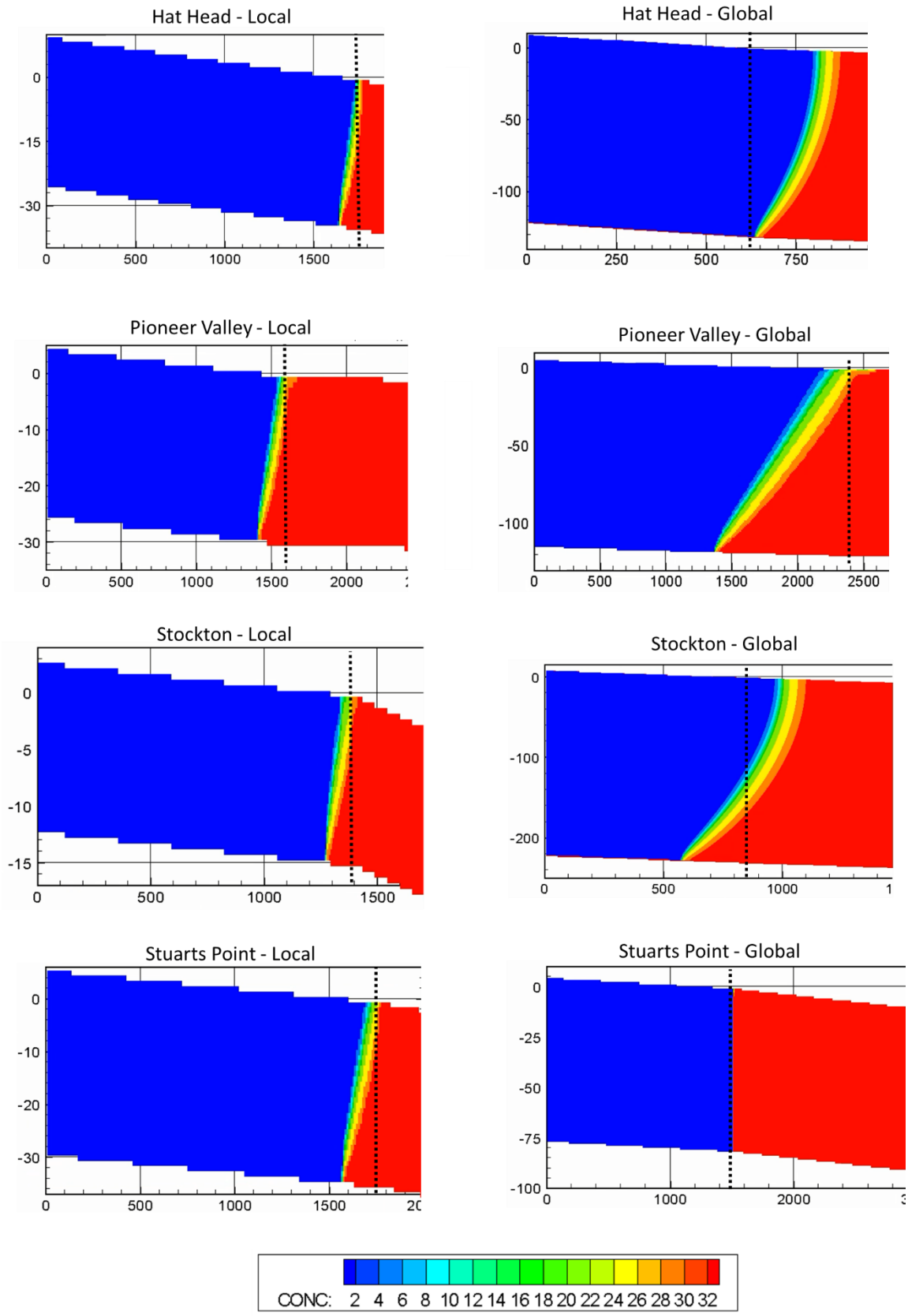

Figure 38: Concentration profiles (g Cl^-/l) for M3 - Part 2.

Note: The total length of the model was cropped in the images for a better visualization. The black dashed line represents the location of the coastline.

In the case of Hat Head, when using global datasets, the saltwater intrusion length was equal to 0 m, however, the effect observed here was different than in the other cases with no saltwater intrusion that were mentioned in the previous paragraph. Figure 39 shows that the intrusion shape exists but it has been shifted towards the sea. This is caused by the large head value at the inland boundary condition (9.6 m), which is located at a short distance from the coast (625 m) in comparison to the other areas. These conditions produced a large hydraulic gradient which is related to a high flow of freshwater discharge which is pushing the seawater away from the coastline boundary. The same occurs with Stockton-global, where the hydraulic gradient is producing the presence of freshwater in the offshore part.

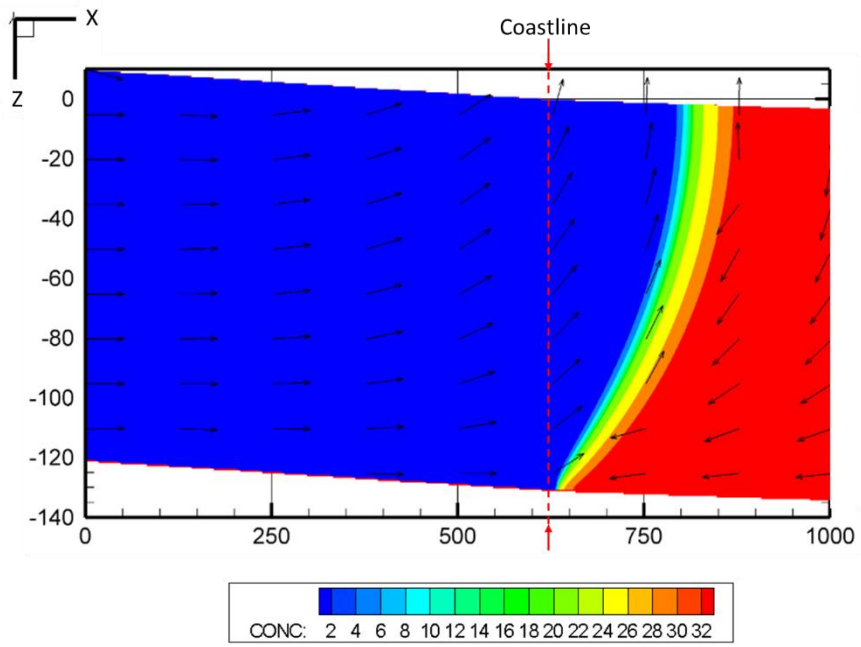

Figure 39: M3 – Concentration (g/l) - Hat Head simulation using global datasets.

These models simulated using SEAWAT set all model layer's type as confined as it was considered that the unsaturated zone would be very small. However, in the case of Stockton, there was a difference of some meters between the surface elevation at the inland boundary condition and the water table elevation. This particular condition of the case study area caused problems related to the flow vectors during the simulations. A better way to represent this case would have been choosing the model layer type as convertible, however, the latter caused convergence issues.

Figure 40 shows the freshwater volumes estimated for each of the case study areas. It is important to mention that in some areas, due to the characteristics of the system, such as the hydraulic gradient, it may occur that there is freshwater in the continental shelf area, as it was previously explained for Hat Heat. The values presented in Figure 40 consider this volume as well as the inland freshwater volume.

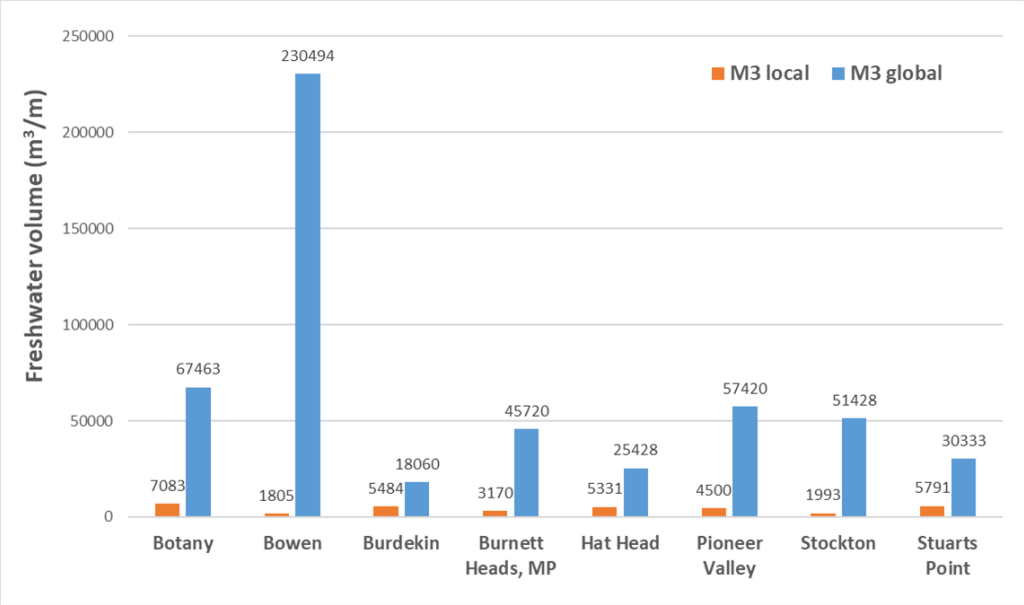

Figure 40: M3 – Freshwater volume (m^3/m)

4.2.4 Methodology 4 (M4): Complex conceptualization modelling using global datasets

In the case of Methodology M4, these models comprised only the use of global datasets coupled with more complex setups, while the simulations are done with SEAWAT. Out of the initial 8 case study areas, only 6 could be assessed using this methodology because the other 2 case study areas models were still in development process. Out of all the profiles available for each case study area (Zamrsky et al., 2018), one of them was selected as the most representative. Table 8 indicates which cross-sections were selected based on this methodology.

Table 8: M4 - Cross-sections selected

id_cs	Case study area
51219	Botany
50679	Bowen
50652	Burdekin
51110	Hat Head
51169	Stockton
51106	Stuarts Point

*id_cs (cross section identification number) from Zamrsky et al. (2018)

For each of the 6 case study areas, five realizations for geology and recharge (Section 3.3.4) were run, having a total of 30 simulations. Figure 41 shows an example of the first realization for Botany. The information for the other realizations can be found in Appendix G.

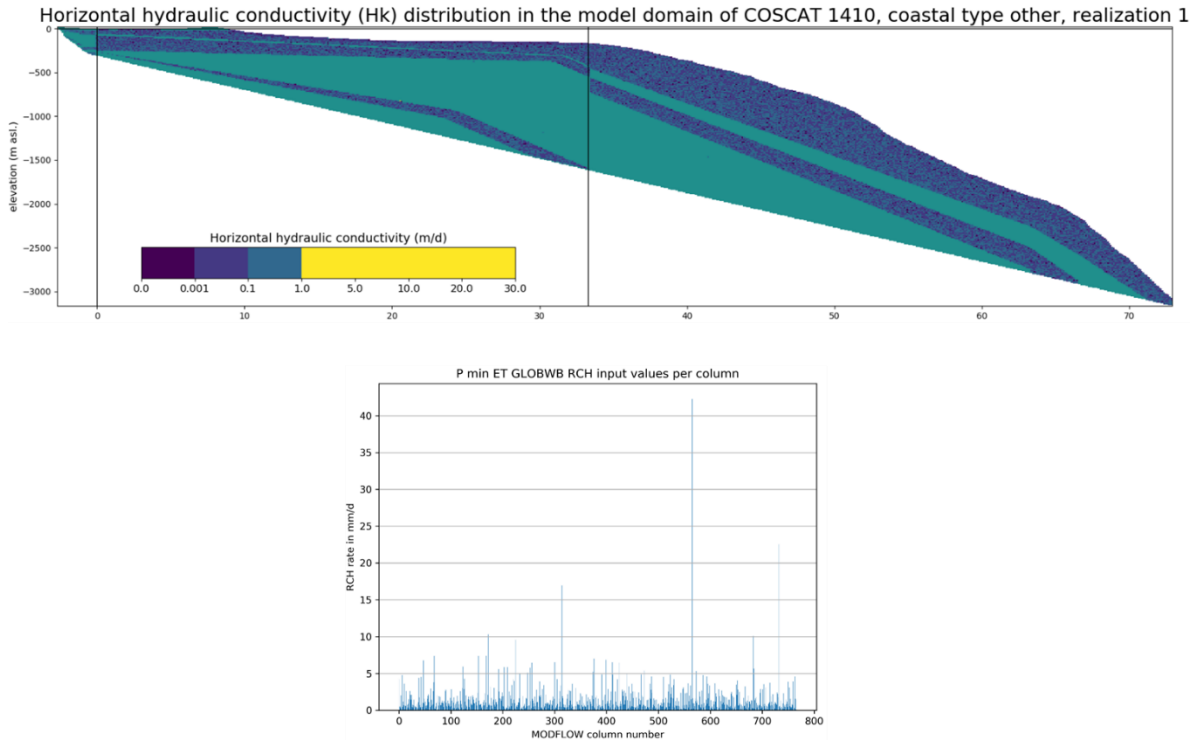

Figure 41: M4 – Botany - Geology and recharge input for the first realization.

The recharge considered has specific values per top model cell along the profile. These values were generated based on the mean and standard deviation obtained from fitting the recharge values of each area to a lognormal distribution. Because of this, very high recharge values were obtained in some of the cells. To counteract this effect, the conceptualization of these models included drains in the top layer to adjust the actual recharge that enters the model by working as an outflow condition for the overflow.

Figure 42 shows the average saltwater intrusion lengths for the available profiles. Details of the lengths obtained for the 5 realizations considered per area can be found in Appendix H. In the case of Stockton and Stuarts Point, these values are equal to zero, which represent that there is no intrusion as the saline groundwater is being pushed away from the inland area. In these cases, there are processes and specific conditions of the groundwater system which are causing this effect, as it will be explained.

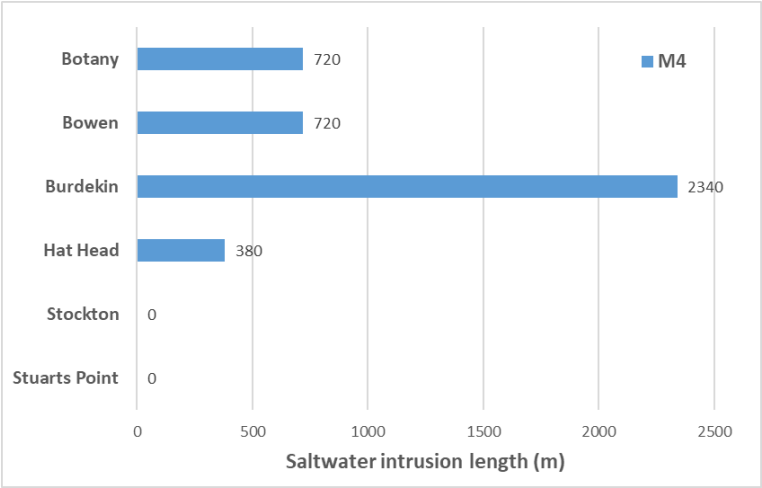

Figure 42: Methodology M5 – Saltwater intrusion length - average (m).

Figure 43 shows the concentration profiles for all the case study areas and their corresponding 5 realizations, where the variations of geology and the recharge are showing consistent results between the realizations.

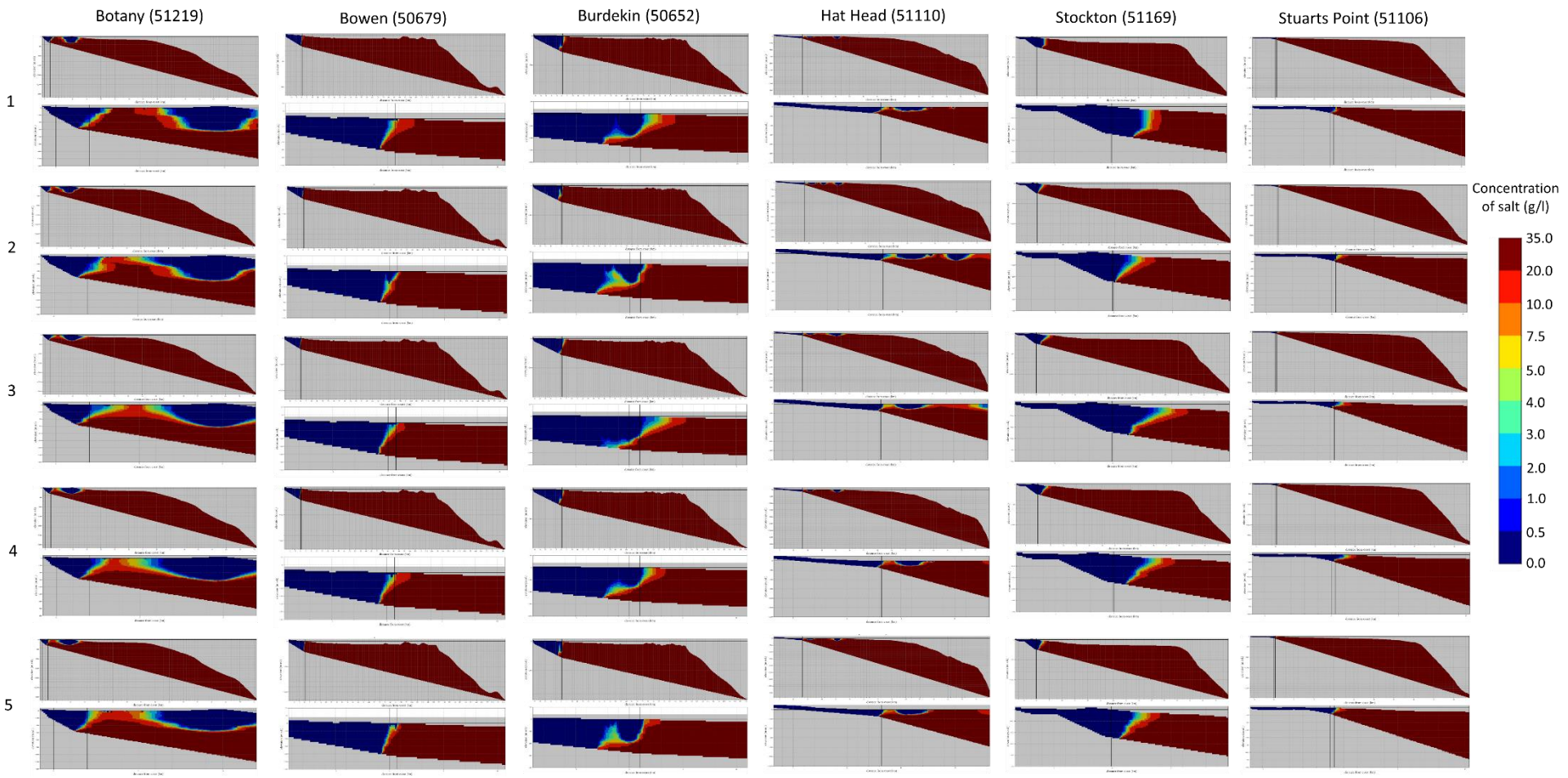

Figure 43: Concentration profiles (g Cl^-/l) for M4. Number on the right side represent the corresponding number of realization.

To explain why there is no saltwater intrusion present in these two cases, Figure 44 and Figure 45 show the head distribution for Stockton and Stuarts Point obtained after reaching the steady state for realization 1, as example. In both cases there are two sections of the profile with high elevation, also correlated with high head values (yellow colour in legend). These secondary zones with high topography are located very close to the coast, producing a large hydraulic gradient and high flux over a very short length. However, this flow cannot be discharged because of the presence of a superficial clay layer (as seen in the geological input graphs). The sum of all these effects caused that the freshwater flux is pushing the saltwater back and explains this "no intrusion" conditions.

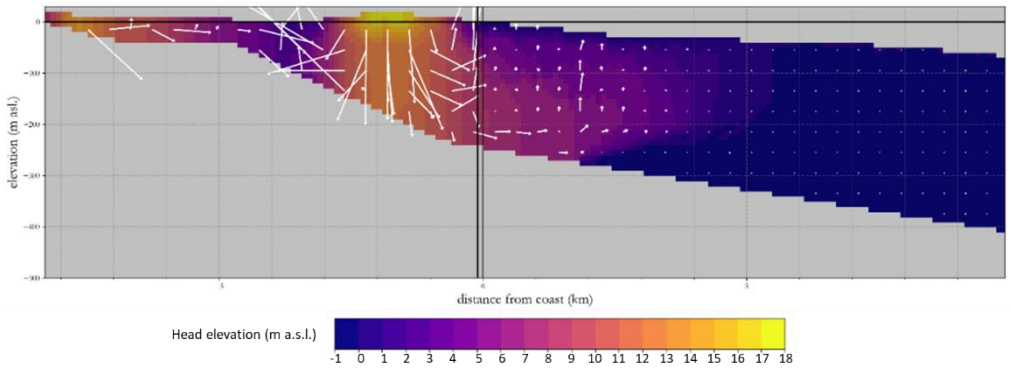

Figure 44: Head elevation (m a.s.l) – Stockton – Realization 1

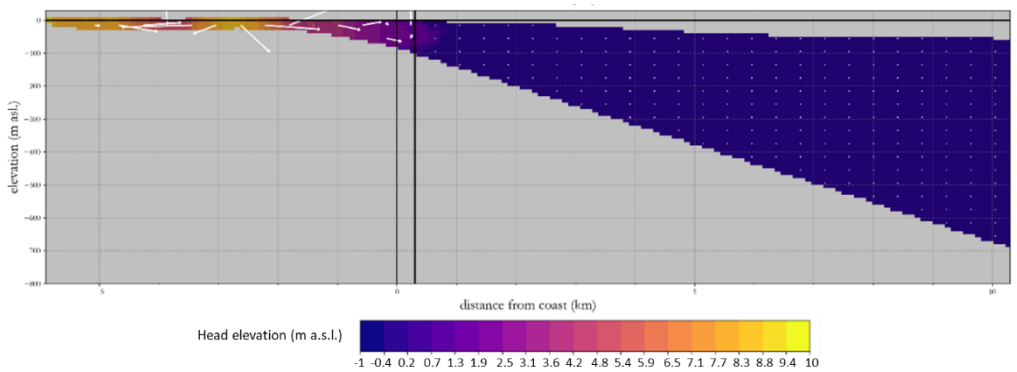

Figure 45: Head elevation (m a.s.l) – Stuarts Point – Realization 1

It is important to consider if the conceptualisation contemplated in these models is adequate to represent these particular topographical conditions, which are high elevation areas close to the coast. The model settings are considering all the layers of the groundwater system as confined, as it was assumed that the unsaturated zone would be negligible, however, under these conditions, it would have been advisable to consider this zone.

Figure 46 shows the freshwater volumes obtained in Methodology M4. It is also relevant to see in that the freshwater volumes found are not only located in the inland area, but also in the continental shelf part of the model (Appendix I), meaning that there is some fresh groundwater is being discharged from the coastal part of the groundwater system towards the sea part.

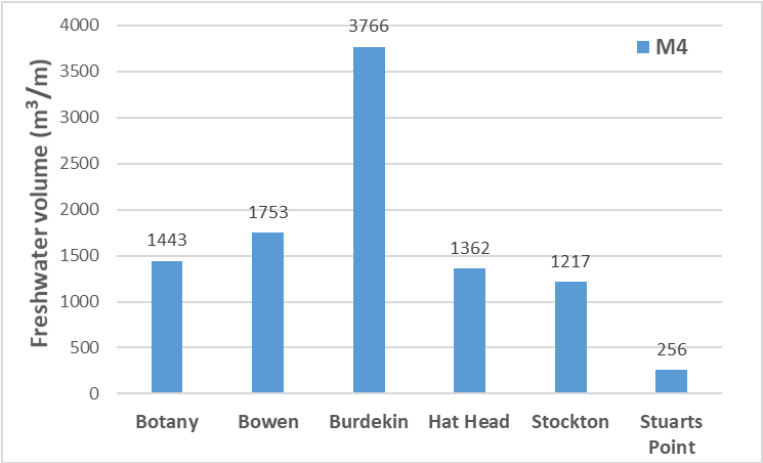

Figure 46: M4 – Freshwater volumes

It is important to note that the particular case of Botany (Figure 47) and Hat Head (Figure 48), these profiles cross other land areas nearby, so there is an extra freshwater recharge condition being applied in the shelf area, which is not related to the processes considered for the inland part of these zones. This is causing an overestimation of the shelf freshwater volume, as in Botany the extra freshwater offshore is ~50% of the total freshwater and this figure is ~30% for Hat Head.

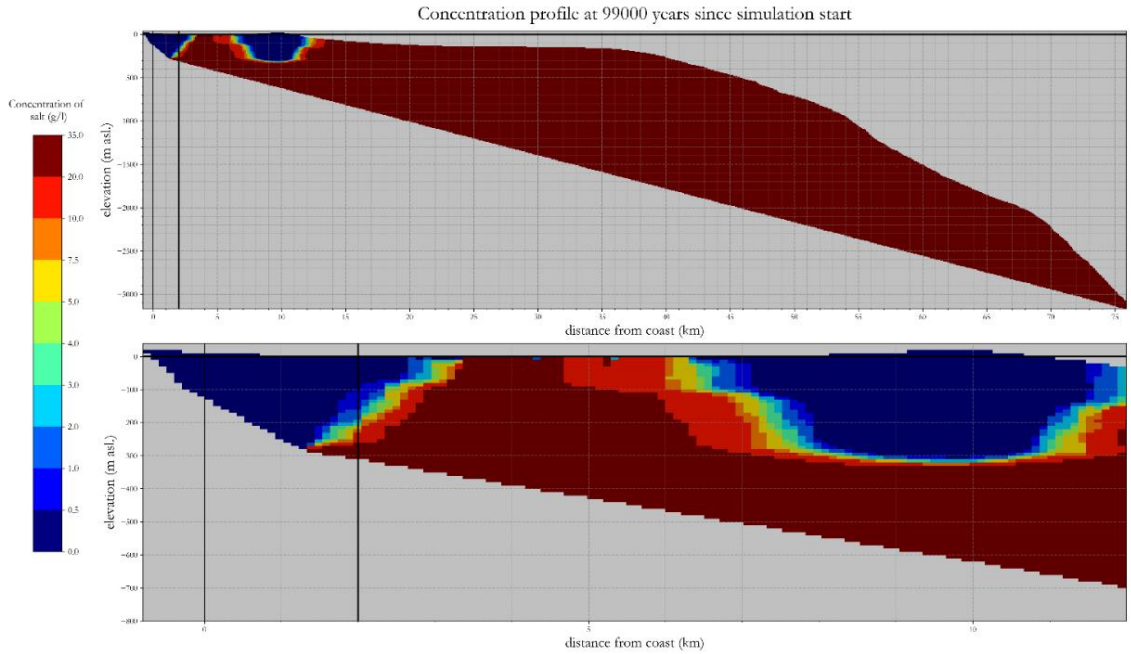

Figure 47: Concentration profile (g Cl^-/l)) – M4 – Botany.

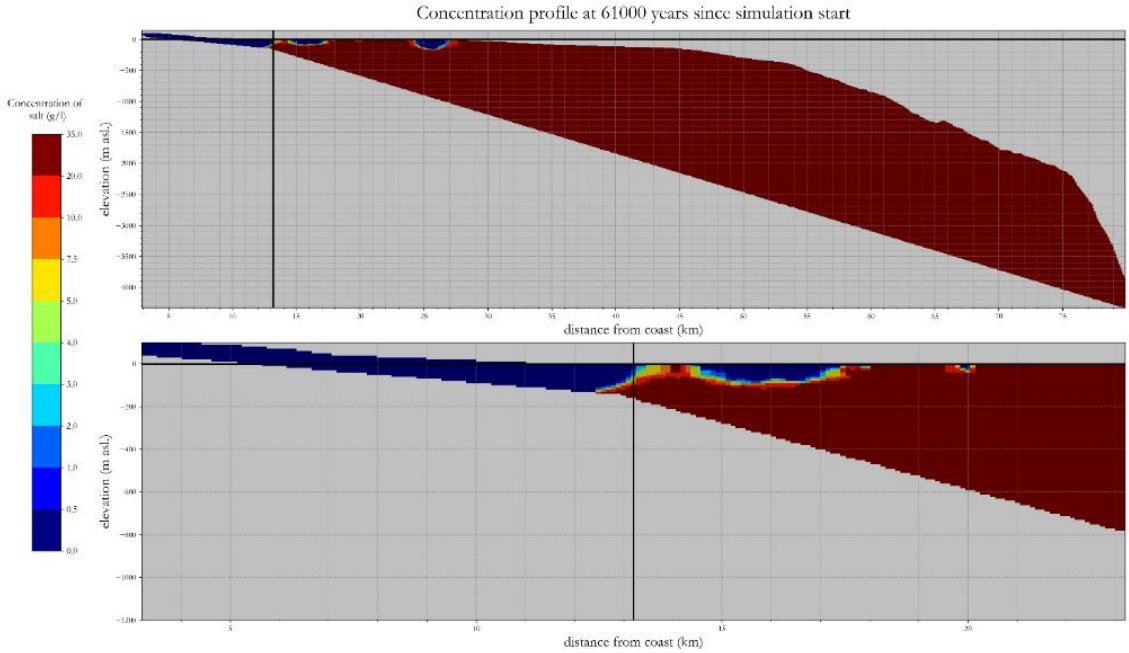

Figure 48: Concentration profile (g Cl^-/l)) – M4 – Hat Head.

4.2.5 Methodology 5 (M5): Complex conceptualization modelling using collected bore log data

In the case of the simulations using bore log data, the same 6 case study areas from M4 were used, which were the ones that already had available information for the modelling. For geology, the corresponding information was extracted from the bore log analysis (see Table 6) for each of the areas. The geology profiles obtained can be seen in Figure 49. For recharge, 5 realizations were considered, and these took the same values as in M4 (Appendix G). Using different randomizations for the recharge and keeping the geological distribution constant aimed to evaluate if the recharge uncertainty could be affecting the saltwater intrusion extent.

The geology profiles show that the two areas located on the north (Bowen and Burdekin) have differentiated sediment layers, while the other four (Botany, Hat Head, Stockton and Stuarts Point) are composed mostly of highly permeable sediments, mostly sand. The conceptualisation considered that the permeable sediments (gravel and sand) would have a hydraulic conductivity equal to 30 m/d, while for the less permeable sediments (silt and clay) it was equal to 0.01 m/d, based on the corresponding ranges presented by Freeze & Cherry (1979).

When comparing these values with the collected local-scale hydraulic conductivities (Table 7), the value considered in M5 for the permeable sediments is less than the median (40 m/d) of the values off all case study areas. Figure 50 represents the concentration profiles for this methodology. As in M4, the overall response on the simulation show similar behaviour among the realizations considering the variable recharge and geology.

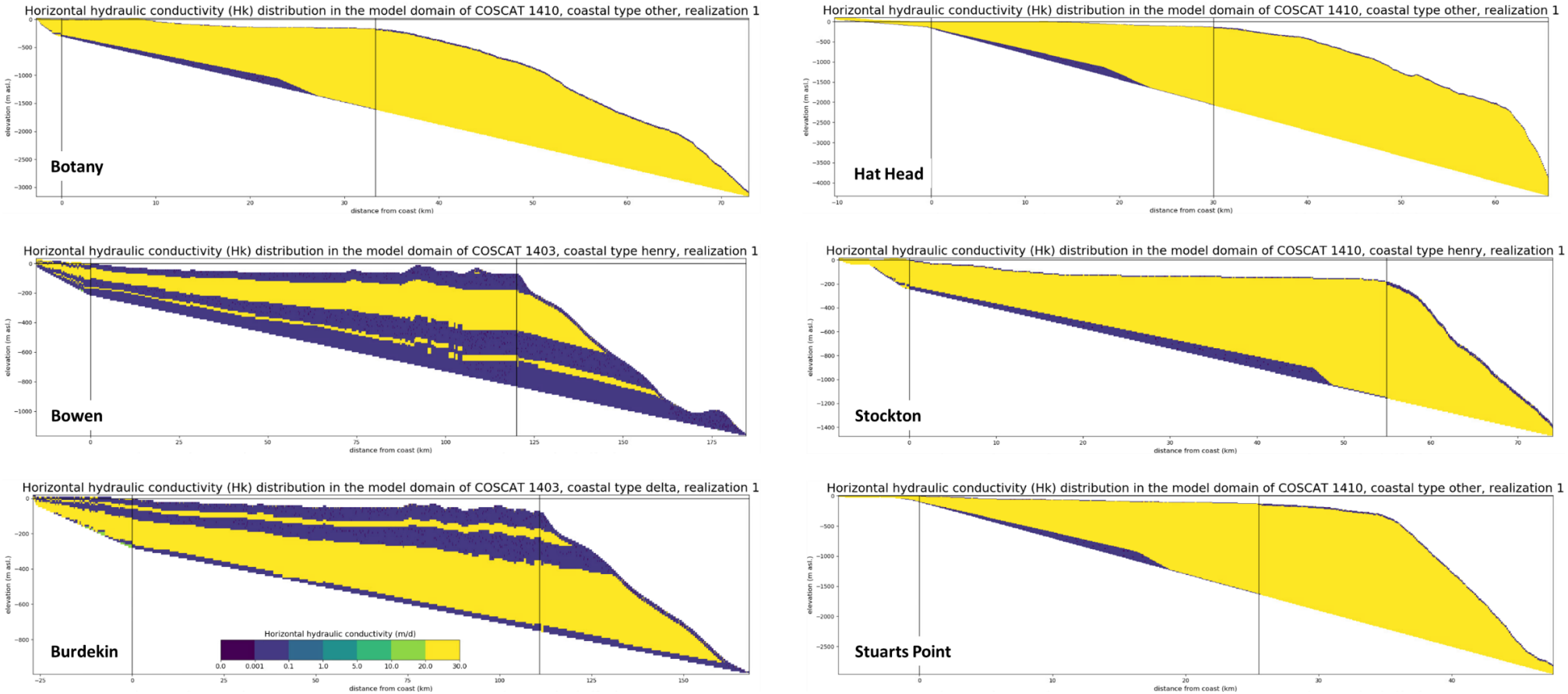

Figure 49: M5 – Geological layers based on bore logs analysis.

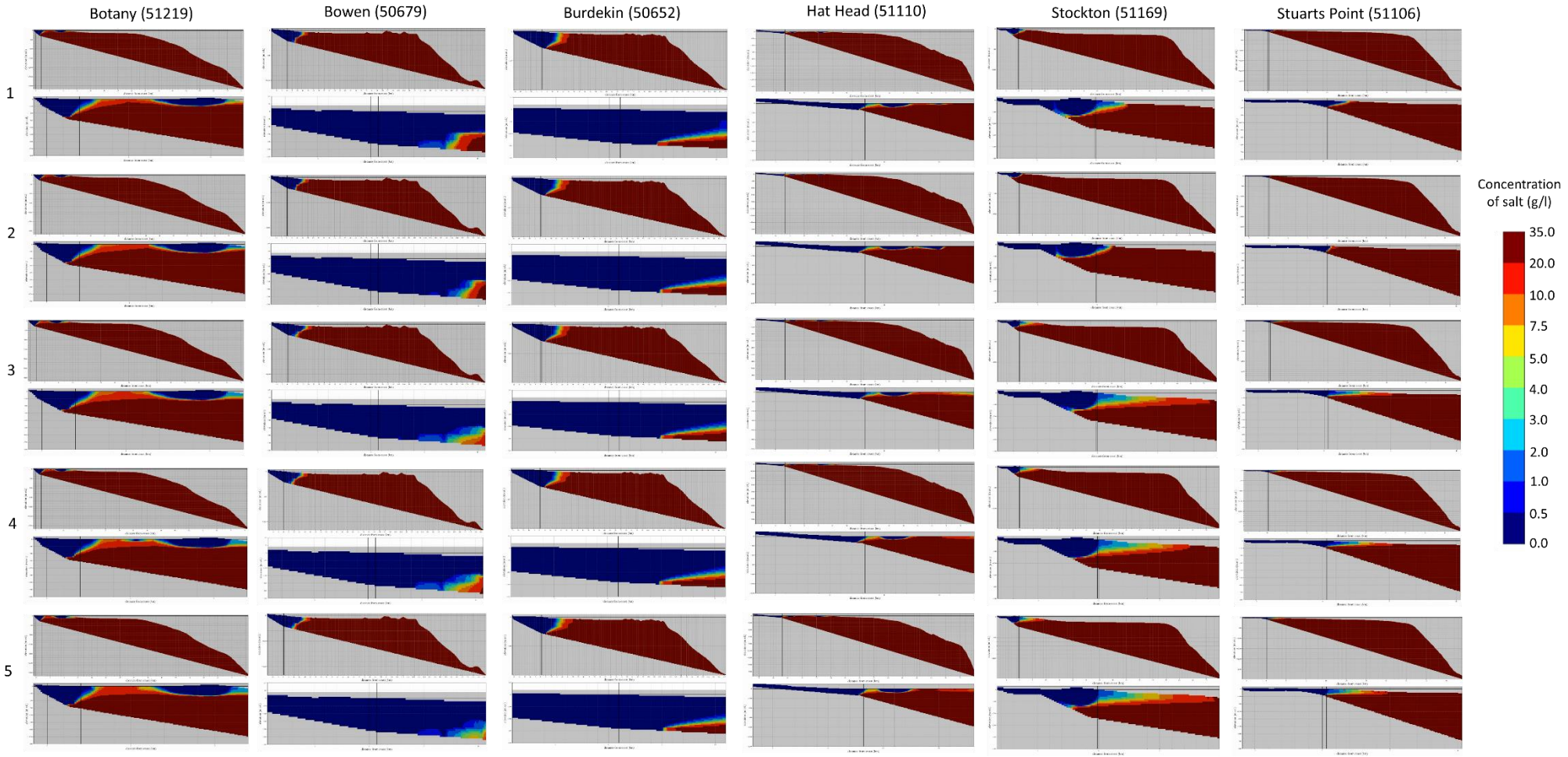

Figure 50: Concentration profiles (g Cl^-/l) for M5. Number on the right side represent the corresponding number of realization.

Figure 51 shows the average saltwater intrusion length calculated based on the 5 realization for the 6 case study areas evaluated. It was seen that half of these areas show no intrusion after the modification of the hydraulic conductivity to values estimated from the bore logs analysis. Stockton shows the highest intrusion equal to 2280 m, while Hat Heads shows the lowest, being 460 m. Appendix J contains the detailed information of the intrusion lengths obtained for all the five realizations per zone.

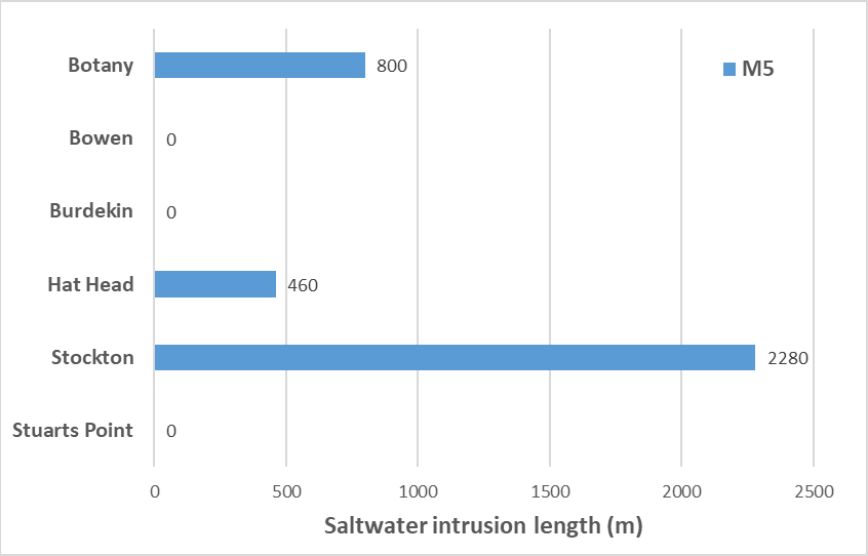

Figure 51: M5 – Average saltwater intrusion length (m).

Figure 52 shows the freshwater volumes in the inland and coastal shelf zones of the model. Burdekin is the area that shows the largest freshwater volume, while Stuarts Point is the smallest. Appendix K has more information about the volumes obtained for each area in all the realizations.

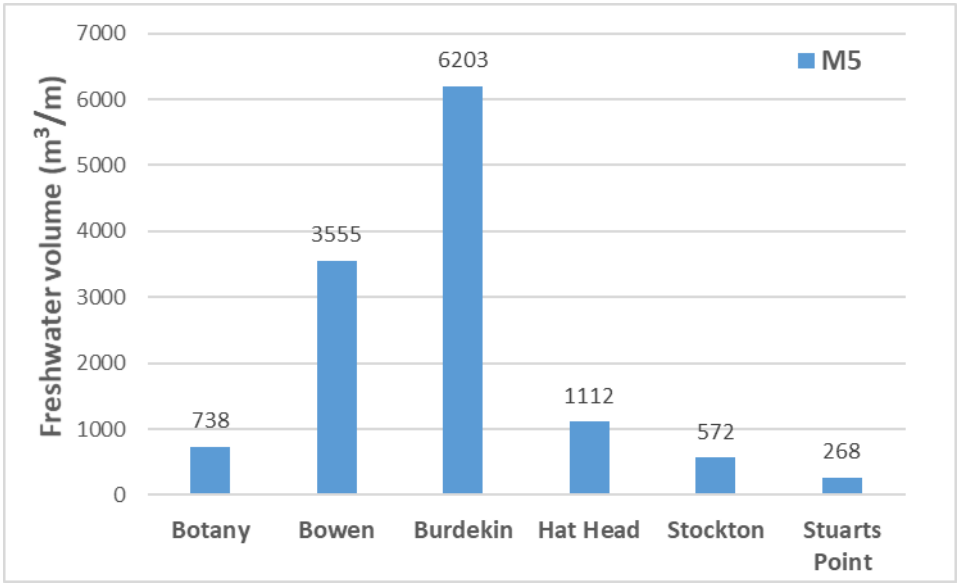

Figure 52: M5 – Freshwater volume (m^3/m).

4.2.6 Comparison between methodologies

This section presents a comparison between the results obtained from each of the methodologies, to assess how different these are when applied to the evaluation of the freshwater-saltwater distribution in coastal aquifers.

a) Saltwater intrusion length

Figure 53 shows the comparison of the saltwater intrusion lengths calculated using the five methodologies in evaluation and considering local or global-scale data, if applicable. In general, it is seen that the lengths obtained using M1-local, M2-local and M3-local have similar values between each other. This also occurs in the case of M1-global, M2-global, M3-global. For M4 and M5, these lengths present variable values and do not follow a trend between each other or the other methodologies. Because of this, the analysis will first relate M1, M2 and M3, while the second part will be focused on M4 and M5.

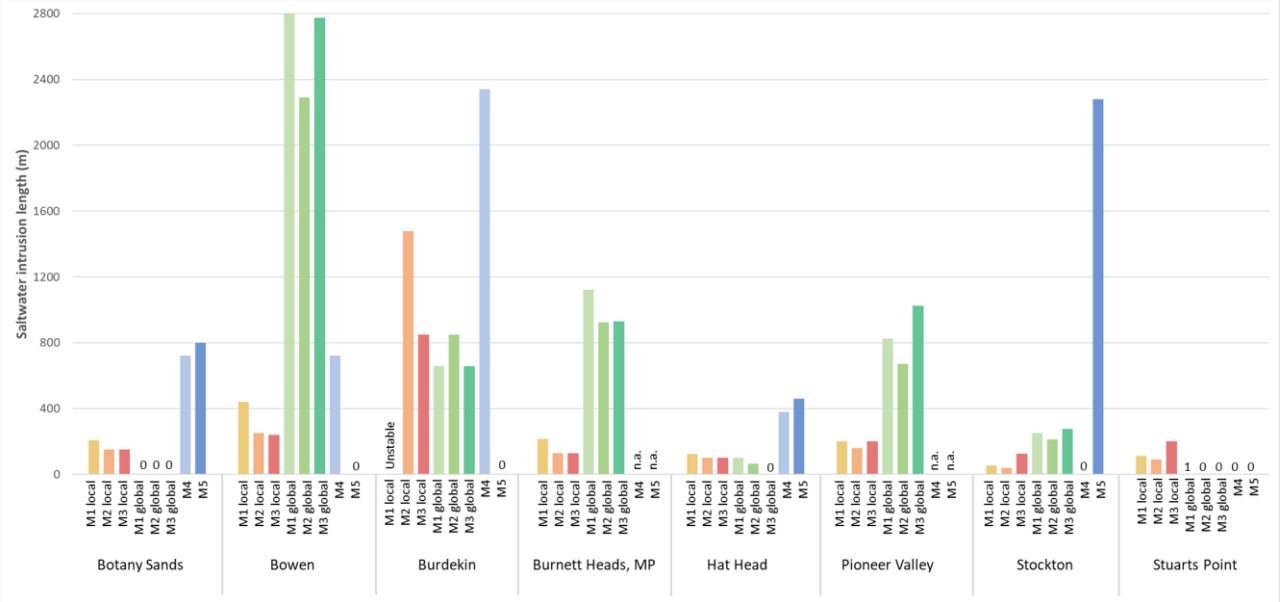

Figure 53: All methodologies - Saltwater intrusion length (m)

M1, M2 and M3

While evaluating the results from M1, M2 and M3, it was seen that their results are similar between each other when considering the same input data. This means that these three methodologies are consistent between each other.

In the case of M1 and M2, the conceptualization is similar, using a rectangular area starting from the coast up to the inland boundary condition in the X axis and the aquifer thickness in the Z axis. In addition, the boundary conditions are the ones that define the head inland and at the coast, and the net recharge. However, M3 has the variation of considering the area in the continental shelf as part of the model, being able to represent offshore processes, and it also considers the topography. Another

characteristic is that in M3, due to the presence of the drain boundary condition on the surface, the net recharge entering the model should be less than in the case of M1 and M2 and could represent a closer-to-reality system as it is limiting the recharge entering the model.

About the offshore processes, Hat Head showed that due to the high hydraulic gradient found, the freshwater flow towards the sea was very large, producing the presence of freshwater in the continental zone area. This process was only seen in M3, and it was not possible to be identified in M1 or M2 given the geometry of these model's conceptualisations.

In M3, at first it would be expected to have a larger saline intrusion as there is less recharge, due to the presence of the drains, to reduce this process. However, there is no a clear trend showing that the saline intrusion in M3 is larger than in M1 or M2 (where no drains are considered), meaning that probably the other boundary conditions could be compensating this effect.

It is seen that in all cases the estimated global hydraulic conductivity is less than the local one. In Botany Sands and Stuarts Point it is clear how this parameter is influencing the behaviour of the intrusion length: in M1-global, M2-global and M3-global this is equal to about 0 m due to the very small hydraulic conductivity value (0.0001 m/d). This parameter is important; however, it is not the only parameter influencing the system. Bowen, Burnett Heads, Pioneer Valley and Stockton show that the saltwater intrusion length in M1-global, M2-global and M3-global are larger than M1-local, M2-local and M3-local, respectively; while for Hat Heads, both groups show similar results. Comparing the relation between the inland head and the distance from the coast to this condition, this parameter is larger for the global data than for the local data. This means that there is a larger head gradient pushing the water towards the sea in the global case, however, its hydraulic conductivity is low, being the density effects more important.

M4 and M5

It was decided to analyse M4 and M5 separately from the other three methodologies, as their input data and conceptualisation differs from the others. This is consequent when seeing that the lengths calculated are not close to the ones obtained using the other methodologies.

At first, it was expected that M4 would have similar results to M1-global, M2-global and M3-global since all of them are considering global datasets as input information. However, due to the different and more complex approaches in M4, such as the condition of spatially-variable recharge and the geological heterogeneity, these are differently influencing the system in comparison to the other three methodologies mentioned.

When comparing M4 and M5, it was also seen that the results between each other were not similar in some cases, as the difference between them is the sediment layers and the hydraulic conductivity. In

the case of Stockton, M5 presents intrusion, where in M4 it is equal to 0 m. Another area where important differences are found is Bowen, where M4 shows around 700 m of intrusion, but M5 shows 0 m. As well, Burdekin shows an intrusion of around 2400 m in M4 and no intrusion in M5. Botany Sands and Hat Head present more similar values of M4 and M5 between each other but being M5 larger in both cases.

To evaluate these methodologies, it is decided to separate them into two groups based on the geology type defined in M5: (1) groundwater systems with highly permeable sediments (Botany Sands, Hat Head, Stockton and Stuarts Point) and (2) groundwater systems with layers of high and low permeability (Bowen and Burdekin).

In the case of the first group (1): the main characteristic is that the geology of these groundwater systems is modified from M4 where they have intercalated layers of high and low permeable material and a capping clay layer on the surface of the continental shelf, to only having highly permeable material and a thin superficial clay layer. An example is shown in Figure 54 for Botany Sands.

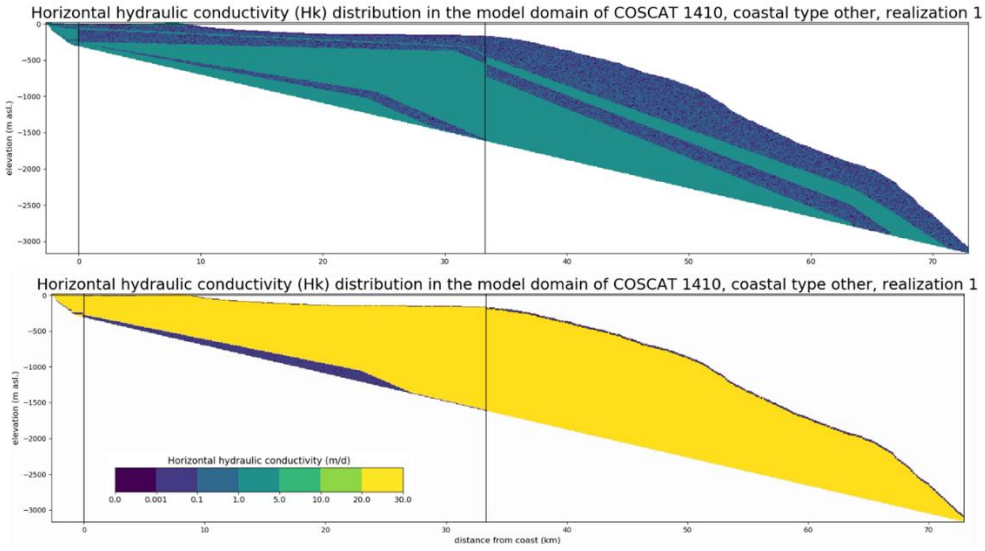

Figure 54: Botany Sands - Comparison between geology for M4 (realization 1) (upper) and M5 (lower).

Evaluating the heads for Stockton (Figure 55), in M4 the heads at the dune nearby the coast were larger than in M5, where they have decreased. In M4, the larger hydraulic gradient was causing the freshwater flow to be pushed towards the sea, causing no intrusion. In M5 the heads at the dune are lower, and now the large heads are occurring far from the coast. This has reduced the hydraulic gradient meaning that the discharge flow is less, so there are more possibilities for the saltwater intrusion to occur as there is a lower flow coming from inland. It is likely that the larger heads in M4 were caused by the clay capping layer that existed in this case, which is not occurring in M5 due to the change in geology. In the case of Botany Sands and Hat Head, the same effect is occurring but at a

lower scale, therefore there is saltwater intrusion in M4 (and not everything is flushed as in Stockton), but still this intrusion is less than in M5, where there is no clay capping layer.

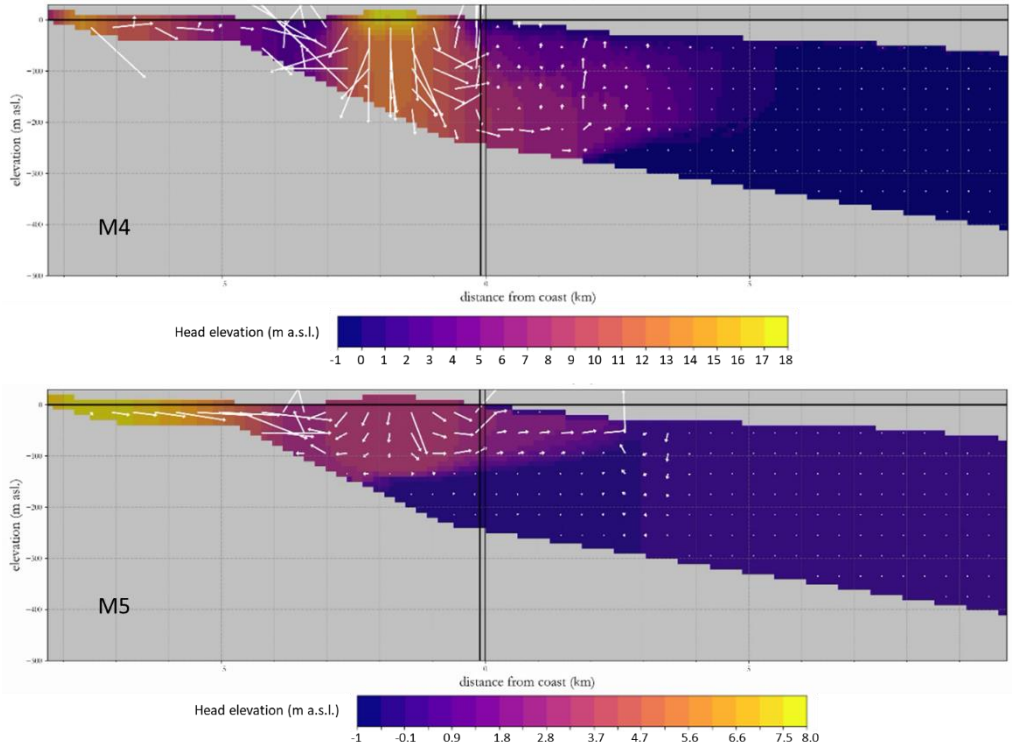

Figure 55: M4 and M5 – Stockton – Hydraulic Head (m).

In the case of Stuarts Point (Figure 56), M4 and M5 show no intrusion, however, when checking the concentration plots, it is possible to compare what is occurring in the shelf area. In the case of M4 (Figure 57), the lower hydraulic conductivity reduces the movement of freshwater towards the sea, encouraging saltwater intrusion to happen, specifically due to the presence of the clay capping layer stopping the flow. In M5, the hydraulic conductivity is larger, so it is possible to have an easier flow movement which is pushing the saline groundwater away from the coast.

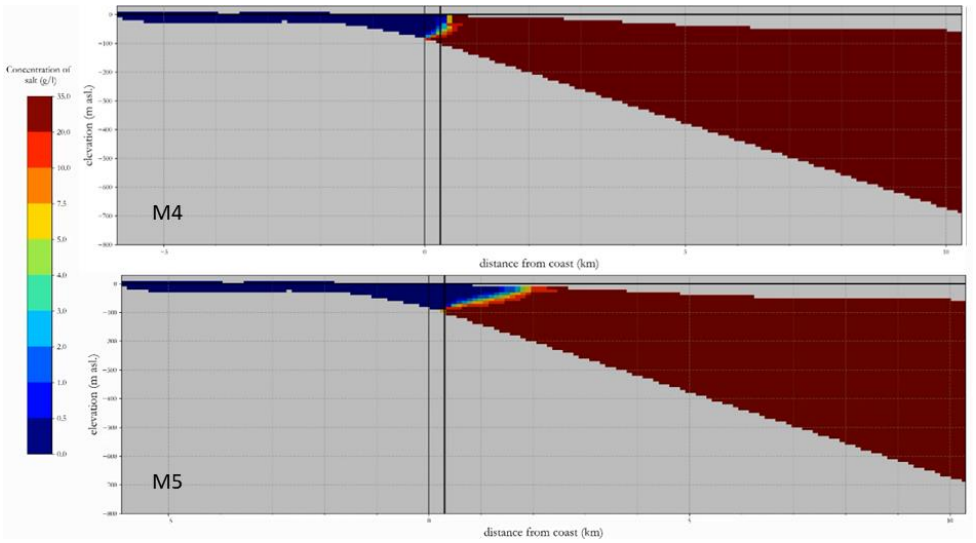

Figure 56: Stuarts Point - Comparison of saline intrusion in M4 and M5 – First realization.

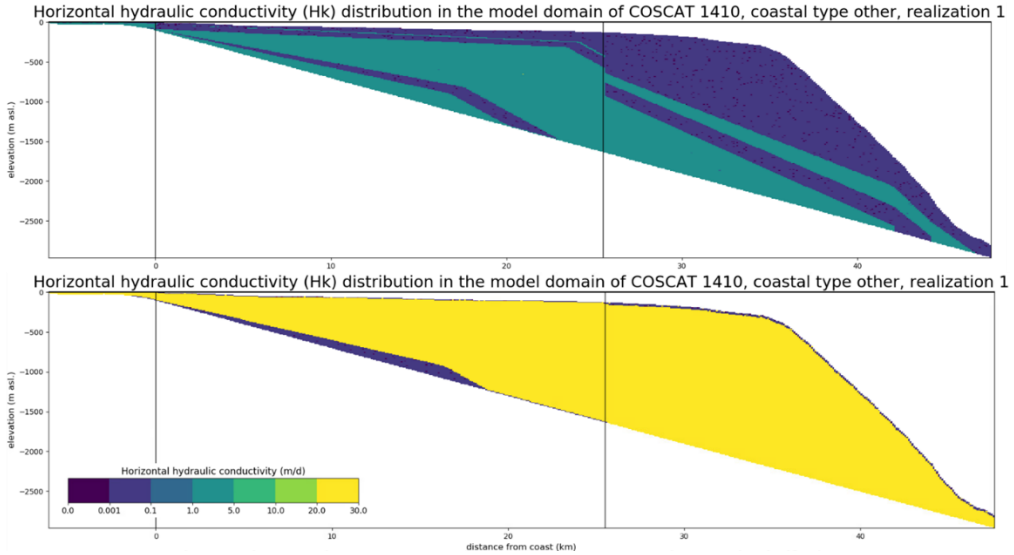

Figure 57: Stuarts Point - Comparison between geology for M4 (realization 1) (upper) and M5 (lower).

In the case of the second group, where Bowen and Burdekin (Figure 58) are found, there are intercalated hydraulic conductivity layers of high and low permeability sediments. These two cases show the same behaviour, where M4 presents saltwater intrusion but in the case of M5 it is 0 m. According to the geology of M4 and M5, there is a thick clay layer on top of the system which is affecting the possibility of discharging freshwater at the coast, causing an increase of heads in the system. However, in M5 the hydraulic conductivity value of the highly permeable material is equal to 30 m/d while in M4 it is between 0.1 and 1 m/d. In both cases, the groundwater flow tries to discharge but it is not possible because of the clay layer. However, in M5, due to the larger hydraulic conductivity, it is easier for freshwater to continue to move horizontally towards the shelf area, avoiding saltwater intrusion. In M4, the same process occurs but the magnitude differs: the lower hydraulic conductivity

does not allow for an easy movement of freshwater, so saltwater intrusion occurs driven by the density variation effects.

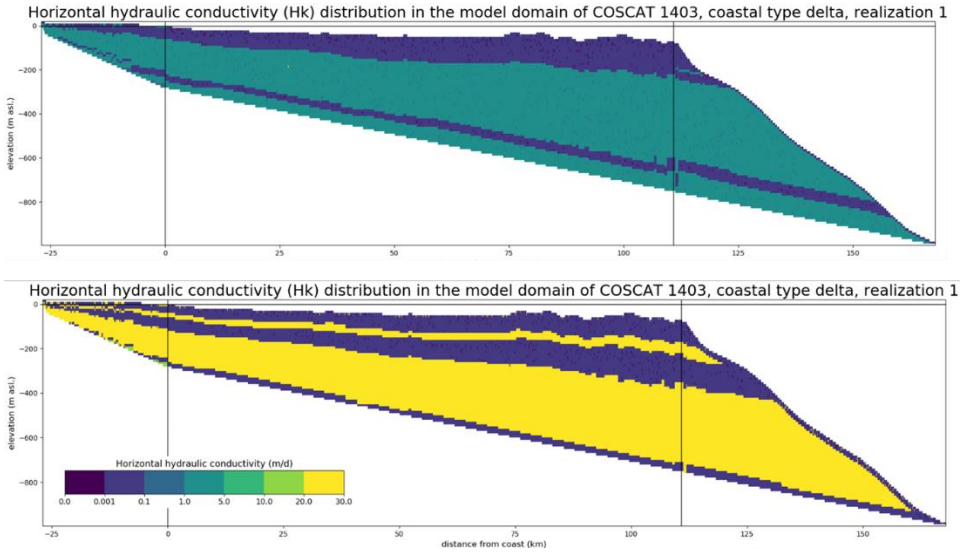

Figure 58: Burdekin - Comparison between geology for M4 (realization 1) (upper) and M5 (lower).

b) Freshwater volume

Figure 59 shows the calculated freshwater volumes that can be found in the inland and continental shelf area. It is seen that for M1-global, M2-global and M3-global, these values are very high in comparison to the ones obtained for M1-local, M2-local, M3-local, M4 and M5. In the case of M4 and M5, the volumes provided by the methodology should be checked as they seemed to be very small given the size of the area in evaluation.

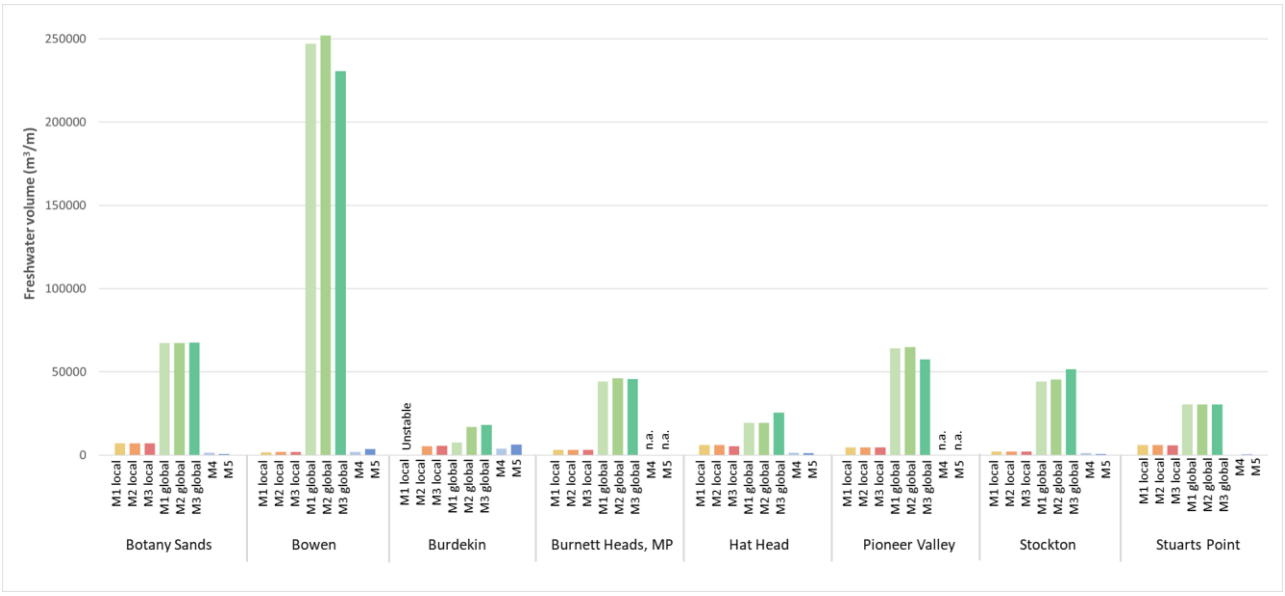

Figure 59: Freshwater volume in inland and continental shelf area (m3/m)

To use absolute volumes for comparison may not be adequate because of the following issues: (1) the uncertainty in the volumes from M4 and M5, (2) the global models have much larger dimensions than the local ones so, in consequence, the freshwater volume available will be larger and (3) the different porosities considered between the models could affect the calculated volumes as it defines the total available water. As way to overcome these issues, it was decided to work with normalised volumes, which were calculated dividing the actual freshwater volume in the model by the maximum freshwater volume that could be found in this area and calculated as a percentage, to know how much freshwater is available in relation to the maximum freshwater volume available inland. However, for a better comparison, only the volumes in the inland part of the models were considered. This applied to M3, M4 and M5 as M1 and M2 do not consider the continental shelf area. Figure 60 shows that, in most cases, this percentage is over 80%, meaning that in relative terms, there is a large availability of fresh groundwater inland.

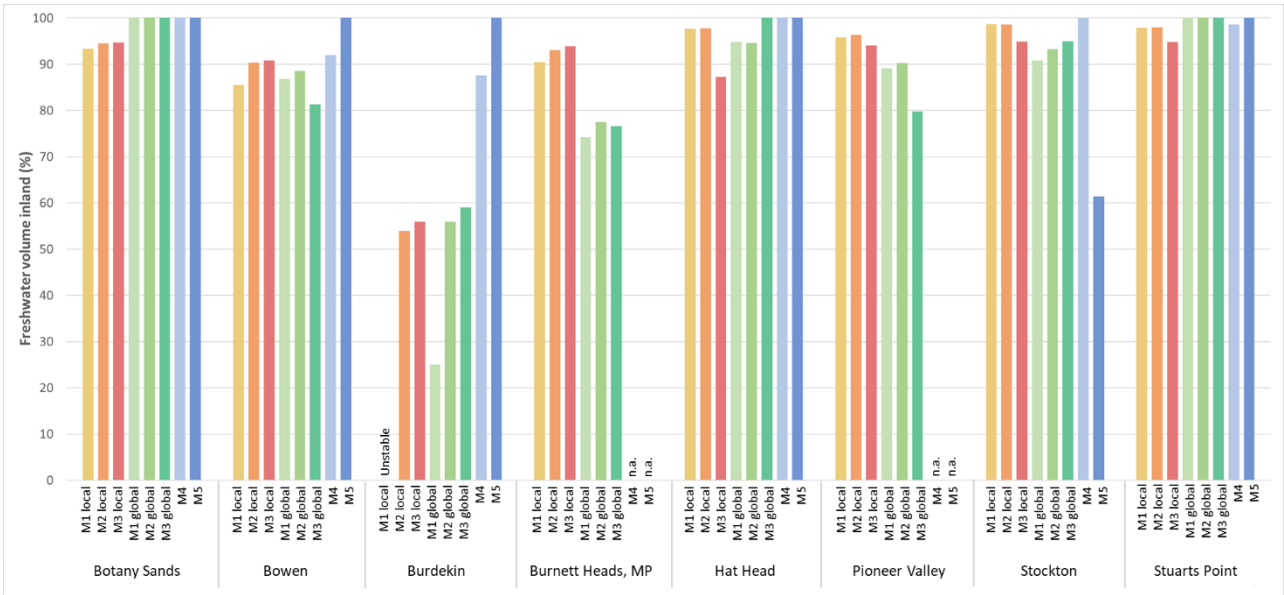

Figure 60: Freshwater volume inland (%)

In the case of Stockton-M5, this value shows a big difference from the others, mainly because of the geological information considered, as this is the only variable different from M4.

For Burnett Heads, there is a clear difference from the inland freshwater percentage obtained using the local information in M1, M2 and M3 than when using the global one applied in the same methodologies. Nonetheless, the difference between the two groups is only around 10%.

For Burdekin, M4 and M5 show that most of the area is freshwater, meaning that there is no intrusion or that it is minimal. On the other hand, M2 and M3 show that the percentage of freshwater inland is around 50%. This fact indicated that the methodologies are representing differently the saltwater intrusion most likely due to geology variations.

4.3 Climate change scenarios simulations

These simulations were performed to evaluate the possible future risks for these groundwater systems under different climate change scenarios. The model used in this evaluation is the one used in M5, as it considered to be the most complex.

Due to the time availability, the climate change simulations were done for two case study areas: Stockton and Stuarts Point.

4.3.1 Case 1: Stockton

For Stockton, Table 9 and Table 10 show the saltwater intrusion length (in kilometres) for the global and local recharge values, respectively. The matrix shows the multipliers applied to the recharge and the increases in sea level considered.

Table 9: Saltwater intrusion length (km) – Stockton – Global RCH

ΔH_{sea} \ K_{RCH}	0.25	0.75	1	1.25
0	3.5	2.8	2.5	2.2
0.2	3.6	2.8	2.6	2.1
1	3.8	3.6	3.2	3.0
2	4.2	4.1	3.8	3.8

Table 10: Saltwater intrusion length (km) – Stockton – Local RCH

ΔH_{sea} \ K_{RCH}	0.25	0.75	1	1.25
0	3.6	3.5	3.5	3.4
0.2	3.8	3.5	3.5	3.4
1	3.8	3.8	3.8	3.6
2	4.2	4.2	4.1	4.1

Note: K_{RCH} = Recharge multiplier, ΔH_{sea} = Change in sea level (m)

The results from both datasets (using a constant recharge value from a local source or using the variable-per-cell recharge estimated from global sources) follow a similar pattern. It is observed that as the sea level increases, the saltwater intrusion will also increase, while in the case of recharge, as it is reduced, the intrusion will increase as suggested in the analytical solutions. This effect indicated that the input of a fresh groundwater source is helping to reduce the intrusion. Based on the baseline case, where there is no sea level rise and the recharge multiplier is equal to 1, the saltwater intrusion has a length expected to be equal to 2.5 km in the global case and 3.5 km in the local case.

In both cases, the most critical scenario is when the sea level increases two meters and the recharge is reduced in 25%. Here, the saltwater intrusion length is the same for both input data sources and it is equal to 4.2 km, meaning that it increased 1.7 km for the global recharge and 0.7 km for the local recharge.

The most favourable scenario is when there is no sea level rise and the recharge is increased in 25% (multiplier = 1.25). The results using the global recharge gave an intrusion value equal to 2.2 km while, when using the local recharge, it is equal to 3.4 km. In the first case, the intrusion decreased 0.3 km and in the second case it reduced 0.1 km.

Table 11 and Table 12 show the freshwater volumes when considering global and local recharge values, respectively. As there is uncertainty in the volumes, the comparison will be qualitative, more than quantitative. The volumes, as expected, follow the same pattern as the intrusion lengths. When comparing the baseline scenario with the less favourable one, using global recharge or local, the freshwater volume decreased in around 60%.

Table 11: Freshwater volume (m3/m) – Stockton – Global RCH

ΔH_{sea} \ K_{RCH}	0.25	0.75	1	1.25
0	404	504	551	605
0.2	378	486	527	569
1	302	392	424	459
2	231	311	393	393

Table 12: Freshwater volume (m3/m) – Stockton – Local RCH

ΔH_{sea} \ K_{RCH}	0.25	0.75	1	1.25
0	335	432	458	486
0.2	313	415	441	460
1	255	323	346	365
2	202	256	276	291

Note: K_{RCH} = Recharge multiplier, ΔH_{sea} = Change in sea level (m)

4.3.2 Case 2: Stuarts Point

For Stuarts Point, both global and local recharge scenarios showed that for all the recharge multipliers evaluated and in the conditions of no sea level rise or a sea level rise equal to 0.2 m, the intrusion will be 0 m in all cases. Variations in the intrusion start to be seen when the sea level rise reaches 1 m, because the saltwater intrusion had not reached the coastline and it is in the continental shelf area. In general, the saltwater intrusion obtained using local recharge are larger than for the global recharge because the recharge in the latter is larger.

In the first case, the intrusion reaches a maximum value when it is equal to 0.6 km under the conditions of sea level rise equal to 2 m and a hydraulic conductivity multiplier of 0.25 m/d. For the local recharge, it shows a maximum intrusion of 0.55 km for a multiplier equal to 0.25 and a sea level rise equal to 2 m.

Table 13: Saltwater intrusion length (km) – Stuarts Point – Global RCH

ΔH_{sea} \ K_{RCH}	0.25	0.75	1	1.25
0	0	0	0	0
0.2	0	0	0	0
1	0.2	0.15	0.1	0.1
2	0.6	0.5	0.5	0.5

Table 14: Saltwater intrusion length (km) – Stuarts Point – Local RCH

ΔH_{sea} \ K_{RCH}	0.25	0.75	1	1.25
0	0	0	0	0
0.2	0	0	0	0
1	0.2	0.2	0.15	0.1
2	0.55	0.5	0.5	0.5

Note: K_{RCH} = Recharge multiplier, ΔH_{sea} = Change in sea level (m)

Table 15 and Table 16 show the freshwater volumes for the global and local recharge considerations. In both cases the most critical scenario is when only the 25% of the current recharge is occurring and

the sea level rise is equal to two meters. In both cases it is deduced that the freshwater volumes have been reduced with around 30% of the baseline condition.

Table 15: Freshwater volume (m3/m) – Stuarts Point– Global RCH

ΔH_{sea} \ K_{RCH}	0.25	0.75	1	1.25
0	262	281	287	287
0.2	251	262	263	266
1	227	232	234	235
2	199	205	205	205

Table 16: Freshwater volume (m3/m) – Stockton – Local RCH

ΔH_{sea} \ K_{RCH}	0.25	0.75	1	1.25
0	255	264	268	270
0.2	247	255	262	261
1	224	228	230	231
2	194	201	205	205

Note: K_{RCH} = Recharge multiplier, ΔH_{sea} = Change in sea level (m)

Chapter 5 Discussion

The main objective of this research was to compare the different available methodologies to estimate the freshwater-saltwater distribution in coastal aquifers. This is related to three research questions which are necessary to achieve this goal. The corresponding discussions to each of them are presented in this chapter.

Research question 1: What are the differences between the local-scale and global-scale data collected for the case study areas to be used in the proposed methodologies to evaluate the freshwater-saltwater distribution in coastal aquifers?

The first research question aimed at evaluating the different data sources available to be used as input data in the methodologies for the evaluation of the freshwater-saltwater distribution in coastal aquifers. The sources used were local-scale information and global-scale datasets. At the beginning of the thesis, it was expected that the results of the different methodologies to be applied will highly depend on the accuracy of the input data used. This section will explain the differences and similarities found for the parameters evaluated based on the information from both data sources for eight case study areas located in Australia.

Prior to the analysis of the parameters to be used in the methodologies, it was considered important to use the available bore logs information, as these provided a better characterisation of the aquifer conditions. One of the parameters defined from the bore logs was the depth to bedrock, which worked as a validation for the depth to bedrock obtained from local and global datasets. Furthermore, it helped to identify the heterogeneity conditions of some of the groundwater systems, showing that half of the case study areas were composed of layers of different sediment types. These conditions will modify the groundwater flow movement in comparison to how it would be in the case of a homogeneous media.

The first parameter in evaluation was the hydraulic conductivity. The shapefiles from where the global data was obtained, presented more than one hydraulic conductivity value per case study area. The values closest to the coast were chosen as the most representative for each of the areas. Nonetheless, these values obtained from the global-scale sources were very low in comparison to the ones from local-scale sources, showing some extremes that are probably not representative of the main geological conditions found in the bore logs. Considering that the local information is the most precise,

it would mean that the global dataset is underestimating the hydraulic conductivity values. It is also possible that the dataset used does not have a fine resolution to be used at this scale of evaluation. Further into the analysis, this parameter was influential in the determination of the saltwater intrusion length. Given this situation, it would have been useful to obtain pumping tests information to also validate the hydraulic conductivity values.

The parameter depth to aquifer base from mean sea level also presented an important difference in the values coming from local sources and the ones from global sources, being the latter always larger. The bore logs were used to validate these values, showing that the local information was the closest in magnitude. However, it could happen that the bore logs were not deep enough to show other low permeable systems which are considered in the global dataset. The large values of aquifer thickness from the global dataset would directly affect the calculation of volumes, as these would give the idea of more freshwater resources available than in the real conditions.

For the net recharge, the estimated values were obtained from the difference of precipitation and evapotranspiration rasters based on global datasets. This approach is very general and could be improved as there are other processes such as river-aquifer exchange or pumping, that may be influencing the recharge in these zones. It is also possible that calculating a spatial average of the recharge for the area would be too simple for the definition needed in this type of study. In contrast, the local collected data considers processes such as pumping or infiltration, if these exist. The recharge rates are based on water balances for the area or percentages of precipitation. From the evaluation of the results, there is no general trend defining if the local or global information is the largest or the lowest. In some of the global cases, the calculated net recharge is negative, indicating that there is a deficit of precipitation in the system, in average. A negative net recharge is not realistic unless the groundwater level above the extinction depth.

The distance to the inland boundary condition and the head at this point, are two parameters that define the groundwater gradient which had an important influence in the saltwater intrusion, as observed in the analytical solution and in the simulations. The estimation of the first parameter (distance) did not show any trend between the local and global values, while in the case of the head, the values from global sources are in almost all cases larger than the ones from the local sources. Since these heads are measured at different distances, this comparison is not representative.

Finding the location of the inland boundary condition only using a topography dataset may not be too accurate, as the location of this condition could be influenced by local factors of each groundwater system, and not only based on the topographical variations. It is true that the topography could be used as a first estimation of where the water divide is located but it may not work in all cases. A more

accurate way of defining this condition would be using values obtained from the monitoring of hydraulic heads or from a groundwater calibrated model for the area. Estimating the head at the inland boundary condition based on the difference between the topography and the distance to water table datasets is an approach with less uncertainty, as this difference directly represents the required parameter. However, it could still be incorrectly representing the groundwater system if the location of the boundary condition defined is not properly defined.

Related to porosity, there was no global dataset available to define it so, based on the default values used in groundwater models simulations, it was assumed to be equal to 0.25. This is an intermediate value between the upper and lower presented in the local sources.

In general, it has been observed that there are many differences in the local and global sources of information considered and a lot of variability was found when comparing the results. These results should imply that the global datasets evaluated in this research would not be accurate enough for representing local conditions. This does not necessarily mean that the quality of the global datasets is bad, but it may be more representative at a different scale. This information is generally used in data-scarce zones, so it would be very important to consider these limitations in the data. A practical approach to consider would be the use of downscaling methods to improve the results of the global datasets.

Research question 2: How influential are the input data and the conceptualizations in the different methodologies for the evaluation of the freshwater-saltwater distribution in coastal aquifers and how do these affect the calculated results?

Five methodologies were applied to evaluate the freshwater-saltwater distribution in coastal aquifers. These were chosen to cover a broad group of approaches, from the simplest to the most complex. Where possible, local and global information was applied to see their influence in the results obtained.

The first methodology (M1) is the analytical solution calculation. It presented an easy approach for calculating the saltwater intrusion by applying mathematical formulas. This is a convenient tool when a first estimate is needed and there are not computational facilities available. It does not consider detailed information about the aquifer, such as the local pumping, variation in recharge along the profile, heterogeneity of the aquifer or freshwater discharge offshore.

The second methodology (M2) is a density-variable groundwater flow simulation considering a conceptualization based on the Henry case problem. This conceptualization is very similar to M1 by considering a homogeneous aquifer, constantly distributed recharge values along the profile and an aquifer that ends at the coastline. This simulation was the easiest of all the ones considered in this research.

The third methodology (M3) was also a groundwater model simulation but considering an area that encompasses the inland and offshore parts of the aquifer, as well as outflow processes on the surface of the aquifer. This methodology showed that offshore freshwater discharge could occur in certain cases, however, this was not identified in M1 or M2. From this conceptualization, it was determined that it is important to consider the continental shelf area in models aimed at evaluating the saltwater intrusion. Another important aspect found when simulating this approach was related to the conceptualization of the aquifer layers. This model also considered the topography at the coast (equal to zero m a.s.l) and the value at the inland condition. This approach showed that in some cases it could be important to consider the depth of the unsaturated zones in the simulations, as it should not be neglected in some cases.

Comparing these three methodologies so far, it is seen that the results obtained in M1 (analytical solution), are very similar to M2 and M3 (numerical modelling approaches), when considering the same input data (local or global). This means that it would be adequate to use any of these methodologies for obtaining a first estimate, unless there is large offshore discharge occurring. When the influence of more processes is necessary to be considered, such as river effects, M2 and M3 would need to be improved to include them. In the case of the analytical solution (M1) this is not possible as the equations used do not explicitly include processes like drainage and rivers.

M4 was a more complex methodology based on global datasets, considering the uncertainty in recharge and geology named in this study as “realizations”. The estimated recharge, based on statistical methods, was variable along the model columns, which is representative of the different recharge rates occurring in a groundwater system. As part of the geology, these models considered the presence of the capping clay layers present in the system, as well as the different sediment layers which influence the groundwater flow.

The application of this model was simple, as it is just necessary to indicate the ID of the cross-section to evaluate and the number of realization desired. It is important to consider that this methodology is currently under modification as part of a PhD research, so the future versions of the code may have different input data and the results may vary. A drawback of this method is that the locations of the profiles are predefined and, even though they are located at a distance of 500 m between each other, in some cases a profile for the desired area was not available, or some profiles were not yet available. Another aspect to consider is that, due to the complexity of these models, the larger modelling domain, the number of cells and the low permeable layers, the simulation time to reach the steady state takes longer than in M2 or M3.

In the case of M5, this conceptualization is similar to M4, but considering the geology layering from the bore logs analysis. Due to limitations in the conceptualization of M4, only two types of sediment were used in the model. The two hydraulic conductivity values used were estimated from bibliography based on the sediment type. The values estimated for the low permeable sediment in M4 were lower than the one considered in M5. This methodology also showed that some areas had no saline intrusion, which were not necessarily the same as in M4, showing the influence of the geology input in the results.

M4 and M5 did not show similar results for the saline intrusion length. However, when comparing the results between them, the conceptualization of the layers was important for the groundwater flow simulations. In the case of geology, where intercalated geological layers were simulated, the heads distribution are affected by the clay capping layers which reduce the possibility of freshwater discharge at the coast. The behaviour will also be influenced by the hydraulic conductivity, which defines the interface shape.

Increasing the complexity of the model conceptualization and using global information (M4 and M5) gave very different results from the ones found in the simpler approaches (M1, M2, M3). At the same time, there are differences between using global and local input data in M1, M2 and M3. The results are mostly influenced by the input data, since the data collection section showed large differences between the global datasets and the local data. It was important to define more complex scenarios, such as M4 and M5, to represent coastal groundwater systems but, at the same time, take into account the degree of uncertainty that came from the use of global hydraulic conductivity and recharge values in these two cases. The conceptualization of M5 is improved by a more precise geological layering. But could be better by correlating this with measured values of hydraulic conductivity.

The freshwater volumes in the aquifer are influenced by the groundwater system's dimensions. Because of this, it was necessary to normalise these results, based on the maximum freshwater volume available. Note that only the inland fresh groundwater volumes were considered in the analysis, as in some cases there was freshwater volume in the shelf area that was not related to processes at the inland groundwater system. Normalised volumes of fresh groundwater of at least 80% occur in most of the cases, meaning that the intrusion is incipient or does not have potential of reaching further inland under the conditions evaluated.

Research question 3: What are the possible effects of climate change on the saltwater intrusion process in coastal aquifers?

It was not only important to consider the current saltwater intrusion, but also to evaluate possible climate change scenarios, as these will be of vital importance in the coming tens of years. This evaluation was performed for two case study areas (Stockton and Stuarts Point) and considering two types of recharge: (1) the global recharge used in M4 and M5 and (2) the local recharge used in M1, M2 and M3.

When evaluating the saltwater intrusion length, it was observed that higher recharge rates reduce the intrusion effect, as this process helps to increase the freshwater flow discharged. The sea level rise is a head increase at this point, causing the conditions for intrusion to increase as well. This analysis was consequent with the results, where largest intrusion occurred under a sea level rise of 2 m and a recharge of 25% of the original rate. The net increase in the intrusion length from the baseline condition will depend on the aquifer and climate conditions of the area. The intrusion length in Stockton increased in 1.7 km and 0.7 km for the global and the local recharge cases, respectively. For Stuarts Point, the increases from the baseline condition are 0.6 km and 0.55 km for the global and local recharge scenarios, respectively. There is a large uncertainty in the possible climate change scenarios to occur; however, in case the recharge and sea level rise are taken to more extreme conditions, it is expected that the intrusion will be even larger.

The freshwater volumes in Stockton showed a decrease of 60% of the initial value, while in the case of Stuarts Point this percentage is equal to 30%, considering the less favourable scenario. These numbers show an important decrease of fresh groundwater resources in the groundwater system.

Chapter 6 Conclusions

The comparison of different methodologies to estimate the freshwater-saltwater distribution in coastal aquifers was successfully achieved. This followed a stepwise approach where 5 methodologies were evaluated based on two types of input data, which were local and global scale data. The research considered the use of 8 case study areas located in Australia which had the necessary data to apply these methodologies, such that a comparative analysis could be done.

The first part of the research compared the different sources of input data available. The results showed that the global datasets had important differences from the local data. It means that this information should be used carefully and consider the scale of evaluation when applying it. This data is important as global datasets are used in areas where the necessary information for saline water intrusion assessments is scarce. The use of bore logs information provided important details about the groundwater system, such as its dimensions and geological layering which can be used for obtaining better results from the methodologies.

The second part of the research evaluated the influence of the input data on the results obtained from applying the methodologies. The analysis showed that the main parameters that influenced the results were the hydraulic conductivity, the groundwater system heterogeneity and conceptualization of layers (mainly the clay layers) and the hydraulic gradient (related to the head and position of the inland boundary condition). Another important feature was the importance of including the offshore parts of the groundwater system in the simulation for insight in the processes occurring in the continental shelf area. These were related to the heads that produced large hydraulic gradients and, in consequence, high flows of freshwater discharge which pushed the seawater away from the coastline boundary. The obtained values of saltwater intrusion length and freshwater volumes showed that the accuracy of the input data has an eminent effect on the estimated freshwater-saltwater distribution. Furthermore, in general, the obtained results were very different from each other; the only similarities where found between M1, M2 and M3 whenever the same input data is used. However, it is not possible to define which is the most accurate methodology of all, as there is no parameter considered to validate the results of this research.

The third part of the research analysed the effect of climate change in the freshwater availability of the groundwater. Results show that the most critical conditions of saltwater intrusion would occur

when the recharge rates are decreased to and the sea water level rises. After evaluating all scenarios and case study areas, the saltwater intrusion increased up to 1.7 km and reductions of 60% of the initial freshwater volume. The results per case study area highly depend on the characteristics of the groundwater systems in question.

Given the limitations of the research, the most accurate methodology could not be defined. However, for a quick first estimate M1 would be an advisable option since no computational resources are needed. In the case this is not a restriction, M3 would be the next step as it allows for the use of different boundary conditions that better represent the system as well as the use of topography and bathymetry. Finally, the next step would be to use M5 which dynamically simulates more processes and parameters in a way closer to reality, using global datasets and local information, where available. The most important factor of M5 was including geological layering from boreholes which showed to be an important parameter in the determination of the saline intrusion.

Chapter 7 Recommendations

This research did not consider a reference for the validation of the saline intrusion length. It would be advisable to use approaches such as geophysical methods and saline monitoring techniques (Delsman et al., 2018). This would provide a better definition of the precision of the methods in evaluation and to define which was the most accurate.

The use of global datasets is very important for the evaluations as these fill the gaps in data-poor areas where information is not available, however, these should be used carefully. In addition, if possible, apply downscaling methods or validation from field measurements (such as bore logs information) to check its accuracy. Global datasets can be used as a first approach where no other data available.

The evaluation of coastal groundwater systems is very complex due to the number of parameters that influence its behaviour such as the hydraulic conductivity, recharge, pumping rates, geological layers, etc. Moreover, it is important to carefully conceptualize the area, considering the relevant processes affecting the saltwater intrusion and the general groundwater flow processes in the area.

It is important to consider the offshore area in the modelling as it is possible to find fresh groundwater in these locations which would increase the total volume available.

References

Australian Government - Bureau of Meteorology. (n.d.). Australian Groundwater Explorer. Retrieved May 19, 2019, from http://www.bom.gov.au/water/groundwater/explorer/map.shtml

Börker, J., Hartmann, J., Amann, T., & Romero-Mujalli, G. (2018). Terrestrial Sediments of the Earth: Development of a Global Unconsolidated Sediments Map Database (GUM). *Geochemistry, Geophysics, Geosystems*. https://doi.org/10.1002/2017GC007273

De Graaf, I. E. M., Sutanudjaja, E. H., Van Beek, L. P. H., & Bierkens, M. F. P. (2015). A high-resolution global-scale groundwater model. *Hydrology and Earth System Sciences*, *19*(2), 823–837. https://doi.org/10.5194/hess-19-823-2015

Delsman, J., Van Baaren, E. S., Siemon, B., Dabekaussen, W., Karaoulis, M. C., Pauw, P., … Oude Essink, G. H. P. (2018). Large-scale, probabilistic salinity mapping using airborne electromagnetics for groundwater management in Zeeland, the Netherlands. *Environmental Research Letters*, *13*. https://doi.org/10.1088/1748-9326/aad19e

Fan, Y., Li, H., & Miguez-Macho, G. (2013). Global patterns of groundwater table depth. *Science*, *339*(6122), 940–943. https://doi.org/10.1126/science.1229881

Freeze, R. A., & Cherry, J. A. (1979). *Groundwater* (Prentice-Hall, Ed.). New Jersey.

Gleeson, T., Moosdorf, N., Hartmann, J., & van Beek, L. P. H. (2014). A glimpse beneath earth's surface: GLobal HYdrogeology MaPS (GLHYMPS) of permeability and porosity. *Geophysical Research Letters*, *41*(11), 3891–3898. https://doi.org/10.1002/2014GL059856

Harbaugh, A. W. (2005). MODFLOW-2005 , The U . S . Geological Survey Modular Ground-Water Model — the Ground-Water Flow Process. In *U.S. Geological Survey Techniques and Methods 6- A16*. Virginia: U.S. Geological Survey.

Hartmann, J., & Moosdorf, N. (2012). The new global lithological map database GLiM: A representation of rock properties at the Earth surface. *Geochemistry, Geophysics, Geosystems*, *13*(12), 1–37. https://doi.org/10.1029/2012GC004370

Huscroft, J., Gleeson, T., Hartmann, J., & Börker, J. (2018a). *Compiling and mapping global permeability of the unconsolidated and consolidated Earth: GLobal HYdrogeology MaPS 2.0 (GLHYMPS 2.0). [Supporting Data]*. https://doi.org/https://doi.org/10.5683/SP2/TTJNIU

Huscroft, J., Gleeson, T., Hartmann, J., & Börker, J. (2018b). Compiling and Mapping Global Permeability of the Unconsolidated and Consolidated Earth: GLobal HYdrogeology MaPS 2.0 (GLHYMPS 2.0). *Geophysical Research Letters*, *45*(4), 1897–1904. https://doi.org/10.1002/2017GL075860

Ivkovic, K. M., Dixon-Jain, P., Marshall, S. K., Sundaram, B., Clarke, J. D. A., Wallace, L., & Werner, A. D. (2013). *A national-scale vulnerability assessment of seawater intrusion: Literature review, data review, and method development*. Geoscience Australia, Canberra, and National Centre for Groundwater Research and Training, Adelaide.

Ivkovic, K. M., Marshall, S. K., Carey, H., Morgan, L. K., Sundaram, B., Dixon-Jain, P., … Werner, A. D. (2013). *A national-scale vulnerability assessment of seawater intrusion: Coastal aquifer typology*. Geoscience Australia, Canberra, and National Centre for Groundwater Research and Training, Adelaide.

Ivkovic, K. M., Marshall, S. K., Morgan, L. K., Werner, A. D., Carey, H., Cook, S., … Simon, D. (2012). *National-scale vulnerability assessment of seawater intrusion: summary report*.

https://doi.org/Online ISBN: 978-1-922136-00-8 National-scale

Karssenberg, M. (2018). *The geology of coastal aquifers worldwide as input for a global coastal groundwater flow model*. Utrecht University.

Langevin, C. D., Thorne, D. T. J., Dausman, A. M., Sukop, M. C., & Guo, W. (2008). SEAWAT Version 4: A Computer Program for Simulation of Multi-Species Solute and Heat Transport. In *Techniques and Methods Book 6, Chapter A22* (p. 39). U.S. Geological Survey.

Laruelle, G. G., Dürr, H. H., Lauerwald, R., Hartmann, J., Slomp, C. P., Goossens, N., & Regnier, P. A. G. (2013). Global multi-scale segmentation of continental and coastal waters from the watersheds to the continental margins. *Hydrology and Earth System Sciences*, *17*(5), 2029–2051. https://doi.org/10.5194/hess-17-2029-2013

Morgan, L. K., & Werner, A. D. (2015). A national inventory of seawater intrusion vulnerability for Australia. *Journal of Hydrology: Regional Studies*, *4*, 686–698. https://doi.org/10.1016/j.ejrh.2015.10.005

Morgan, L. K., Werner, A. D., Ivkovic, K. M., Carey, H., & Sundaram, B. (2013). *A national-scale vulnerability assessment of seawater intrusion: First-order assessment of seawater intrusion for Australian case study sites*. Geoscience Australia, Canberra, and National Centre for Groundwater Research and Training, Adelaide.

Morgan, L. K., Werner, A. D., Morris, M. J., & Teubner, M. D. (2013). *Application of a Rapid-Assessment Method for Seawater Intrusion Vulnerability: Willunga Basin, South Australia*. 205–225. https://doi.org/10.1007/978-94-007-5648-9

Natural Earth. (2017). Natural Earth. Retrieved August 21, 2017, from http://www.naturalearthdata.com/downloads/10m-physical-vectors

NTSG. (n.d.). MODIS Global Evapotranspiration Project (MOD16). Retrieved March 25, 2019, from Numerical Terradynamic Simulation Group (NTSG) - University of Montana website: http://www.ntsg.umt.edu/project/modis/mod16.php

Oude Essink, G. H. P. (2001). *Density Dependent Groundwater Flow*. Utrecht University, Institute of Earth Sciences, The Netherlands.

Oude Essink, G. H. P., & Boekelman, R. H. (1996). Problems with large-scale modelling of salt water intrusion in 3D. *14th Salt Water Intrusion Meeting*, (0), 288–299.

Pelletier, J. D., Broxton, P. D., Hazenberg, P., Zeng, X., Troch, P. A., Niu, G., … Gochis, D. (2016). A gridded global data set of soil, intact regolith, and sedimentary deposit thicknesses for regional and global land surface modeling. *Journal of Advances in Modeling Earth Systems*, *8*(1), 41–65. https://doi.org/10.1002/2015MS000526

Post, V. E. A. (2005). *Fresh and saline groundwater interaction in coastal aquifers: Is our technology ready for the problems ahead?* 120–123. https://doi.org/10.1007/s10040-004-0417-2

Shangguan, W., Hengl, T., Mendes de Jesus, J., Yuan, H., & Dai, Y. (2017). Mapping the global depth to bedrock for land surface modeling. *Journal of Advances in Modeling Earth Systems*, *9*(1), 65–88. https://doi.org/10.1002/2016MS000686

UN-Oceans. (n.d.). UN Atlas of the Oceans. Retrieved March 22, 2019, from http://www.oceansatlas.org/home/en/

Verkaik, J., & Janssen, G. M. C. M. (2015). *iMOD-SEAWAT User Manual*. Deltares.

Vermeulen, P. T. M., Roelofsen, F. J., Minnema, B., Burgering, L. M. T., Verkaik, J., & Rakotonirina, A. D. (2018). *iMOD User Manual* (4.3). Deltares.

Visser, M., & Bootsma, H. (2019). *imod-python*. Retrieved from

https://gitlab.com/deltares/imod/imod-python

Weatherall, P., Marks, K. M., Jakobsson, M., Schmitt, T., Tani, S., Arndt, J. E., … Wigley, R. (2015). A new digital bathymetric model of the world's oceans. *Earth and Space Science*, *2*(8), 331–345. https://doi.org/10.1002/2015EA000107

Werner, A. D. (2009). A review of seawater intrusion and its management in Australia. *Hydrogeology Journal*, *18*(1), 281–285. https://doi.org/10.1007/s10040-009-0465-8

Werner, A. D. (2017). On the classification of seawater intrusion. *Journal of Hydrology*, *551*, 619–631. https://doi.org/10.1016/j.jhydrol.2016.12.012

Werner, A. D., Bakker, M., Post, V. E. A., Vandenbohede, A., Lu, C., Ataie-Ashtiani, B., … Barry, D. A. (2012). Seawater intrusion processes, investigation and management: Recent advances and future challenges. *Advances in Water Resources*, *51*, 3–26. https://doi.org/10.1016/j.advwatres.2012.03.004

Werner, A. D., & Simmons, C. T. (2009). *Impact of Sea-Level Rise on Sea Water Intrusion in Coastal Aquifers*. *47*(2), 197–204. https://doi.org/10.1111/j.1745-6584.2008.00535.x

Werner, A. D., Ward, J. D., Morgan, L. K., Simmons, C. T., Robinson, N. I., & Teubner, M. D. (2012). Vulnerability indicators of sea water intrusion. *Ground Water*, *50*(1), 48–58. https://doi.org/10.1111/j.1745-6584.2011.00817.x

Zamrsky, D. (2019). *Rapid coastal groundwater modelling and scenarios for strategic policy development (Unpublished doctoral thesis)*. Utrecht University.

Zamrsky, D., Oude Essink, G. H. P., & Bierkens, M. F. P. (2018). Estimating the thickness of unconsolidated coastal aquifers along the global coastline. *Earth System Science Data*, *10*(3), 1591–1603. https://doi.org/10.5194/essd-10-1591-2018

Appendices

Appendix A Case study areas characteristics

The characteristics of each case study area are presented in the next section (Ivkovic, Marshall, et al., 2013):

1. Botany

- Location: Sydney, New South Wales, on the eastern Australian coast.
- Climate: Humid during summer and temperate most of the year. Temperature varies from 26.1 °C in summer and 17.6 °C in winter. Rainfall is seasonal (mostly falling during summer and autumn), with a value of mean annual rainfall equal to 1084 mm. Evaporation rates exceed rainfall during most of the year.
- Hydrogeology: The Botany Sand Beds aquifer is characterized for being shallow and unconfined to semi-confined., which highly permeable sediments. Its hydraulic conductivity varies along the aquifer due to its heterogeneity.
  The main recharge mechanism is rainfall infiltration. Surface drainage is influenced by the urban environment.
- Land and water use: Oldest producing groundwater system in Australia still in use. Used for domestic garden, industrial and recreational.
- Incidence of SWI: In the 1960's is was reported to have experienced SWI because of groundwater extraction for industry. Measures were taken by shutting down these bores and moving the aquifer production inland.

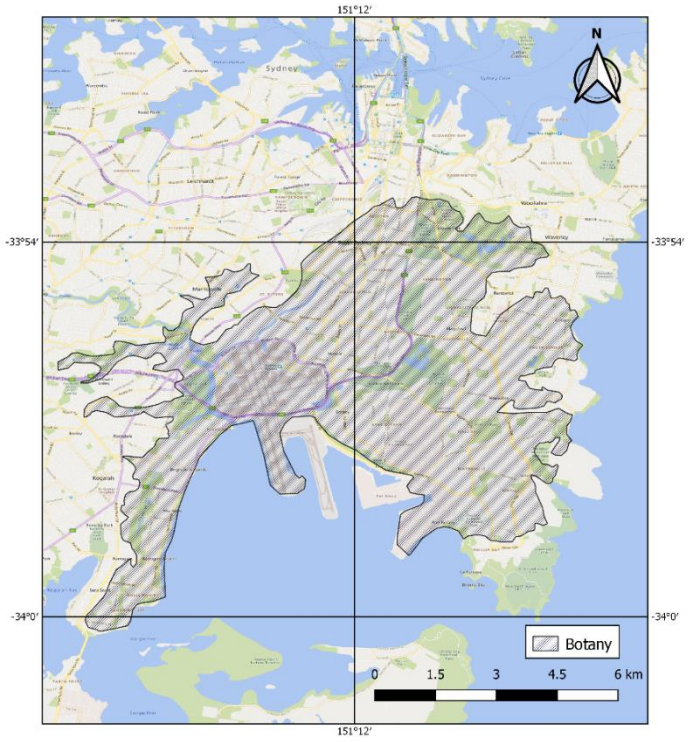

Figure 61: Location map for Botany (WGS 84 coordinate system).

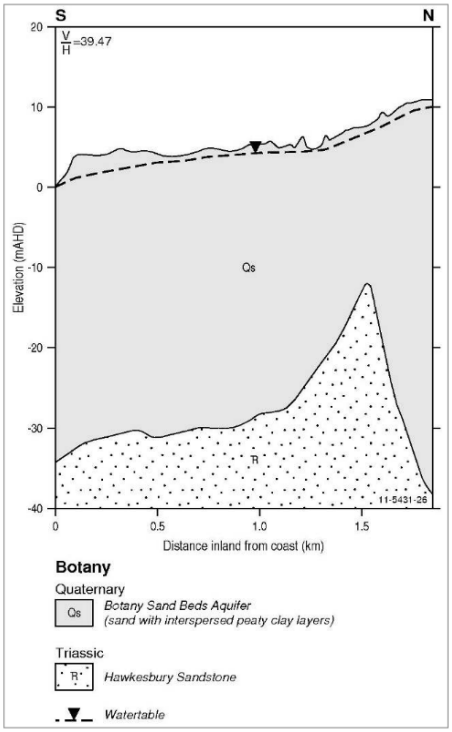

Figure 62: Geological cross-section through the Botany area.

2. Bowen

- Location: Queensland's central coast. Groundwater use mainly in Bowen Irrigation Area.
- Climate: Mean daily maximum temperature of 32 °C in January and 24 °C in July. Rainfall is seasonal, 75% falls from December to March. Average rainfall is 1020 mm. Area prone to periods of drought. High evaporation rates (1900 mm/y class A pan evaporation rate).
- Hydrogeology: The most significant aquifer is formed by the unconsolidated Quaternary fluvio-deltaic sediments. Groundwater flow direction is seawards, presence of paleochannels that form preferential flow paths. Unconfined to locally semi-confined. Streams influence aquifer recharge. Overbank flooding during wet season produces recharge. Direct recharge from rainfall or irrigation water.
- Land and water use: Groundwater use is larger than surface water use, mostly for irrigation. This demand increases as land use expands. Potential demand for this use exceeds the availability. Other minor uses are residential, stock and industry.
- Incidence of SWI: Seawater intrusion due to over-pumping of groundwater.

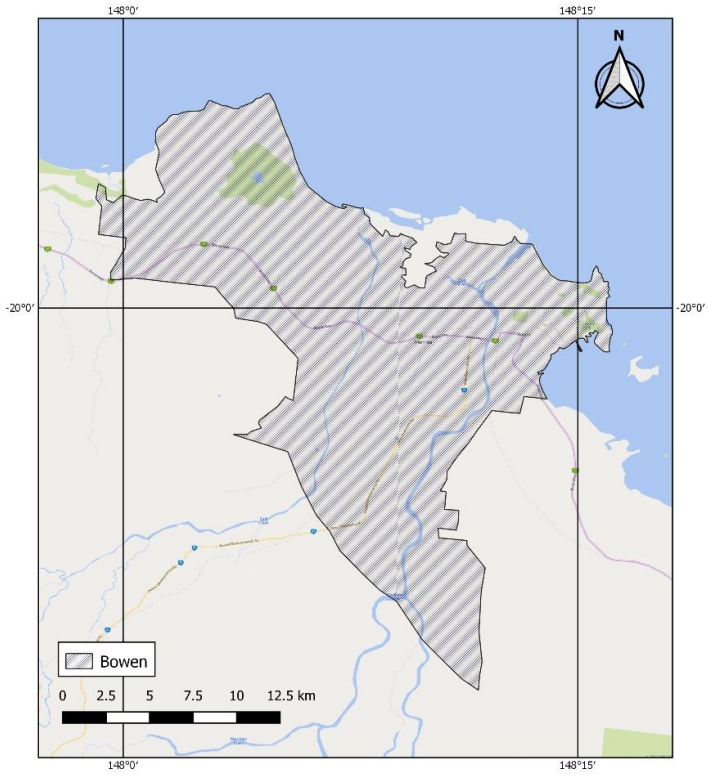

Figure 63: Location map for Bowen (WGS 84 coordinate system)

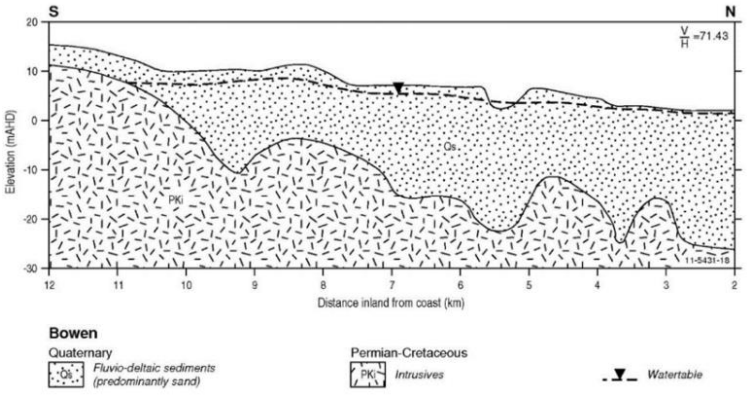

Figure 64: Geological cross-section through the Bowen area.

3. Burdekin

- Location: Located along the central Queensland coastal plain.
- Climate: Tropical climate with highly seasonal rainfall. Mean annual rainfall is 781 mm. Two-thirds occur during summer. Evaporation rates range from 10 mm/d in November to 2.8 mm/d in June.
- Hydrogeology: Main aquifer is shallow and unconfined, composed of heterogeneous, unconsolidated alluvial and deltaic sediments. Mixture of discontinuous lenses of inter-bedded gravel, channel sands, silt, mud and clay. Inclusion of all layers into one hydrostatigraphic units because of complexity of sedimentation and inconsistent distribution of extensive layers. Basement rock is granitic and the groundwater movement through it is negligible.
  Recharge processes include rainfall infiltration, channel seepage, percolation through sites of artificial recharge, flood flows and irrigation returns.
- Land and water use: Groundwater use by the Burdekin Irrigation area, which is one of Australia's main users. Natural flows along the Burdekin River have suffered modifications for irrigation to reticulate surface water to irrigators and artificially recharge aquifers.
- Incidence of SWI: It has been documented and causes are low rainfall and intense groundwater pumping. Water tables have dropped below sea level during intense drought periods.

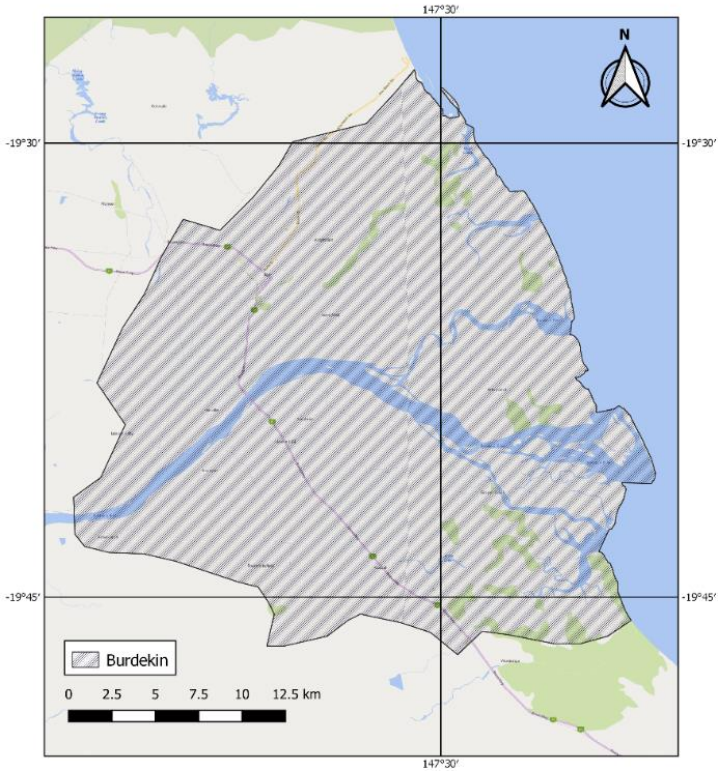

Figure 65: Location map for Burdekin (WGS 84 coordinate system).

Note: The exact delineation of this area was not present in the original report, so an approximate area was delimited based on the explanations present.

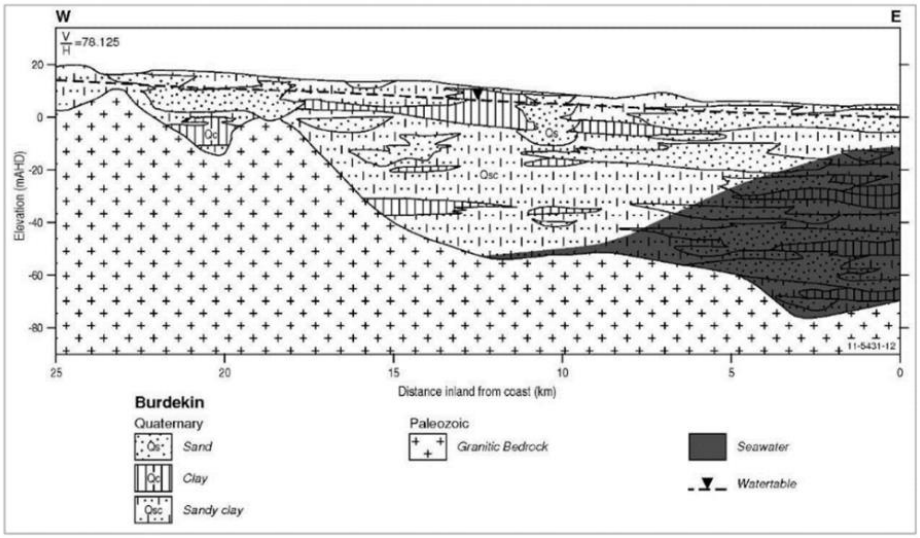

Figure 66: Geological cross-section through the Burdekin area.

4. Burnett Heads (Moore Park)

- Location: Within the Queensland subtropics.
- Climate: Average maximum temperature is 29.8 °C in summer, 22.6 °C in winter and 26.6 °C along the year. The average annual rainfall is around 1023 mm, where 45% occurs in summer and 12% during winter.
- Hydrogeology: Groundwater is found in two main aquifers: the upper Elliot Formation and the underlying Fairymead Beds. It is considered that they have moderate to high groundwater potential, however it may vary along the area. These are composed of Tertiary unconsolidated to semi-consolidated alluvial sediments which overlie the Lower Cretaceous Burrum Coal Measures basement. Both aquifers are separated by the Gooburrum clay, which is a leaky aquitard clay layer of variable thickness and distribution
- Land and water use: Groundwater is the main source of reliable water. It is used for irrigation, industry and urban water supply.
- Incidence of SWI: Many reports of seawater intrusion due to the intensive use for irrigation coupled with drought conditions along time. Many hectares of land have been lost to seawater intrusion. It is estimated that the interface is moving inland at a rate of 100 m/y.

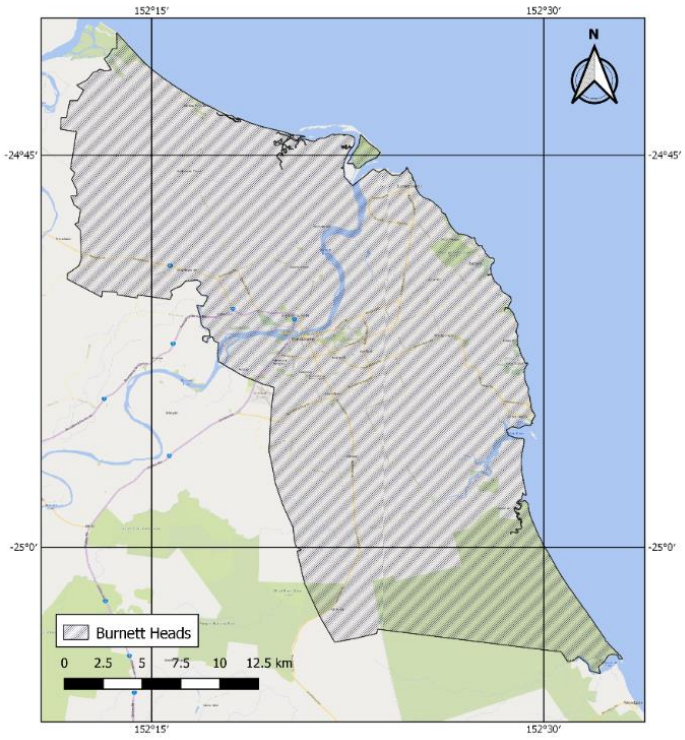

Figure 67: Location map for Burnett Heads (WGS 84 coordinate system).

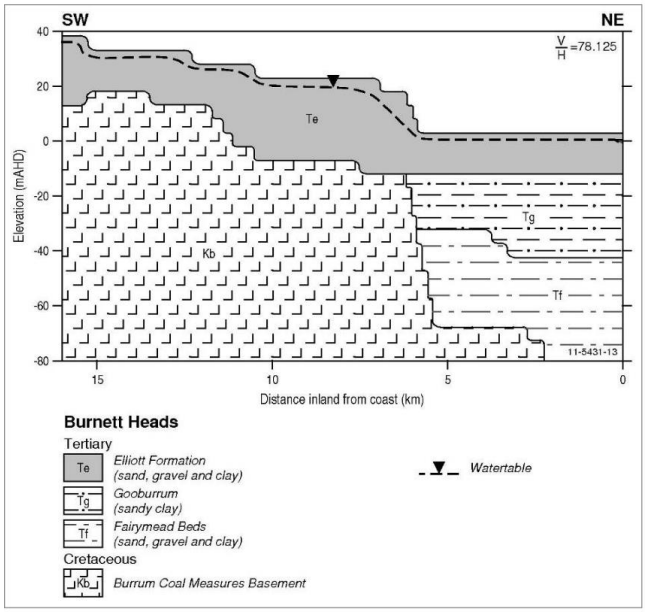

Figure 68: Geological cross-section through the Burnett Heads area.

5. Hat Head

- Location: On the north coast of New South Wales.
- Climate: Temperate, no dry season. Consistent rainfall along the year, with mean annual values of 1493 mm at South West Rocks. The monthly mean maximum temperature in summer is 26.5 °C, 23.2 °C in winter and 23.2 °C for the whole year.
- Hydrogeology: The system is composed of coastal sand dune sediments which are excellent aquifers due to their thickness, extent and permeability. Its high conductivity is affected by a

sand layer with humic and ferruginous material, causing some level of cementation. The basement is composed of marine clay that contains saltwater. It has low permeability and a low-yielding capacity.

Aquifer recharge is via rainfall infiltration and the discharge occurs in local wetlands and estuaries, as well as because of evapotranspiration.

- Land and water use: Groundwater for urban use.
- SWI incidence: Investigations indicate that pumping had not created a long-term decline of water level in the aquifer, however, some deep bores have higher salinities and ionic ratios similar to seawater, so there could be a risk of seawater intrusion.

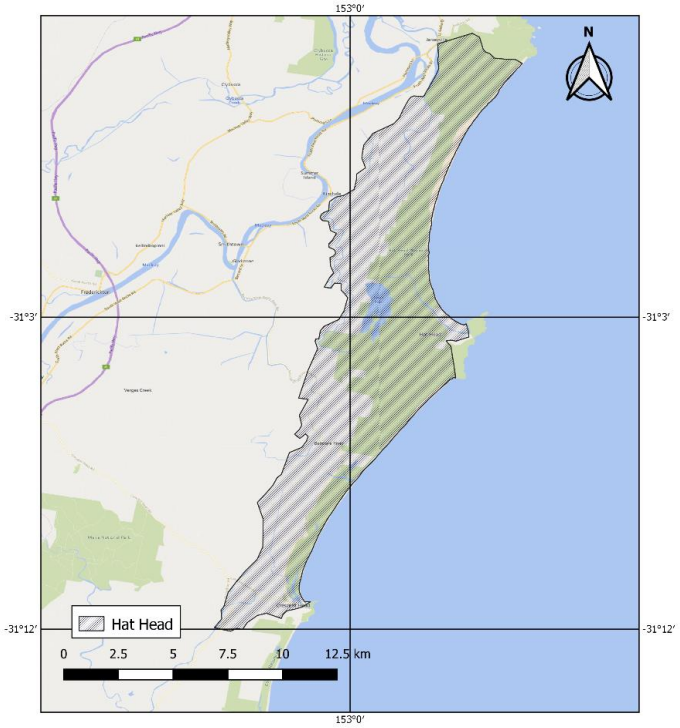

Figure 69: Location map for Hat Head (WGS 84 coordinate system).

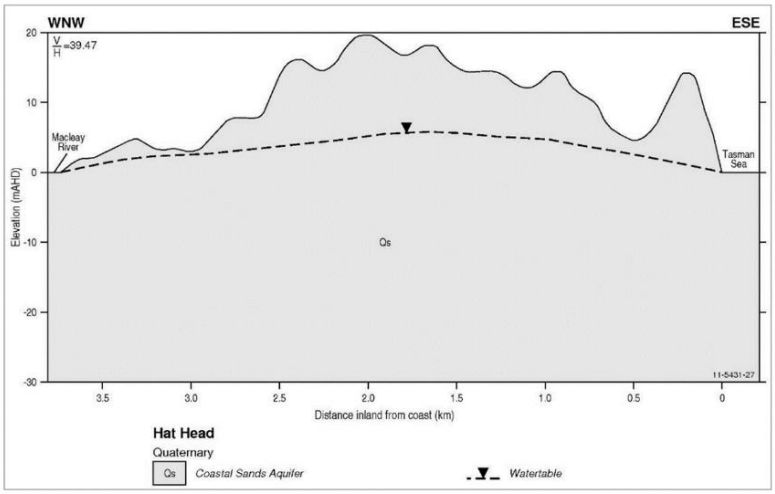

Figure 70: Geological cross-section through the Hat Head area.

6. Pioneer Valley

- Location: Northern central coast of Queensland.
- Climate: Average annual rainfall of less than 1100 mm in the south to over 2000 mm in the west. Mean daily temperatures vary from 13 °C in winter to 30 °C in summer. Mean annual evaporation is around 2000 mm/y.
- Hydrogeology: A singular aquifer system that consists on alluvial deposits and fractured rock units. Higher-yielding deposits of coarse sands and gravels can be found in the lower alluvial domain. Rainfall is the main source of aquifer recharge.
- Land and water use: Majority of groundwater irrigation used to supplement rainfall. Also used by domestic sugar milling industry, urban water supply, stock water, farm and rural domestic water supplies.
- Incidence of SWI: Became a serious concern in the mid-1990s because of rainfall below average from 1991 to 1997 and high irrigation demand.

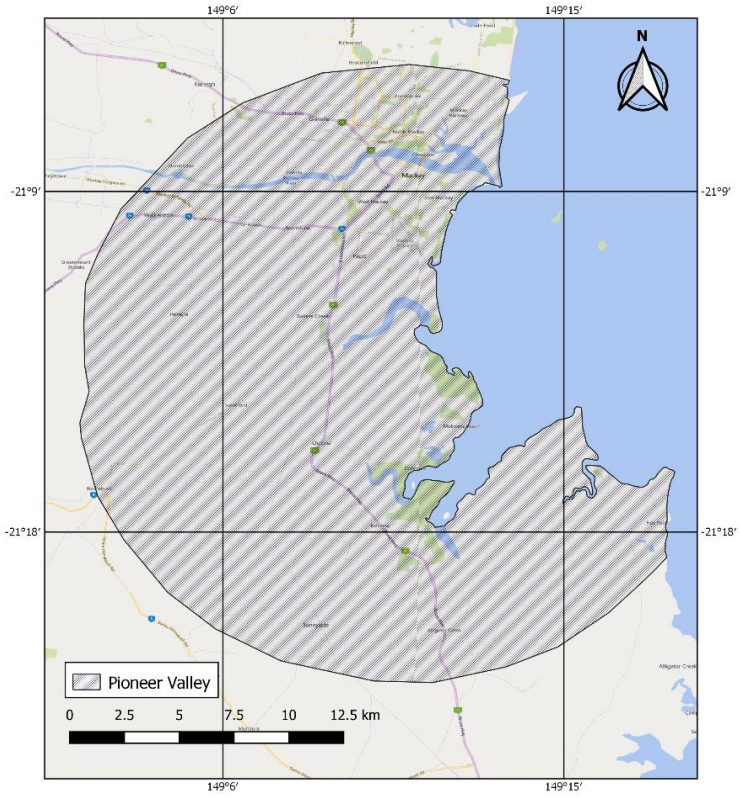

Figure 71: Location map for Pioneer Valley (WGS 84 coordinate system).

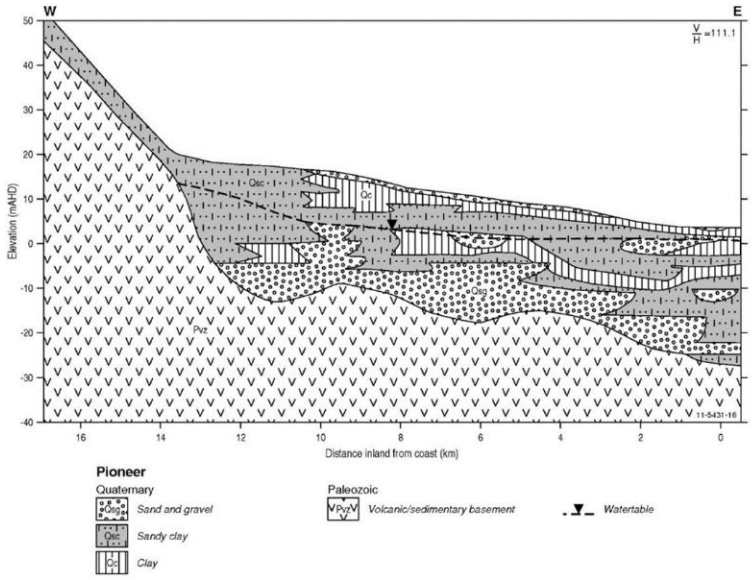

Figure 72: Geological cross-section through the Pioneer Valley area.

7. Stockton

- Location: northeast of the city of Newcastle, on the New South Wales coast.
- Climate: Temperate climate. Rainfall is realitve consistent throughout the year, with a mean annual value of 1134 mm. The monthly mean temperature in simmer is 25.3 °C, 17.4 °C in winter and 21.8 °C during the whole year. Average annual pan evaporation is around 1750 mm.
- Hydrogeology: Aquifers in the area are derived from the North Stockton Sandbeds and the Tomago Sandbeds, which are separated by estuarine mud (Tilligerry Mud member) which can be a confining layer in certain zones. The Medowie Clay member is at the base of these aquifers and forms a continuous aquitard. The basement is composed of Carboniferous and Permian rock which are relatively impermeable.
  Recharge into the aquifer occurs from the rainfall infiltration into the dunes. Discharges occur to the ocean and Tilligerry Creek, also through evapotranspiration, groundwater abstractions or drains.
- Land and water use: groundwater used for stock and domestic activities, sand mine and mineral processing, small scale irrigation and industry.
- SWI incidence: Southward migration of saline water from Tilligerry Creek due to extensive drainage network on the southern banks of the estuary. No increase of salinity seen at the seaward coastline.

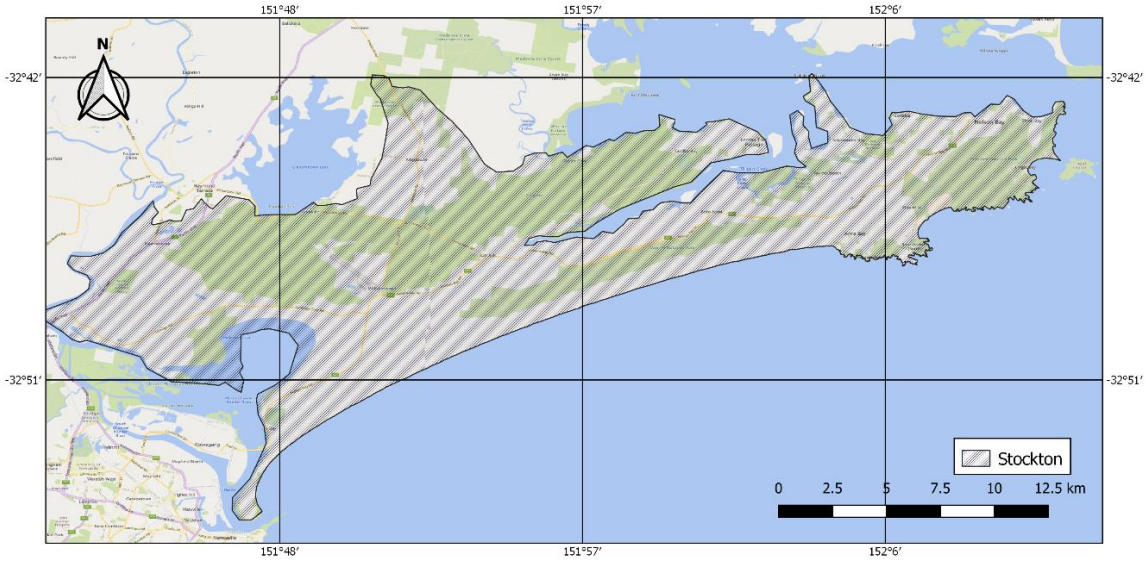

Figure 73: Location map for Stockton (WGS 84 coordinate system).

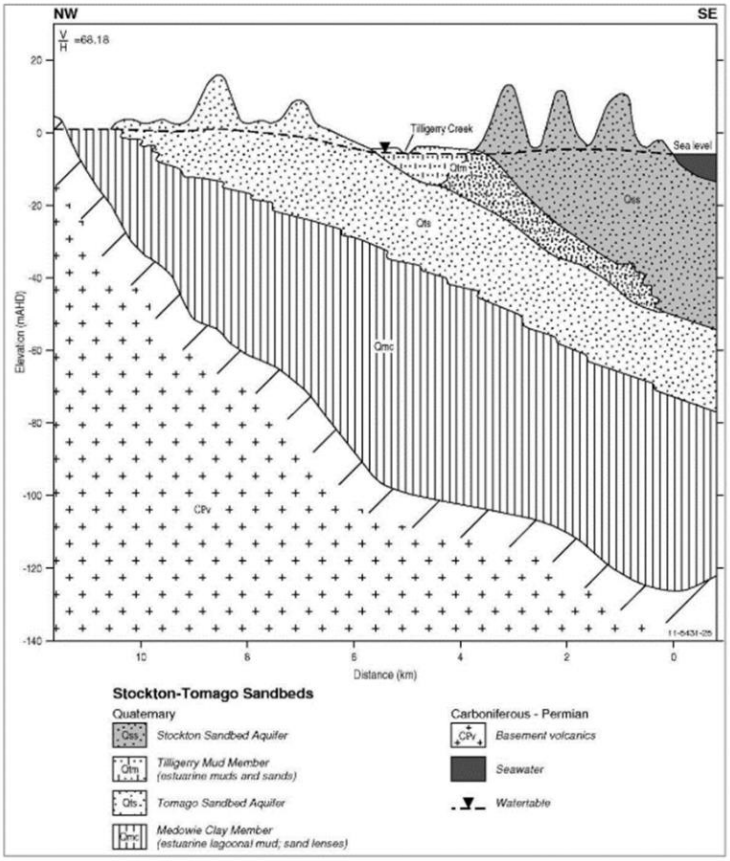

Figure 74: Geological cross-section through the Stockton area.

8. Stuarts Point

- Location: Located on the Mid North Coast in New South Wales.
- Climate: temperate climate. Rainfall relatively consistent throughout the year, with a mean annual rainfall of 1134 mm. The monthly mean maximum temperature in summer is 25.3 °C in summer, 17.4 °C in winter and 21.8 °C along the whole year.
- Hydrogeology: The aquifers are mostly composed of sands. When associated with Mcleay River or estuarine deposits, they may contain muds and clays. Groundwater exists within a shallow unconfined aquifer or as a perched aquifer system. The latter are common but not laterally extensive and are supported by an almost impermeable coffee rock layer. Underneath, there is a shallow sandy aquifer. Both systems are hydraulically connected and considered as one unit in this evaluation.

  The recharge occurs because of direct rainfall infiltration. Discharge is through surface water bodies, groundwater abstraction and evapotranspiration.
- Land and water use: Used for individual domestic use, town supply and horticulture.
- SWI incidence: Clear evidence of seawater intrusion at Stuarts Point as been seen due to observed increase of salinity, nonetheless, the cause has not been identified. In general, the seawater intrusion impact is considered to be minor.

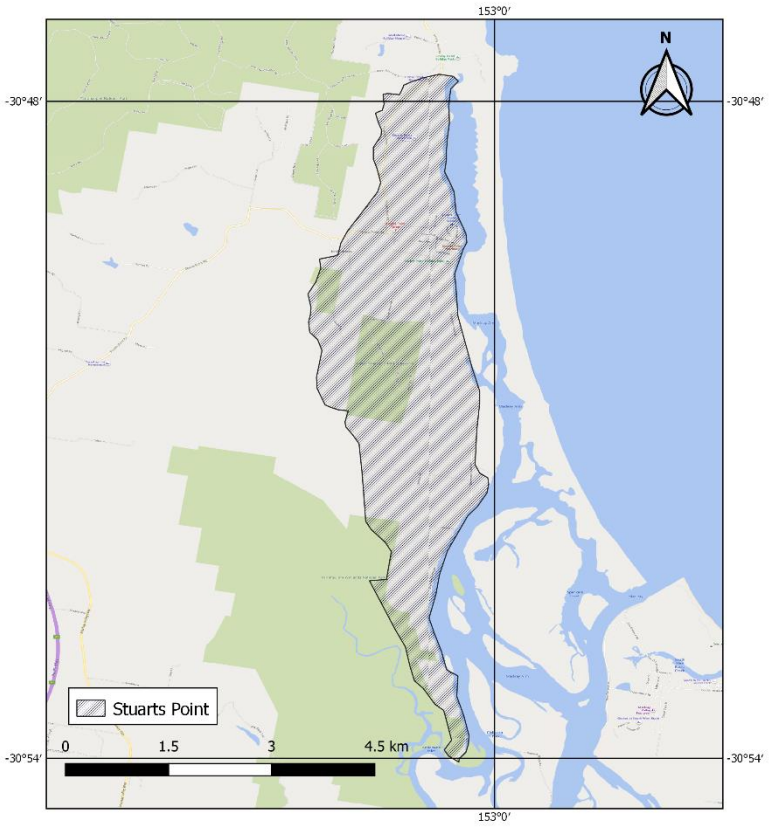

Figure 75: Location map for Stuarts Point (WGS 84 coordinate system).

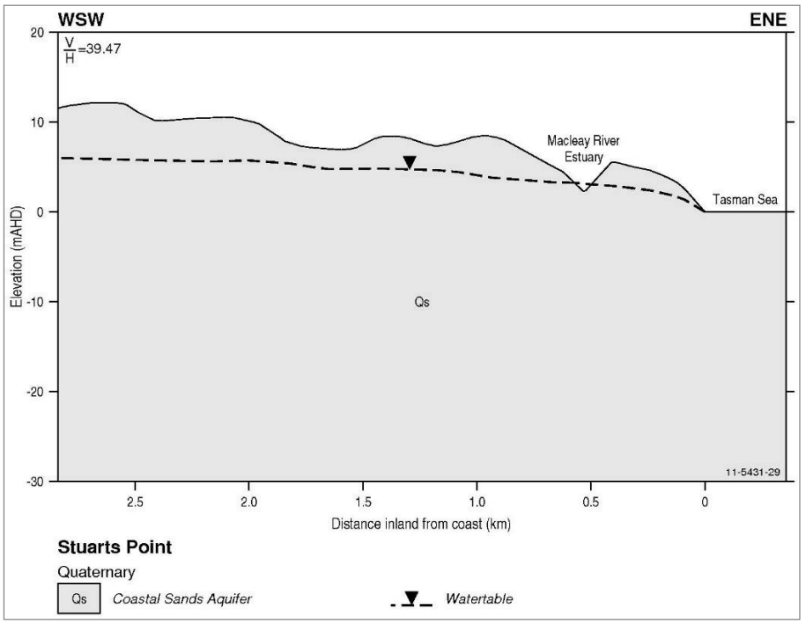

Figure 76: Geological cross-section through the Stuarts Point area.

Appendix B Bore log sediment type (not considering the basement rock)

Case study area	HydroID	Bore log sediment type	Case study area	HydroID	Bore log sediment type
Botany	10088027	Miscellaneous, sand, clay	Hat Head	10151327	Sand, rock
	10092440	Miscellaneous, sand, peat, clay		10016331	Sand, clay
	10096367	Miscellaneous, sand		10051564	Sand
	10102701	Sand		10118341	Sand, rock
	10101495	Sand, regolith		10013095	Sand
	10091717	Sand		10018031	Sand
Bowen	40144579	Silt, clay, sand		10106089	Sand
	40144650	Silt, clay, sand	Pioneer Valley	40051380	Clay
	40144588	Silt, clay, sand		40081867	Clay
	40144365	Silt, clay, sand		40145417	Clay
	40144404	clay, sand		40023197	Clay
	40144402	Silt, clay, sand		40145527	Clay, sand
	40144590	Silt, clay, sand		40145412	Clay
	40144419	clay, sand		40145538	Clay, sand
	40144592	Silt, clay, sand		40145522	Sand, clay
	40144584	Silt, clay, sand		40145794	Sand, clay
	40144355	Clay, silt		40145563	Sand, clay
Burdekin	40144287	Soil, silt, clay		40145791	Clay, sand
	40144698	Clay		40145785	Clay, sand
	40141803	Clay, silt, sand		40145567	Clay, sand
	40141563	Sand, clay		40145976	Sand
	40141789	Sand, clay		40145569	Clay
	40141807	Sand, clay		40145776	Clay, sand
	40141785	Sand		40145784	Sand, clay
	40109521	Clay, sand		40145782	Clay
Burnett Heads	40147891	Clay, sand, silt		40145776	Clay
	40147964	Clay, sand		40145570	Sand
	40148028	Silt, sand, clay	Stockton	10080680	Sand
	40147858	Sand, clay		10104355	Sand
	40147907	Sand, clay		10096642	Sand
	40148023	Sand, clay, silt	Stuarts Point	10014074	Sand
	40147861	Gravel, clay, silt		10008433	Sand
	40148078	Gravel, sand, silt, shale, coal, sandstone		10101302	Sand
	40147968	Sand, clay, gravel		10008594	Sand
	40148265	Clay, sand, silt		10011156	Sand
				10129522	Sand

*HydroID based on the Australian Groundwater Explorer (Australian Government - Bureau of Meteorology, n.d.).

Appendix C Average borehole simplification analysis

Based on the information from the Australian Groundwater explorer website (Australian Government - Bureau of Meteorology, n.d.).

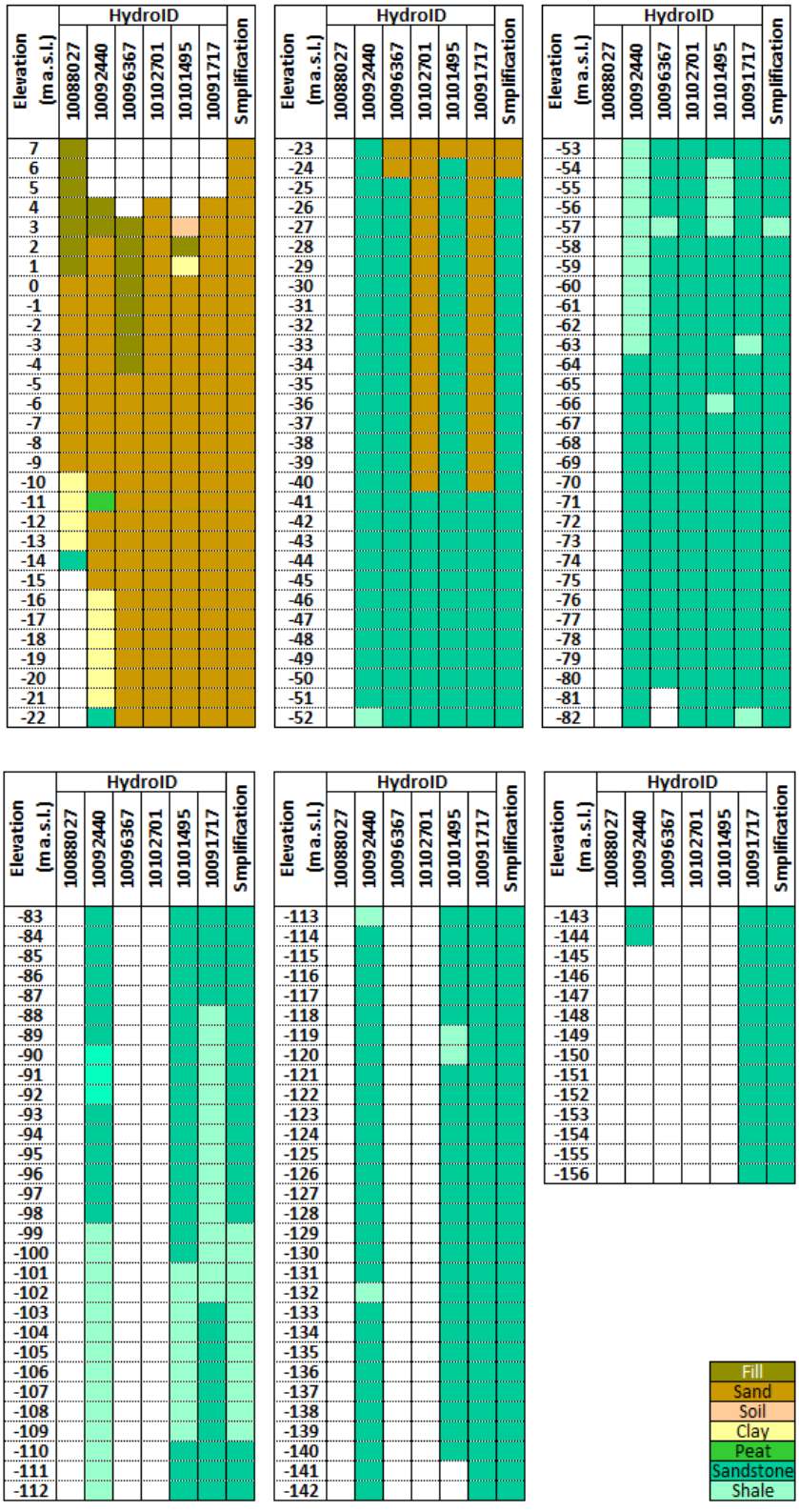

Figure 77: Average borehole simplification – Botany.

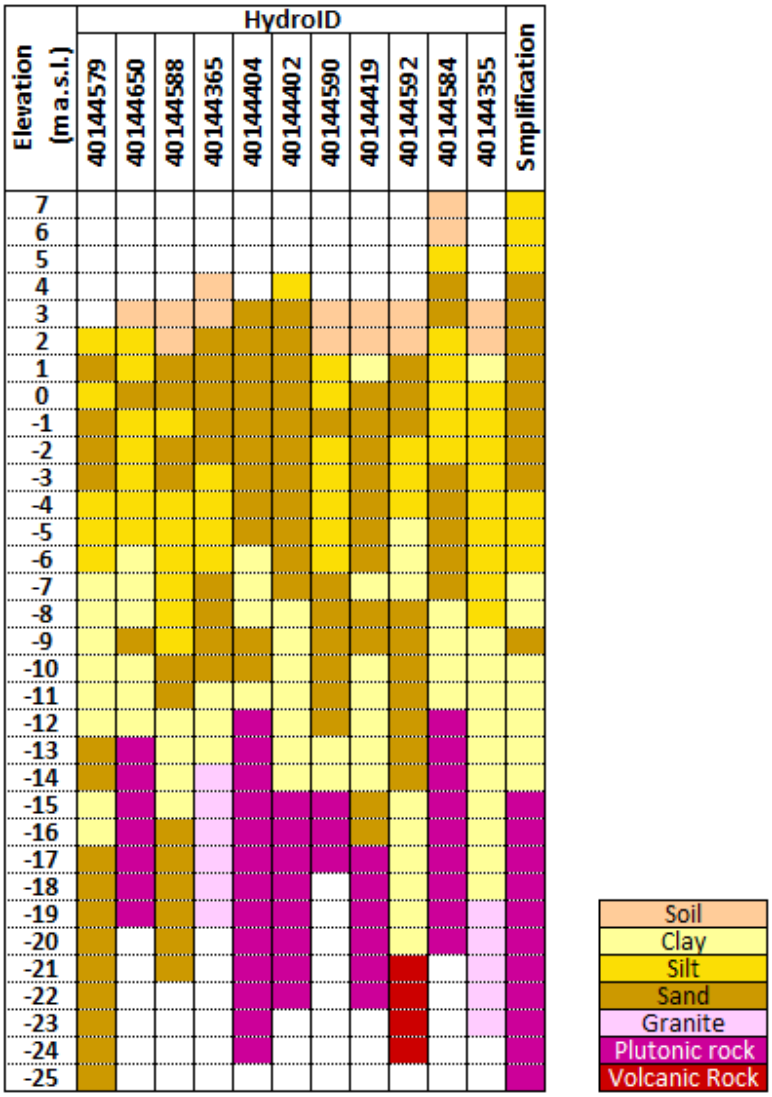

Figure 78: Average borehole simplification – Bowen

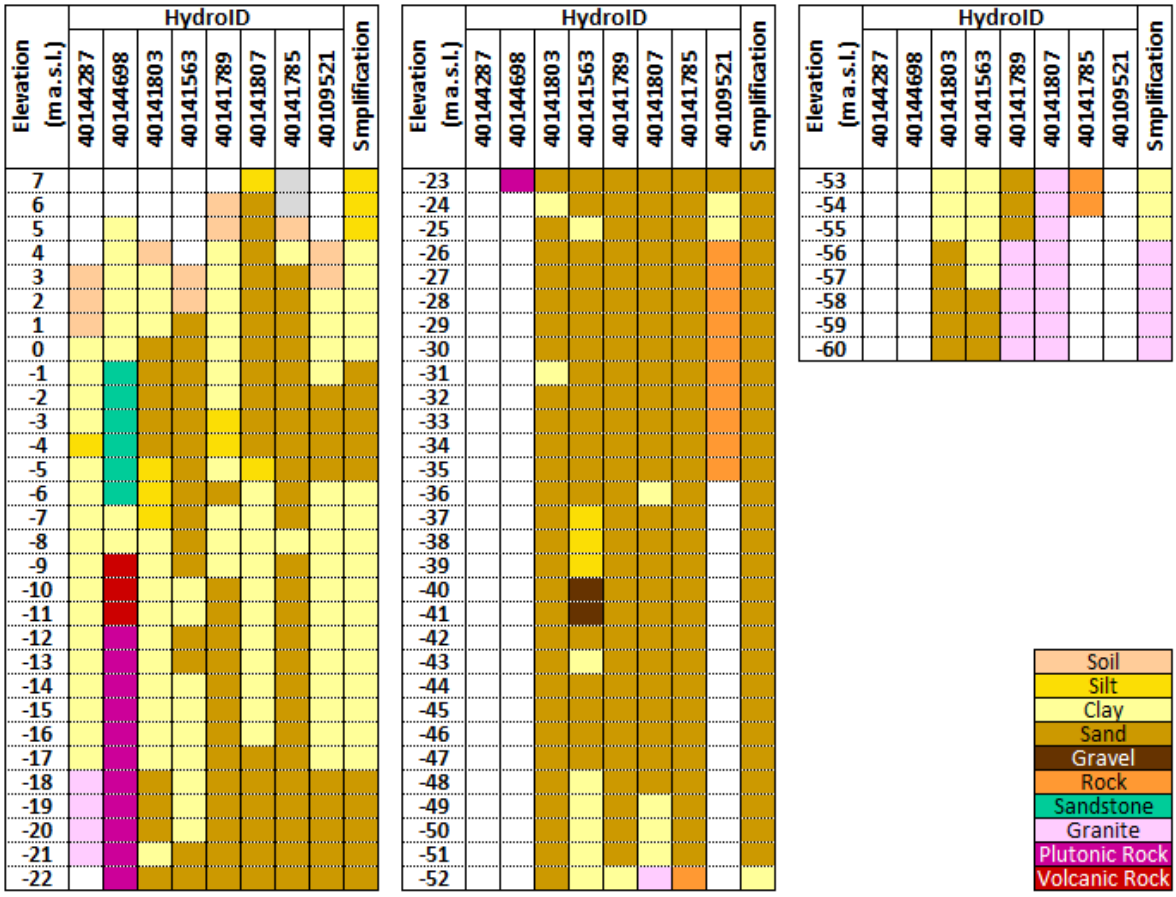

Figure 79: Average borehole simplification – Burdekin

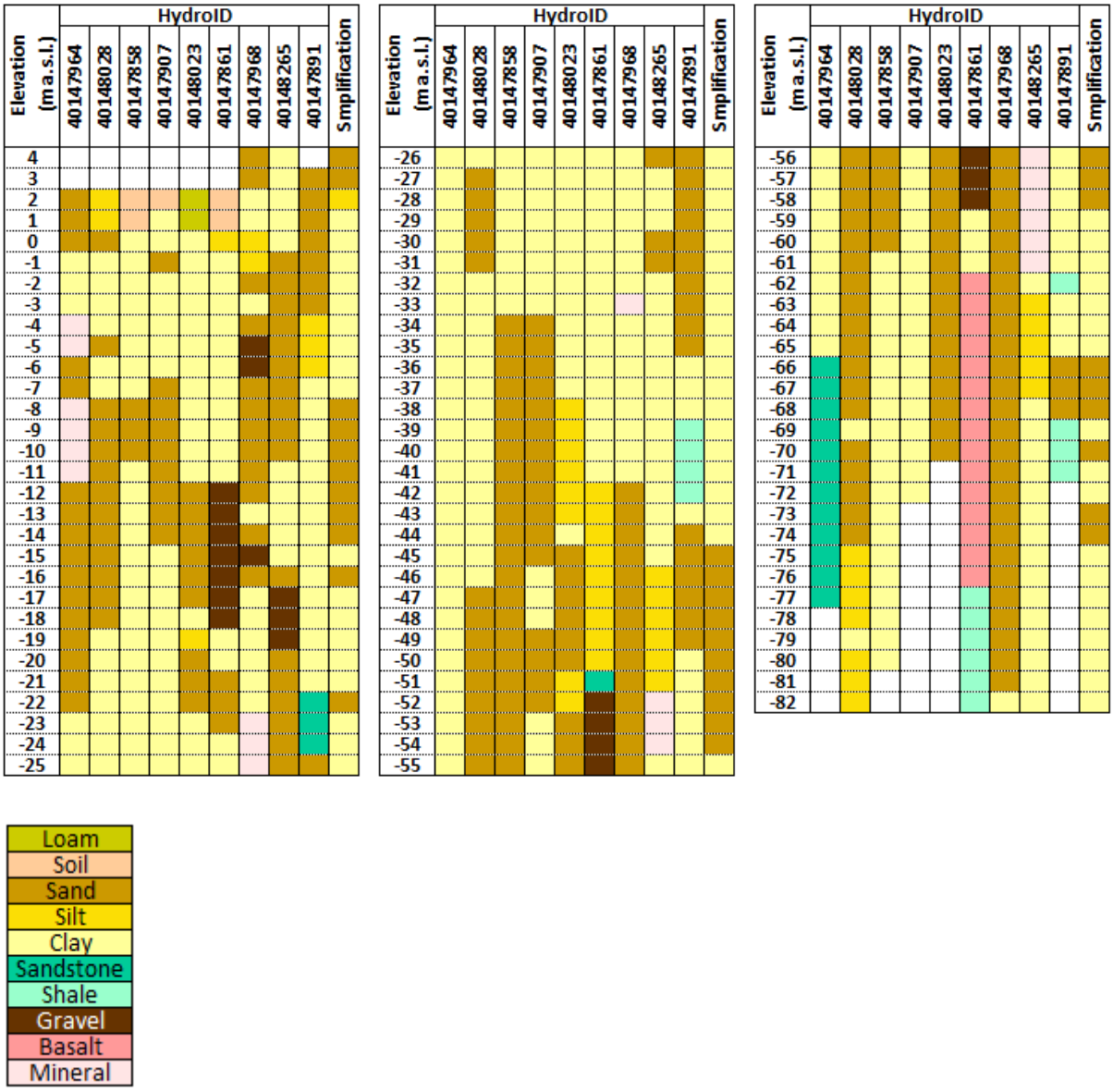

Figure 80: Average borehole simplification – Burnett Heads

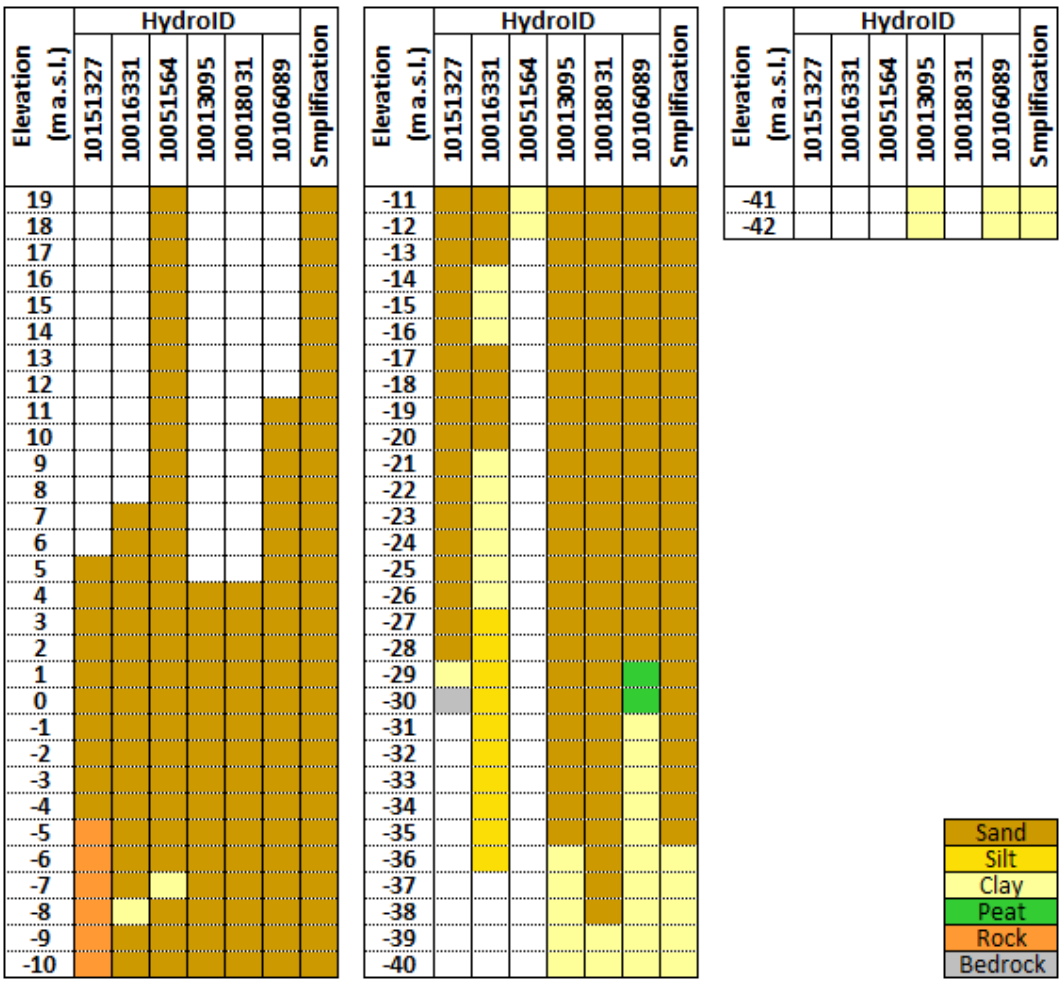

Figure 81: Average borehole simplification – Hat Head

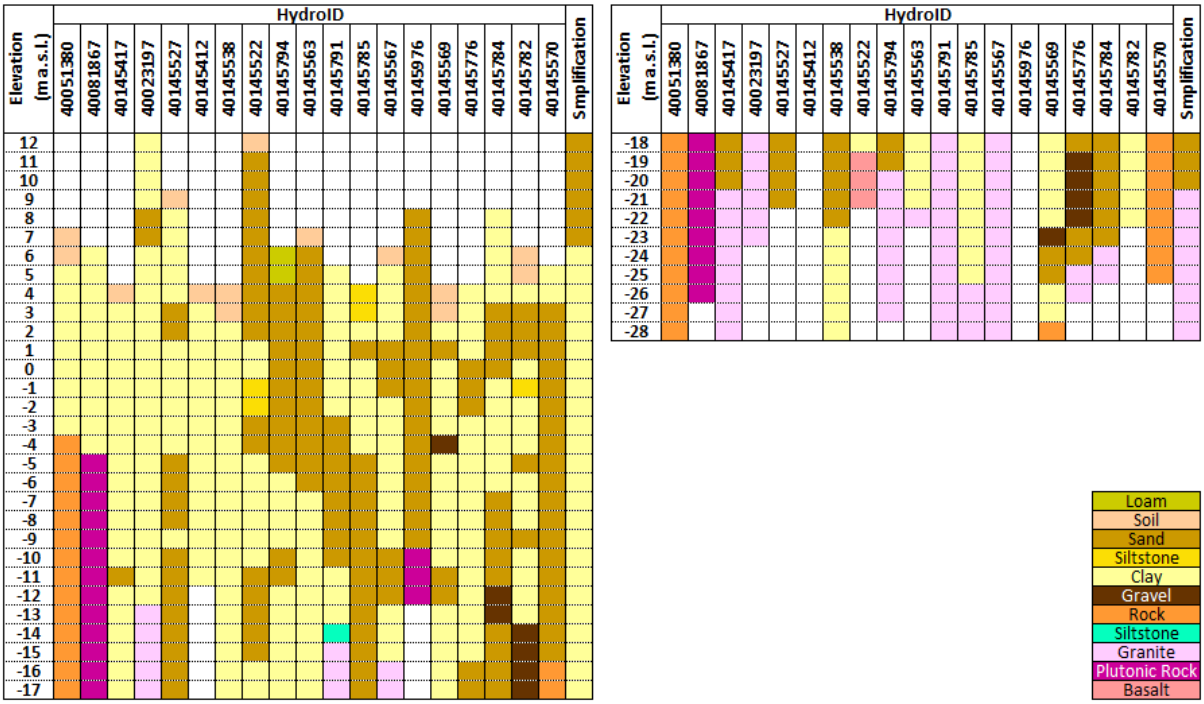

Figure 82: Average borehole simplification – Pioneer Valley

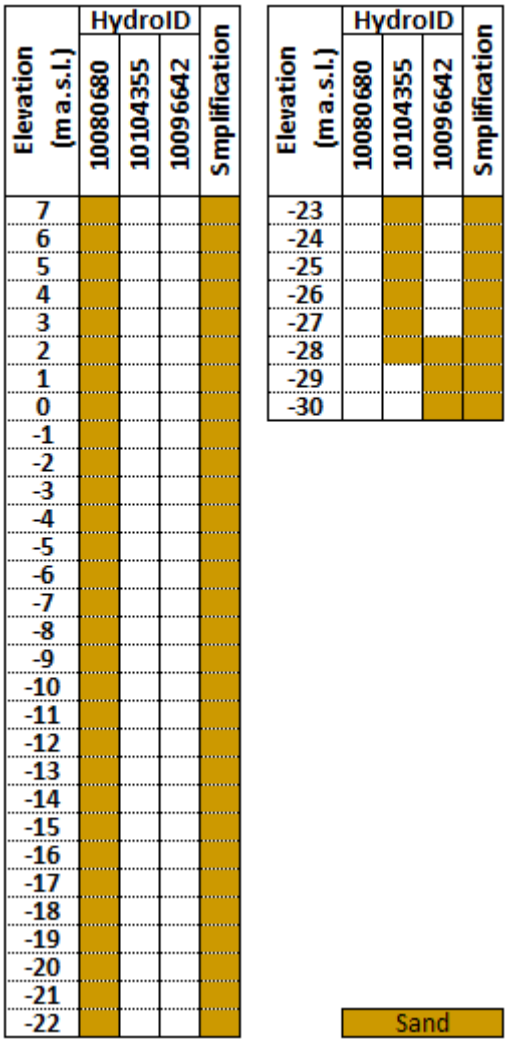

Figure 83: Average borehole simplification – Stockton

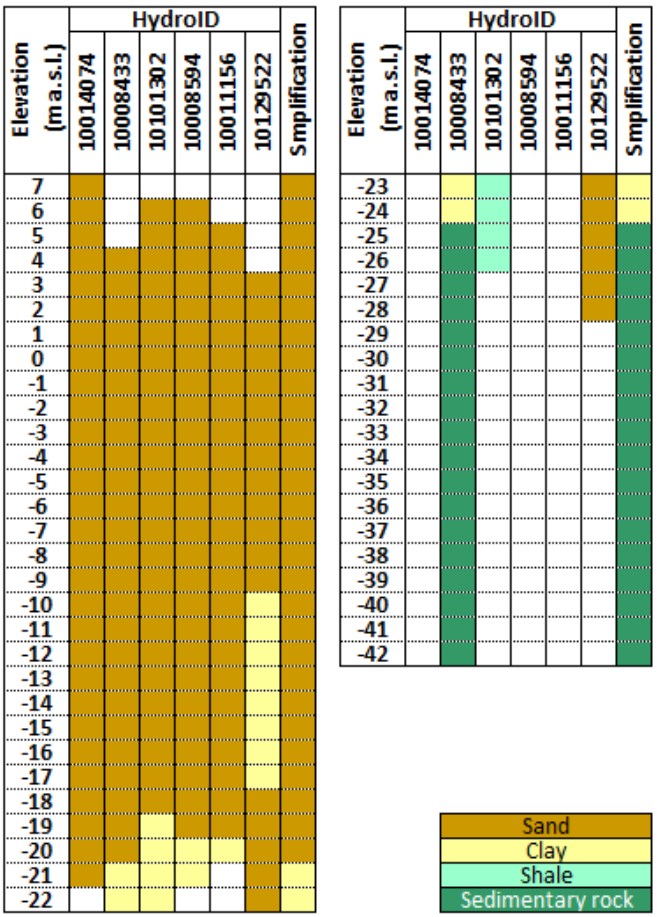

Figure 84: Average borehole simplification – Stuarts Point

Appendix D Average aquifer thickness and standard deviation for each of the profiles considered per case study area

Case study area	id_cs	Average aquifer thickness - ate_avg (m a.s.l.)	Average calculated thickness (m)	Standard deviation of aquifer thickness - ate_stdev (m a.s.l.)
Botany	51218	-77.4	77	57.38
Bowen	50678	-114.41	165	80.74
	50679	-215.98		118.07
Burdekin	50652	-281.73	186	227.47
	50653	-206.42		98.84
	50654	-164.37		69.46
	50655	-157.68		106.84
	50656	-135.74		68.45
	50657	-171.57		87.31
Burnett Heads, MP	50934	-270.15	167	257.86
	50935	-167.89		139.38
	50936	-67.13		68.79
	50937	-160.95		97.52
Hat Head	51110	-151.87	131	118.91
	51111	-110.56		59.92
Pioneer Valley	50751	-198.9	120	234.27
	50752	-58.35		46.57
	50753	-103.79		112.01
Stockton	51172	-202.67	230	182.02
	51171	-222.45		149.48
	51170	-238.72		215.62
	51169	-232.84		218.78
	51168	-350.59		362.61
	51167	-314.04		218.42
	51166	-48.89		21.18
Stuarts Point	51106	-81.28	81	17.95

*id_cs (cross section identification number) from Zamrsky et al. (2018)

Appendix E Bore logs depth to aquifer base and type

Case study area	HydroID	Depth to aquifer base (m)	Aquifer base type	Case study area	HydroID	Depth to aquifer base (m)	Aquifer base type
Botany	10088027	20	Sandstone	Hat Head	10151327	34	Basement
	10092440	25	Sandstone		10016331	33	Sedimentary rock
	10096367	28	Sandstone		10051564	30	Clay
	10102701	42	Sandstone		10118341	30	Clay
	10101495	25	Sandstone		10013095	40	Clay
	10091717	42	Sandstone		10018031	42	Clay
Bowen	40144579	28	Plutonic rock		10106089	40	Clay
	40144650	15	Plutonic rock	Pioneer Valley	40051380	10	Rock
	40144588	24	Plutonic rock		40081867	9	Plutonic rock
	40144365	18	Granite		40145417	25	Granite
	40144404	15	Plutonic rock		40023197	25	Granite
	40144402	17	Plutonic rock		40145527	22	Rock
	40144590	17	Plutonic rock		40145412	19	Granite
	40144419	18	Plutonic rock		40145538	42	Granite
	40144592	23	Volcanic rock		40145522	30	Rock/Basalt
	40144584	17	Plutonic rock		40145794	25	Granite
	40144355	22	Granite		40145563	28	Granite
Burdekin	40144287	20	Granite		40145791	17	Siltstone/granite
	40144698	13	Volcanic rock		40145785	29	Granite
	40141803	85	Granite		40145567	21	Granite
	40141563	80	Rock		40145976	16	Plutonic rock
	40141789	60	Granite		40145569	32	Rock
	40141807	58	Granite		40145776	28	Granite
	40141785	56	Rock		40145784	31	Granite
	40109521	30	Rock		40145782	32	Volcanic rock
Burnett Heads	40147891	70	Shale, sandstone		40145776	28	Granite
	40147964	70	Sandstone		40145570	20	Rock
	40148028	83	Shale	Stockton	10080680	n.a	Superficial
	40147858	62	Clay, sandstone		10104355	n.a.	Superficial
	40147907	75	Clay		10096642	n.a.	Superficial
	40148023	73	Shale	Stuarts Point	10014074	23	Clay
	40147861	62	Basalt, shale		10008433	25	Clay, sandstone
	40148078	70	Basalt		10101302	25	Clay, shale
	40147968	85	Clay		10008594	25	Clay
	40148265	73	Clay		10011156	25	Clay
					10129522	20	Sand

*HydroID from the Australian Groundwater Explorer website (Australian Government - Bureau of Meteorology, n.d.).

Appendix F Determination of distance to inland boundary condition and head at this point

Case study area	id_cs	Distance to inland boundary condition (m)	Average distance to inland boundary condition (m)	GEBCO (m a.s.l.)	GWTD (m)	GEBCO-GWTD (m a.s.l.)	Average GEBCO-GWTD (m)
Botany	51218	3500	3500	35	32.3	2.7	2.7
Bowen	50678	9350	6890	11	2.82	8.18	6.4
	50679	4430		9	4.48	4.52	
Burdekin	50652	400	656	4	ND	-	3.1
	50653	814		5	1.74	3.26	
	50654	400		5	0.61	4.39	
	50655	1011		4	2.5	1.5	
Burnett Heads	50934	650	1425	11	1.33	9.67	4.7
	50935	650		8	0.52	7.48	
	50936	1500		6	6.24	-0.24	
	50937	2900		8	5.98	2.02	
HatHead	51110	500	625	9	0.67	8.33	9.6
	51111	750		12	1.08	10.92	
Pioneer Valley	50751	690	2397	6	1.1	4.9	4.8
	50752	3500		4	0.49	3.51	
	50753	3000		7	1.04	5.96	
Stockton	51166	700	846	9	0.1	8.9	8.5
	51167	990		18	6.8	11.2	
	51168	830		10	0.1	9.9	
	51169	730		16	0.1	15.9	
	51170	1000		13	10.08	2.92	
	51171	825		11	9	2	
Stuarts Point	51106	1500	1500	5	0.4	4.6	4.6

*id_cs (cross section identification number) from Zamrsky et al. (2018)

*GEBCO = GEBCO dataset (Weatherall et al., 2015)

*GWTD = Groundwater table dataset (Fan et al., 2013)

Appendix G M4 - Geology and recharge input for all realizations

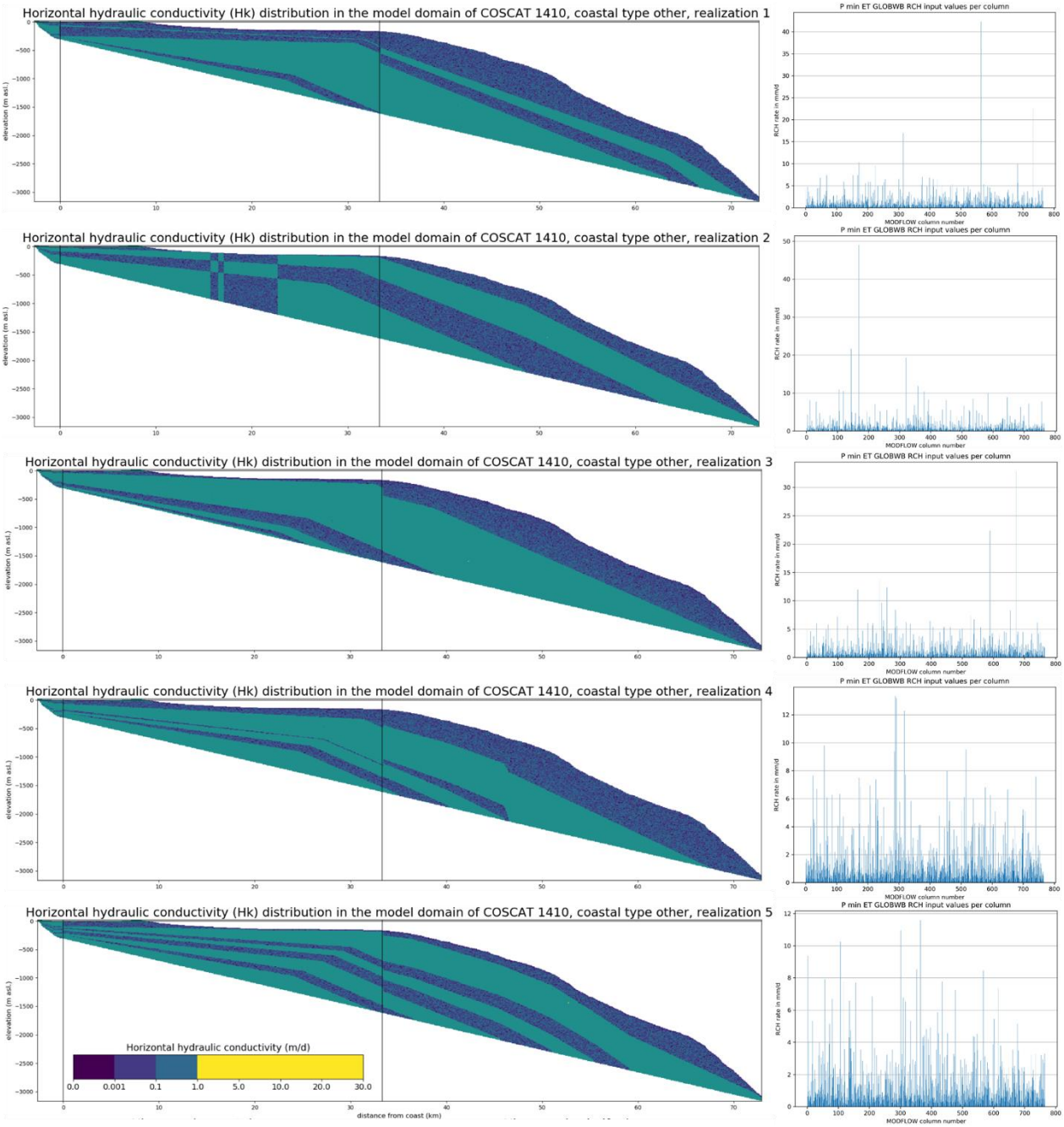

Figure 85: M4 - Botany– Geology and recharge model input

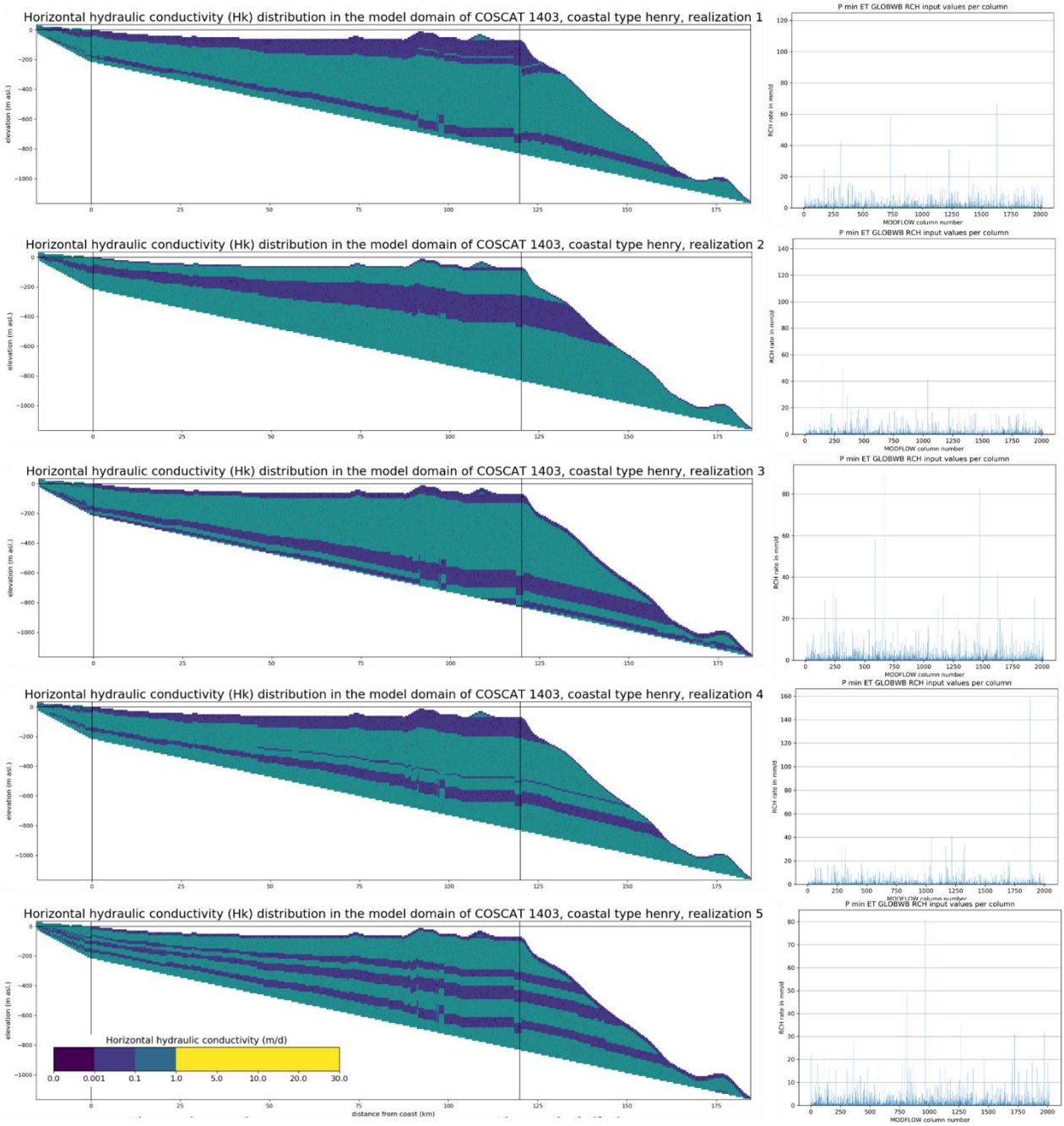

Figure 86: M4 - Bowen– Geology and recharge model input

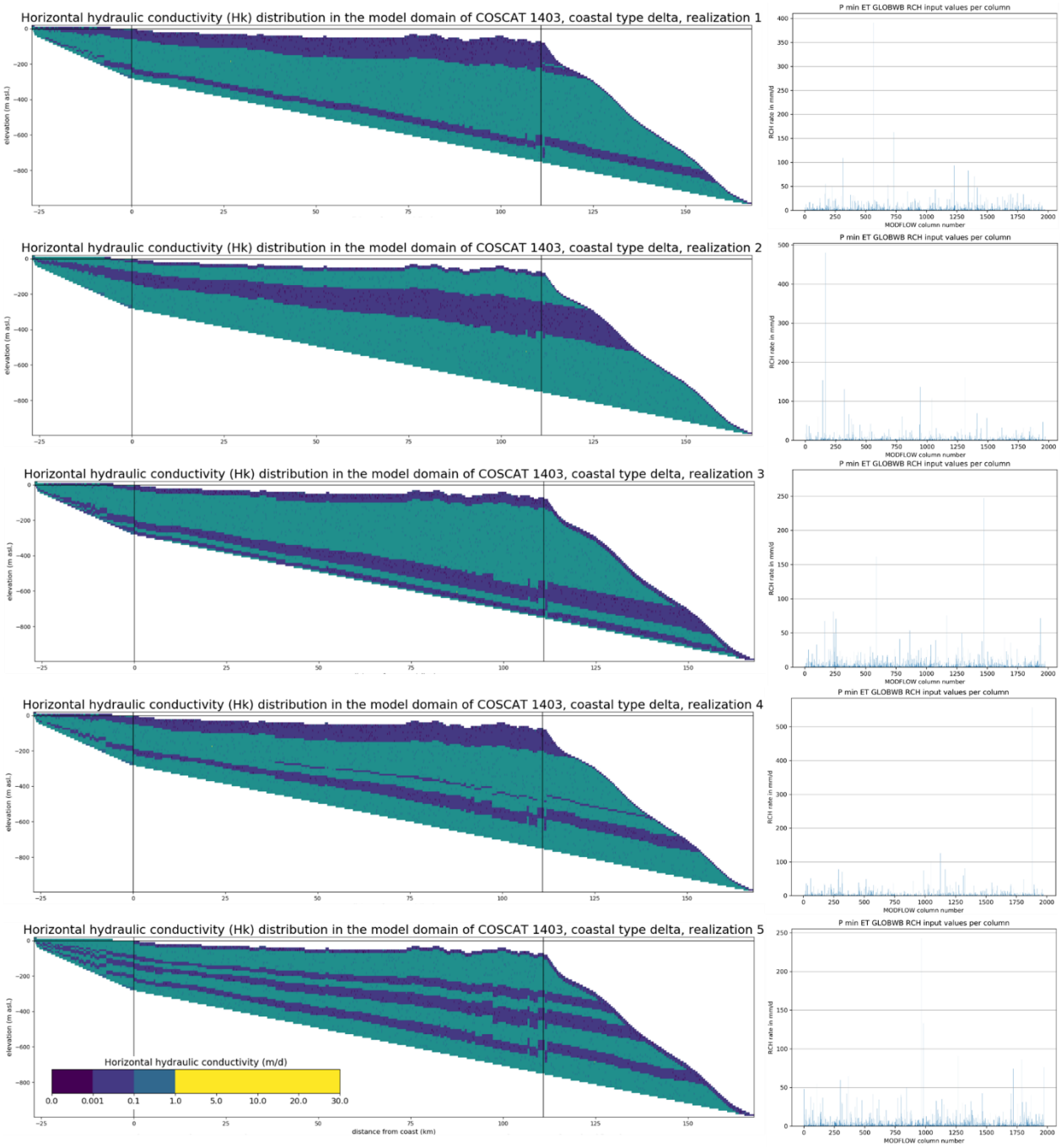

Figure 87: M4 – Burdekin – Geology and recharge model input

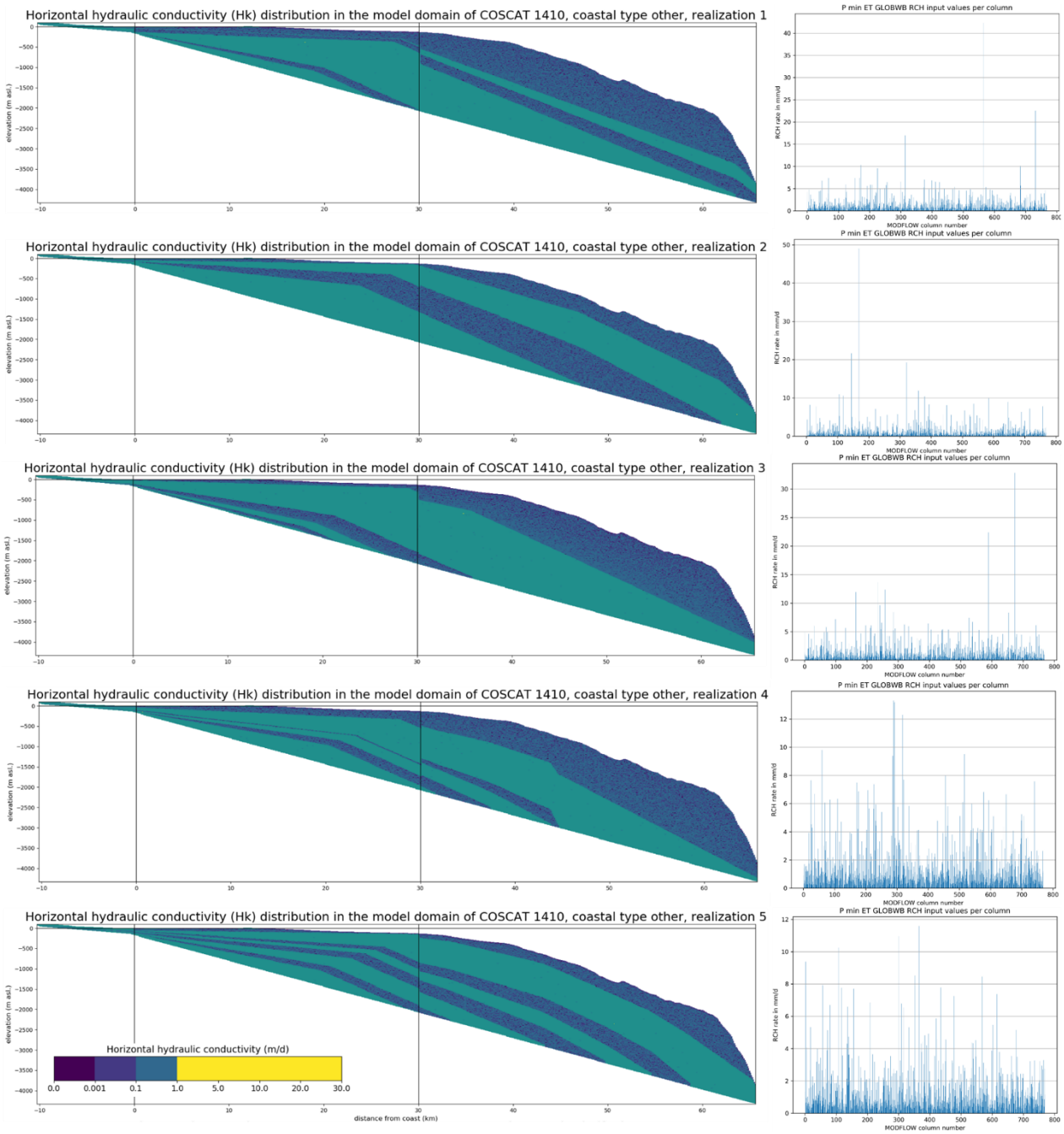

Figure 88: M4 – Hat Head – Geology and recharge model input

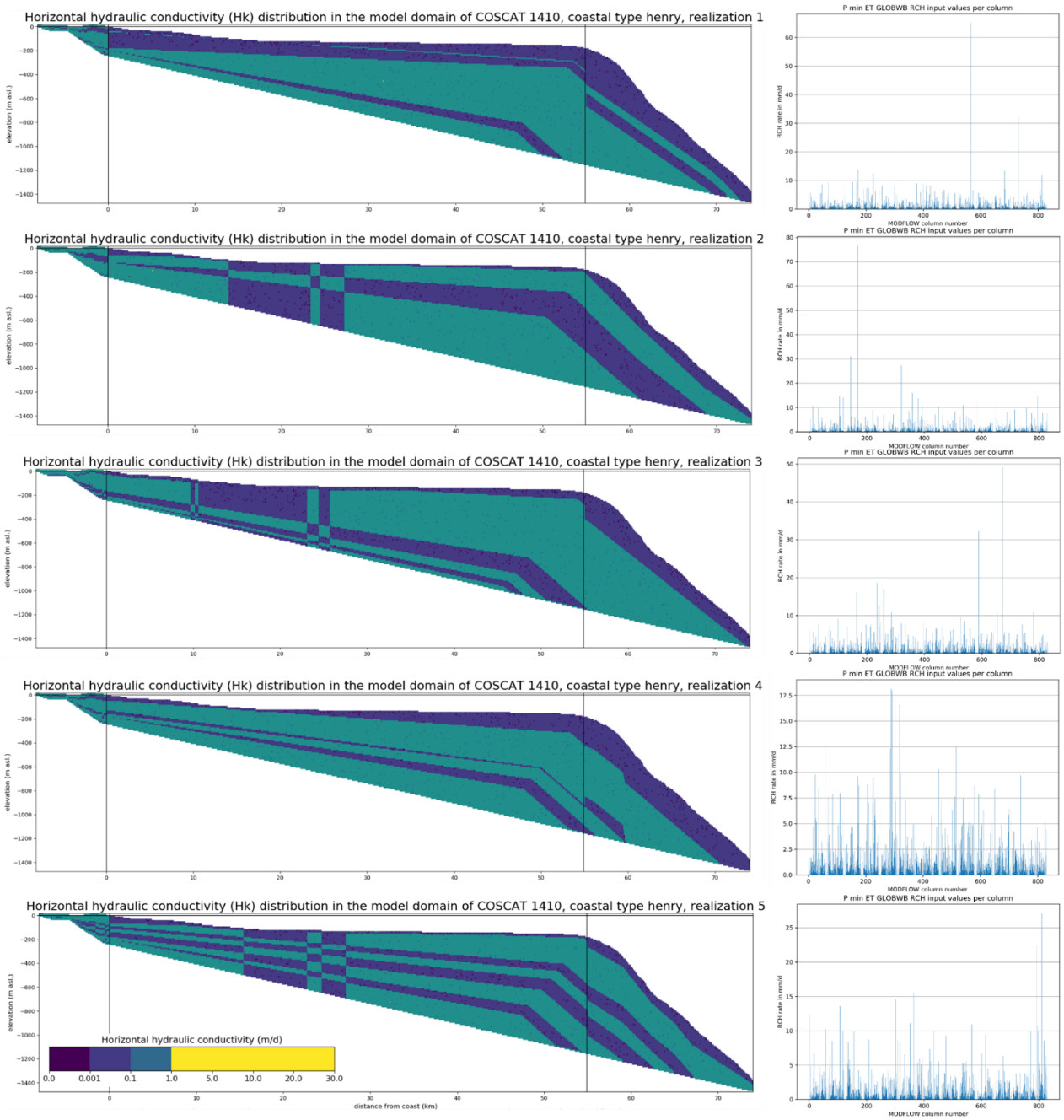

Figure 89: M4 - Stockton – Geology and recharge model input

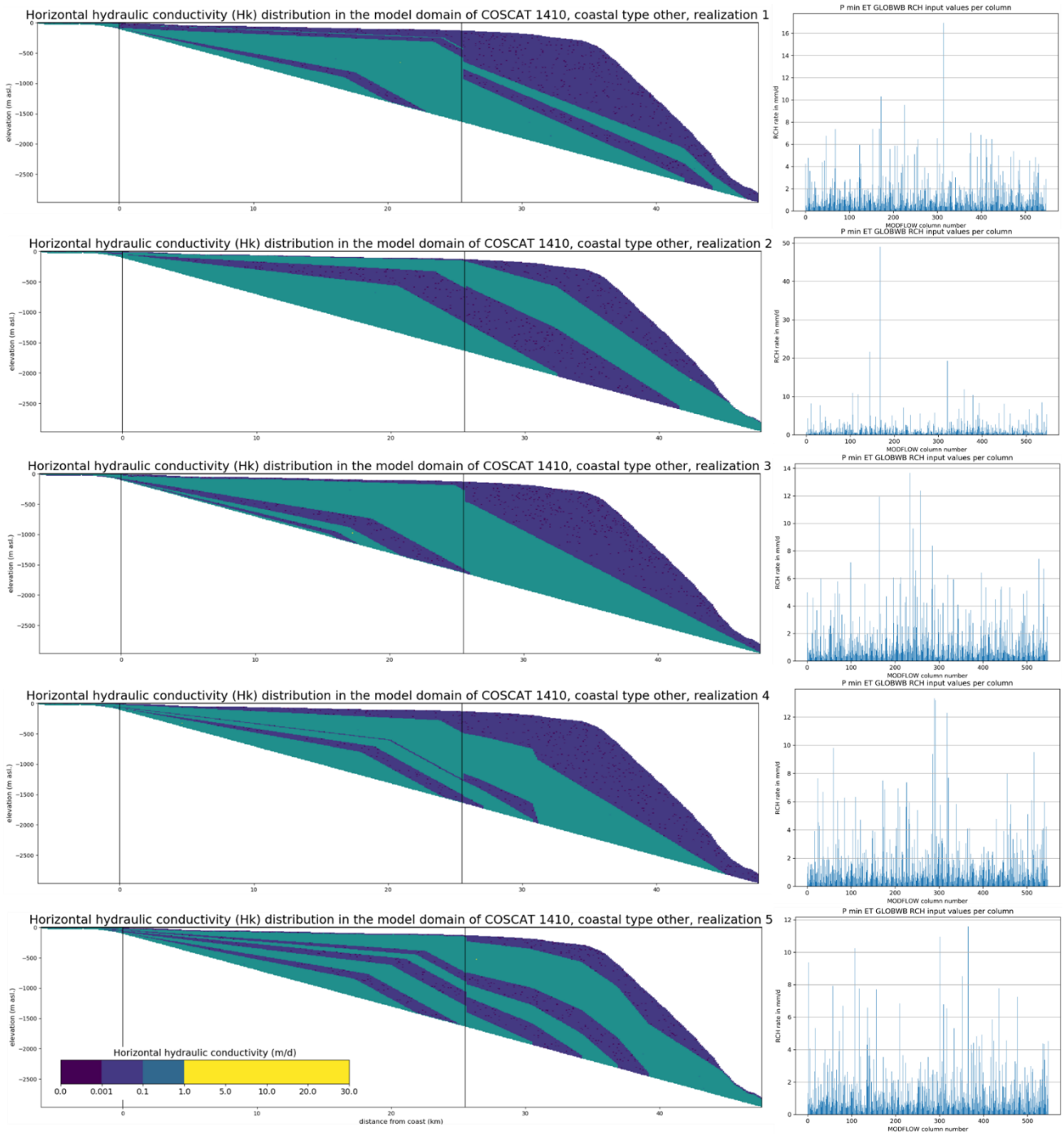

Figure 90: M4 – Stuarts Point – Geology and recharge model input

Appendix H M4 – Saltwater intrusion length (m) for all realizations

Table 17: M4 – Saltwater intrusion length (m) for all realizations

id_cs	Case study area	Realization number	Distance from coast (m)
51219	Botany	1	700
		2	600
		3	800
		4	700
		5	800
50679	Bowen	1	700
		2	700
		3	800
		4	700
		5	700
50652	Burdekin	1	2600
		2	3100
		3	800
		4	2400
		5	2800
51110	Hat Head	1	800
		2	200
		3	200
		4	400
		5	300
51169	Stockton	1	0
		2	0
		3	0
		4	0
		5	0
51106	Stuarts Point	1	0
		2	0
		3	0
		4	0
		5	0

*id_cs (cross section identification number) from Zamrsky et al. (2018)

Appendix I M4 – Freshwater volumes (m^3/m) for all realizations

Table 18: M4 - Freshwater volumes (m^3/m) for all realizations

id_cs	Case study area	Realization	Freshwater volume inland (m^3/m)	Freshwater volume continental shelf (m^3/m)	Total (m^3/m)
51219	Botany	1	49	1290	1339
		2	49	1478	1527
		3	49	1449	1498
		4	49	1457	1506
		5	49	1296	1345
50679	Bowen	1	1765	1	1766
		2	1729	5	1734
		3	1744	3	1747
		4	1756	4	1760
		5	1756	3	1759
50652	Burdekin	1	3731	71	3802
		2	3469	51	3520
		3	3909	96	4005
		4	3729	66	3795
		5	3635	74	3709
51110	Hat Head	1	208	1011	1219
		2	208	1297	1505
		3	208	1204	1412
		4	208	1146	1354
		5	208	1111	1319
51169	Stockton	1	932	458	1390
		2	931	47	978
		3	932	434	1366
		4	932	306	1238
		5	932	183	1115
51106	Stuarts Point	1	249	2	251
		2	253	7	260
		3	247	6	253
		4	250	13	263
		5	249	2	251

*id_cs (cross section identification number) from Zamrsky et al. (2018)

Appendix J M5 – Saltwater intrusion length (m) for all realizations

Table 19: M5 – Saltwater intrusion length (m) for all realizations

id_cs	Case study area	Realization number	Distance from coast (m)
51219	Botany	1	800
		2	800
		3	800
		4	800
		5	800
50679	Bowen	1	0
		2	0
		3	0
		4	0
		5	0
50652	Burdekin	1	0
		2	0
		3	0
		4	0
		5	0
51110	Hat Head	1	400
		2	400
		3	400
		4	800
		5	300
51169	Stockton	1	2400
		2	3000
		3	1900
		4	2000
		5	2100
51106	Stuarts Point	1	0
		2	0
		3	0
		4	0
		5	0

*id_cs (cross section identification number) from Zamrsky et al. (2018)

Appendix K M5 – Freshwater volumes (m^3/m) for all realizations

Table 20: M5 - Freshwater volumes (m^3/m) for all realizations

id_cs	Case study area	Realization	Freshwater volume inland (m^3/m)	Freshwater volume continental shelf (m^3/m)	Total (m^3/m)
51219	Botany	1	49	598	647
		2	49	672	721
		3	49	712	761
		4	49	697	746
		5	49	768	817
50679	Bowen	1	1903	1441	3344
		2	1903	1755	3658
		3	1903	1609	3512
		4	1903	1577	3480
		5	1903	1876	3779
50652	Burdekin	1	4222	1860	6082
		2	4222	1960	6182
		3	4222	1997	6219
		4	4222	1993	6215
		5	4222	2097	6319
51110	Hat Head	1	208	906	1114
		2	208	898	1106
		3	208	932	1140
		4	208	860	1068
		5	208	925	1133
51169	Stockton	1	551	0	551
		2	502	0	502
		3	592	0	592
		4	629	0	629
		5	588	0	588
51106	Stuarts Point	1	253	34	287
		2	253	13	266
		3	253	9	262
		4	253	12	265
		5	253	9	262

*id_cs (cross section identification number) from Zamrsky et al. (2018)